



Chapter 11

Offshore Marine Environment Characterisation

DISCLAIMER

This disclaimer applies to and governs the disclosure and use of this Environmental Impact Statement ("EIS"), and by reading, using or relying on any part(s) of the EIS you accept this disclaimer in full.

This Environmental Impact Statement, including the Executive Summary, and all chapters of and attachments and appendices to it and all drawings, plans, models, designs, specifications, reports, photographs, surveys, calculations and other data and information in any format contained and/or referenced in it, is together with this disclaimer referred to as the "**EIS**".

Purpose of EIS

The EIS has been prepared by, for and on behalf of Wafi Mining Limited and Newcrest PNG 2 Limited (together the "**WGJV Participants**"), being the participants in the Wafi-Golpu Joint Venture ("**WGJV**") and the registered holders of exploration licences EL 440 and EL1105, for the sole purpose of an application (the "**Permit Application**") by them for environmental approval under the Environment Act 2000 (the "**Act**") for the proposed construction, operation and (ultimately) closure of an underground copper-gold mine and associated ore processing, concentrate transport and handling, power generation, water and tailings management, and related support facilities and services (the "**Project**") in Morobe Province, Independent State of Papua New Guinea. The EIS was prepared with input from consultants engaged by the WGJV Participants and/or their related bodies corporate ("**Consultants**").

The Permit Application is to be lodged with the Conservation and Environment Protection Authority ("**CEPA**"), Independent State of Papua New Guinea.

Ownership and Copyright

The EIS is the sole property of the WGJV Participants, who reserve and assert all proprietary and copyright ©2018 interests.

Reliance and Use

The EIS is intended and will be made available to CEPA, for review by CEPA and other applicable agencies of the Government of the Independent State of Papua New Guinea ("**Authorised Agencies**"), for the purpose of considering and assessing the Permit Application in accordance with the Act ("**Authorised Purpose**"), and for no other purpose whatsoever.

The EIS shall not be used or relied upon for any purpose other than the Authorised Purpose, unless express written approval is given in advance by the WGJV Participants.

Except for the Authorised Purpose, the EIS, in whole or in part, must not be reproduced, unless express written approval is given in advance by the WGJV Participants.

This disclaimer must accompany every copy of the EIS.

The EIS is meant to be read as a whole, and any part of it should not be read or relied upon out of context.

Limits on investigation and information

The EIS is based in part on information not within the control of either the WGJV Participants or the Consultants. While the WGJV Participants and Consultants believe that the information contained in the EIS should be reliable under the conditions and subject to the limitations set forth in the EIS, they do not guarantee the accuracy of that information.

No Representations or Warranties

While the WGJV Participants, their Related Bodies Corporate and Consultants believe that the information (including any opinions, forecasts or projections) contained in the EIS should be reliable under the conditions and subject to the limitations set out therein, and provide such information in good faith, they make no warranty, guarantee or promise, express or implied, that any of the information will be correct, accurate, complete or up to date, nor that such information will remain unchanged after the date of issue of the EIS to CEPA, nor that any forecasts or projections will be realised. Actual outcomes may vary materially and adversely from projected outcomes.

The use of the EIS shall be at the user's sole risk absolutely and in all respects. Without limitation to the foregoing, and to the maximum extent permitted by applicable law, the WGJV Participants, their Related Bodies Corporate and Consultants:

- do not accept any responsibility, and disclaim all liability whatsoever, for any loss, cost, expense or damage (howsoever arising, including in contract, tort (including negligence) and for breach of statutory duty) that any person or entity may suffer or incur caused by or resulting from any use of or reliance on the EIS or the information contained therein, or any inaccuracies, misstatements, misrepresentations, errors or omissions in its content, or on any other document or information supplied by the WGJV Participants to any Authorised Agency at any time in connection with the Authorised Agency's review of the EIS; and
- expressly disclaim any liability for any consequential, special, contingent or penal damages whatsoever.

The basis of the Consultants' engagement is that the Consultants' liability, whether under the law of contract, tort, statute, equity or otherwise, is limited as set out in the terms of their engagement with the WGJV Participants and/or their related bodies corporate.

Disclosure for Authorised Purpose

The WGJV Participants acknowledge and agree that, for the Authorised Purpose, the EIS may be:

- copied, reproduced and reprinted;
- published or disclosed in whole or in part, including being made available to the general public in accordance with section 55 of the Act. All publications and disclosures are subject to this disclaimer.

Development of Project subject to Approvals, Further Studies and Market and Operating Conditions

Any future development of the Project is subject to further studies, completion of statutory processes, receipt of all necessary or desirable Papua New Guinea Government and WGJV Participant approvals, and market and operating conditions.

Engineering design and other studies are continuing and aspects of the proposed Project design and timetable may change.

NEWCREST MINING LIMITED DISCLAIMER

Newcrest Mining Limited ("**Newcrest**") is the ultimate holding company of Newcrest PNG 2 Limited and any reference below to "Newcrest" or the "Company" includes both Newcrest Mining Limited and Newcrest PNG 2 Limited.

Forward Looking Statements

The EIS includes forward looking statements. Forward looking statements can generally be identified by the use of words such as "may", "will", "expect", "intend", "plan", "estimate", "anticipate", "continue", "outlook" and "guidance", or other similar words and may include, without limitation, statements regarding plans, strategies and objectives of management, anticipated production or construction commencement dates and expected costs or production outputs. The Company continues to distinguish between outlook and guidance. Guidance statements relate to the current financial year. Outlook statements relate to years subsequent to the current financial year.

Forward looking statements inherently involve known and unknown risks, uncertainties and other factors that may cause the Company's actual results, performance and achievements to differ materially from statements in this EIS. Relevant factors may include, but are not limited to, changes in commodity prices, foreign exchange fluctuations and general economic conditions, increased costs and demand for production inputs, the speculative nature of exploration and project development, including the risks of obtaining necessary licences and permits and diminishing quantities or grades of reserves, political and social risks, changes to the regulatory framework within which the Company operates or may in the future operate, environmental conditions including extreme weather conditions, recruitment and retention of personnel, industrial relations issues and litigation.

Forward looking statements are based on the Company's good faith assumptions as to the financial, market, regulatory and other relevant environments that will exist and affect the Company's business and operations in the future.

The Company does not give any assurance that the assumptions will prove to be correct. There may be other factors that could cause actual results or events not to be as anticipated, and many events are beyond the reasonable control of the Company. Readers are cautioned not to place undue reliance on forward looking statements. Forward looking statements in the EIS speak only at the date of issue. Except as required by applicable laws or regulations, the Company does not undertake any obligation to publicly update or revise any of the forward looking statements or to advise of any change in assumptions on which any such statement is based.

Non-IFRS Financial Information

Newcrest results are reported under International Financial Reporting Standards (IFRS) including EBIT and EBITDA. The EIS also includes non-IFRS information including Underlying profit (profit after tax before significant items attributable to owners of the parent company), All-In Sustaining Cost (determined in accordance with the World Gold Council Guidance Note on Non-GAAP Metrics released June 2013), AISC Margin (realised gold price less AISC per ounce sold (where expressed as USD), or realised gold price less AISC per ounce sold divided by realised gold price (where expressed as a %), Interest Coverage Ratio (EBITDA/Interest payable for the relevant period), Free cash flow (cash flow from operating activities less cash flow related to investing activities), EBITDA margin (EBITDA expressed as a percentage of revenue) and EBIT margin (EBIT expressed as a percentage of revenue). These measures are used internally by Management to assess the performance of the business and make decisions on the allocation of resources and are included in the EIS to provide greater understanding of the underlying performance of Newcrest's operations. The non-IFRS information has not been subject to audit or review by Newcrest's external auditor and should be used in addition to IFRS information.

Ore Reserves and Mineral Resources Reporting Requirements

As an Australian Company with securities listed on the Australian Securities Exchange (ASX), Newcrest is subject to Australian disclosure requirements and standards, including the requirements of the Corporations Act 2001 and the ASX. Investors should note that it is a requirement of the ASX listing rules that the reporting of Ore Reserves and Mineral Resources in Australia comply with the 2012 Edition of the Australasian Code for Reporting of Exploration Results, Mineral Resources and Ore Reserves (the JORC Code) and that Newcrest's Ore Reserve and Mineral Resource estimates comply with the JORC Code.

Competent Person's Statement

The information in the EIS that relates to Golpu Ore Reserves is based on information compiled by the Competent Person, Mr Pasqualino Manca, who is a member of The Australasian Institute of Mining and Metallurgy. Mr Pasqualino Manca, is a full-time employee of Newcrest Mining Limited or its relevant subsidiaries, holds options and/or shares in Newcrest Mining Limited and is entitled to participate in Newcrest's executive equity long term incentive plan, details of which are included in Newcrest's 2017 Remuneration Report. Ore Reserve growth is one of the performance measures under recent long term incentive plans. Mr Pasqualino Manca has sufficient experience which is relevant to the styles of mineralisation and type of deposit under consideration and to the activity which he is undertaking to qualify as a Competent Person as defined in the JORC Code 2012. Mr Pasqualino Manca consents to the inclusion of material of the matters based on his information in the form and context in which it appears.

HARMONY GOLD MINING COMPANY LIMITED DISCLAIMER

Harmony Gold Mining Company Limited ("**Harmony**") is the ultimate holding company of Wafi Mining Limited and any reference below to "Harmony" or the "Company" includes both Harmony Gold Mining Company Limited and Wafi Mining Limited.

Forward Looking Statements

These materials contain forward-looking statements within the meaning of the safe harbor provided by Section 21E of the Securities Exchange Act of 1934, as amended, and Section 27A of the Securities Act of 1933, as amended, with respect to our financial condition, results of operations, business strategies, operating efficiencies, competitive positions, growth opportunities for existing services, plans and objectives of management, markets for stock and other matters. These include all statements other than statements of historical fact, including, without limitation, any statements preceded by, followed by, or that include the words "targets", "believes", "expects", "aims", "intends", "will", "may", "anticipates", "would", "should", "could", "estimates", "forecast", "predict", "continue" or similar expressions or the negative thereof.

These forward-looking statements, including, among others, those relating to our future business prospects, revenues and income, wherever they may occur in this EIS and the exhibits to this EIS, are essentially estimates reflecting the best judgment of our senior management and involve a number of risks and uncertainties that could cause actual results to differ materially from those suggested by the forward-looking statements. As a consequence, these forward-looking statements should be considered in light of various important factors, including those set forth in these materials. Important factors that could cause actual results to differ materially from estimates or projections contained in the forward-looking statements include, without limitation: overall economic and business conditions in South Africa, Papua New Guinea, Australia and elsewhere, estimates of future earnings, and the sensitivity of earnings to the gold and other metals prices, estimates of future gold and other metals production and sales, estimates of future cash costs, estimates of future cash flows, and the sensitivity of cash flows to the gold and other metals prices, statements regarding future debt repayments, estimates of future capital expenditures, the success of our business strategy, development activities and other initiatives, estimates of reserves statements regarding future exploration results and the replacement of reserves, the ability to achieve anticipated efficiencies and other cost savings in connection with past and future acquisitions, fluctuations in the market price of gold, the occurrence of hazards associated with underground and surface gold mining, the occurrence of labour disruptions, power cost increases as well as power stoppages, fluctuations and usage constraints, supply chain shortages and increases in the prices of production imports, availability, terms and deployment of capital, changes in government regulation, particularly mining rights and environmental regulation, fluctuations in exchange rates, the adequacy of the Group's insurance coverage and socio-economic or political instability in South Africa and Papua New Guinea and other countries in which we operate.

For a more detailed discussion of such risks and other factors (such as availability of credit or other sources of financing), see the Company's latest Integrated Annual Report and Form 20-F which is on file with the Securities and Exchange Commission, as well as the Company's other Securities and Exchange Commission filings. The Company undertakes no obligation to update publicly or release any revisions to these forward-looking statements to reflect events or circumstances after the date of this EIS or to reflect the occurrence of unanticipated events, except as required by law.

Competent Person's Statement

The Wafi-Golpu Joint Venture is an unincorporated joint venture between a wholly-owned subsidiary of Harmony Gold Mining Company Limited and a wholly-owned subsidiary of Newcrest Mining Limited.

The information in the EIS that relates to Golpu Ore Reserves is based on information compiled by the Competent Person, Mr Pasqualino Manca, who is a member of The Australasian Institute of Mining and Metallurgy. Mr Pasqualino Manca, is a full-time employee of Newcrest Mining Limited or its relevant subsidiaries, holds options and/ or shares in Newcrest Mining Limited and is entitled to participate in Newcrest's executive equity long term incentive plan, details of which are included in Newcrest's 2017 Remuneration Report. Ore Reserve growth is one of the performance measures under recent long term incentive plans. Mr Pasqualino Manca has sufficient experience which is relevant to the styles of mineralisation and type of deposit under consideration and to the activity which he is undertaking to qualify as a Competent Person as defined in the JORC Code 2012. Mr Pasqualino Manca consents to the inclusion of material of the matters based on his information in the form and context in which it appears.

TABLE OF CONTENTS

11. OFFSHORE MARINE ENVIRONMENT CHARACTERISATION 11-1
11.1. Bathymetry 11-1
11.2. Upper Ocean Profiling 11-5
11.3. Potential for Coastal Upwelling 11-10
11.4. Ocean Currents 11-12
11.4.1. Ocean Current Data Collection 11-12
11.4.2. Ocean Floor Mass Movement Events 11-13
11.4.3. Outfall A Currents 11-15
11.4.4. Canyon Mooring Currents 11-15
11.5. Terrestrial Sediment Supply 11-18
11.6. Sediment Transport Through the Markham Canyon 11-20
11.7. Benthic Sediment Characteristics 11-24
11.7.1. Particle Size Distribution 11-27
11.7.2. Metals 11-27
11.8. Offshore Marine Ecology 11-30
11.8.1. Deep-Slope and Pelagic Fish 11-30
11.8.2. Zooplankton and Micronekton 11-46
11.8.3. Deep-Sea Benthic Ecology 11-54
11.9. References 11-61

LIST OF FIGURES

Figure 11.1: New Britain Trench 11-2
Figure 11.2: Bathymetry of the western Huon Gulf 11-3
Figure 11.3: Huon Gulf deep water bathymetry to over 3,000m 11-4
Figure 11.4: Outfall Area high-resolution bathymetry 11-6
Figure 11.5: Upper ocean profiling locations 11-8
Figure 11.6: Surface mixed layer depth and euphotic zone thickness measured to date 11-9
Figure 11.7: Temperature profiles at transects A and B from February, July and August 2017 11-11
Figure 11.8: Huon Gulf ADCP oceanographic instrument mooring locations 11-14
Figure 11.9: Near-bed current speeds at Canyon B and Canyon C moorings from May to September 2017 11-17
Figure 11.10: Rivers draining to the northern shoreline of the Huon Gulf 11-19
Figure 11.11: Turbidity profiles from CTD location A3 11-21
Figure 11.12: Turbidity profiles from CTD location B5 11-22
Figure 11.13: Echo-sounder trace of acoustic backscatter indicating the presence of large bed waves along the floor of the Markham Canyon up canyon of the Trench Mooring 11-25
Figure 11.14: Benthic sediment and infauna box corer and multi corer sampling locations 11-26
Figure 11.15: Deep-slope and pelagic drop-line fishing locations 11-31

Figure 11.16: Pelagic trolling transects 11-32
Figure 11.17: Dwarf gulper shark (Centrophorus atromarginatus) 11-34
Figure 11.18: Long-finned gulper shark (Centrophorus longipinnis) 11-34
Figure 11.19: Gulper shark (Centrophorus granulosus) 11-34
Figure 11.20: Fatspine spurdog (Squalus crassispinis) 11-34
Figure 11.21: Vertical distribution of dwarf gulper sharks 11-35
Figure 11.22: Saddletail snapper (Lutjanus malabaricus) 11-36
Figure 11.23: Common pike eel (Muraenesox baggio) 11-36
Figure 11.24: Blackspotted croaker (Protonibea diacanthus) 11-36
Figure 11.25: Mean metals concentrations (As, Cu and Fe) in liver and muscle of fishes caught (Nov 2016; May 2017) and sourced from DCA Point fish market (Nov 2016) 11-39
Figure 11.26: Mean metals concentrations (Hg, Se and Zn) in liver and muscle of fishes caught (Nov 2016; May 2017) and sourced from DCA Point fish market (Nov 2016) 11-40
Figure 11.27: Metals concentrations (As, Cu and Fe) in liver and muscle of dwarf gulper shark by total weight and length 11-43
Figure 11.28: Metals concentrations (Hg, Se and Zn) in liver and muscle of dwarf gulper shark by total weight and length 11-44
Figure 11.29: Metals concentrations (Cd) in liver and muscle of dwarf gulper shark by total weight and length 11-45
Figure 11.30: Zooplankton and micronekton sampling locations 11-47
Figure 11.31: Copepod collected during zooplankton sampling 11-49
Figure 11.32: Ostracod collected during zooplankton sampling 11-49
Figure 11.33: Ghost shrimp 'Lucifer' collected during zooplankton sampling 11-49
Figure 11.34: Siphonophore (hydrozoan) collected during zooplankton sampling 11-49
Figure 11.35: Arrow worm (chaetognath) collected during zooplankton sampling 11-49
Figure 11.36: Early juvenile slimehead (possibly Hoplostethus sp. Family: Trachichyidae) collected in night plankton sample 11-51
Figure 11.37: Slickhead (Family: Alepocephalidae) collected during micronekton sampling 11-51
Figure 11.38: Viperfish (Chauliodus sloani) collected during micronekton sampling 11-51
Figure 11.39: Leptocephalus stage larvae of anguilliform (eel) fishes collected during micronekton sampling 11-51
Figure 11.40: Average concentrations of As, Cd, Cu, Fe, Mn, Ni and Zn in zooplankton samples collected in March 2017 from the DSTP and reference study areas 11-52
Figure 11.41: Concentrations of As, Cd, Cu, Fe, Pb, Hg, Mn, Ni, Se and Zn in micronekton taxa collected in the DSTP study area in May 2017 11-53
Figure 11.42: Benthic video characterisation study sites 11-55
Figure 11.43: Sea whip (lower left of frame) at Site 13 (depth 757m). Note mounds and burrows in sediment 11-57
Figure 11.44: Cobble sized rocks of riverine origin at Site 1, 229m depth 11-57
Figure 11.45: Average meiofauna density for box and multi corer replicates 11-60

LIST OF TABLES

Table 11.1: Estimated Speed of Turbidity Current Fronts 11-15

Table 11.2: Estimated suspended sediment load for the Markham and Busu rivers 11-20

Table 11.3: Particle size distribution in bed sediments from box core samples – February 2017 11-27

Table 11.4: Total sediment metals (mg/kg) concentrations from box core samples – February 2017 11-28

Table 11.5: EDTA sediment metals concentrations (mg/kg) from box core samples – February 2017.... 11-29

Table 11.6: Summary of food standards and guidelines 11-38

Table 11.7: Macrofauna abundance and density and meiofauna density in deep-sea sediment samples, February 2017 11-58

Table 11.8: Density (number/10cm^2) of meiobenthic fauna collected in the Markham Canyon survey, December 2017........ 11-58

11. OFFSHORE MARINE ENVIRONMENT CHARACTERISATION

The offshore marine environment is the region seaward of the nearshore zone, encompassing the ocean water column from the surface to and including the sea floor. That is, the zone beyond the foreshore, littoral zone and shallow-water benthic and pelagic habitats and in waters deeper than 20 metres (m) and more than 100m from the shore.

This chapter provides a characterisation of the relevant biophysical characteristics of the offshore marine environment potentially affected by the Project. The Project's proposed use of deep sea tailings placement (DSTP) will, with the exception of pipeline construction, bypass the nearshore zone and occur solely within the offshore marine environment at a depth below 200m, located approximately 1 kilometre (km) from shore.

The information in this chapter is based on a range of specialist studies that are included in this EIS as appendices, including:

- Oceanographic investigations of the Huon Gulf undertaken by IHAconsult (Appendix K)
- Physical, chemical and biological sedimentology of the Huon Gulf undertaken by IHAconsult (Appendix M)
- Benthic video characterisation study undertaken by Coffey (Appendix O)
- Deep-slope and pelagic fish characterisation study undertaken by Marscco and Coffey (Appendix P)
- Zooplankton and micronekton characterisation study undertaken by Marscco and Coffey (Appendix Q)
- Fisheries and marine resource use characterisation study undertaken by EnviroGulf Consulting (Appendix S)

These documents contain additional specific descriptions of the study methods, data and further technical details concerning the information presented in this chapter.

11.1. Bathymetry

Regional scale bathymetry of the Huon Gulf and New Britain Trench has been sourced from the General Bathymetric Chart of the Oceans (GEBCO, 2014; Figure 11.1). This shows the Huon Gulf in the west with its seafloor sloping towards the New Britain Trench in the east which is more than 9,000m deep at its deepest point along the northern margin subduction zone.

More detailed bathymetry for the Huon Gulf has been obtained through multi-beam echo sounding surveys conducted in 1999, 2012, 2016 and 2017 (Appendix K, Oceanographic Investigations of the Huon Gulf). The area and resolution of bathymetric data has progressively increased over these surveys. The most up-to-date and accurate bathymetry of the western Huon Gulf is presented in Figure 11.2 to 1,500m water depth and in Figure 11.3 to 3,000m water depth.

The Markham River discharges into the Huon Gulf west of Lae and directly south of the Atzera Mountain Range and southern slopes of the Finisterre Range. Below sea level, seafloor slopes plunge steeply to a submarine canyon known as the Markham Canyon. The canyon floor (see Figure 11.2) is the main pathway for the transport of terrestrially-derived sediment through the Huon Gulf towards the New Britain Trench.

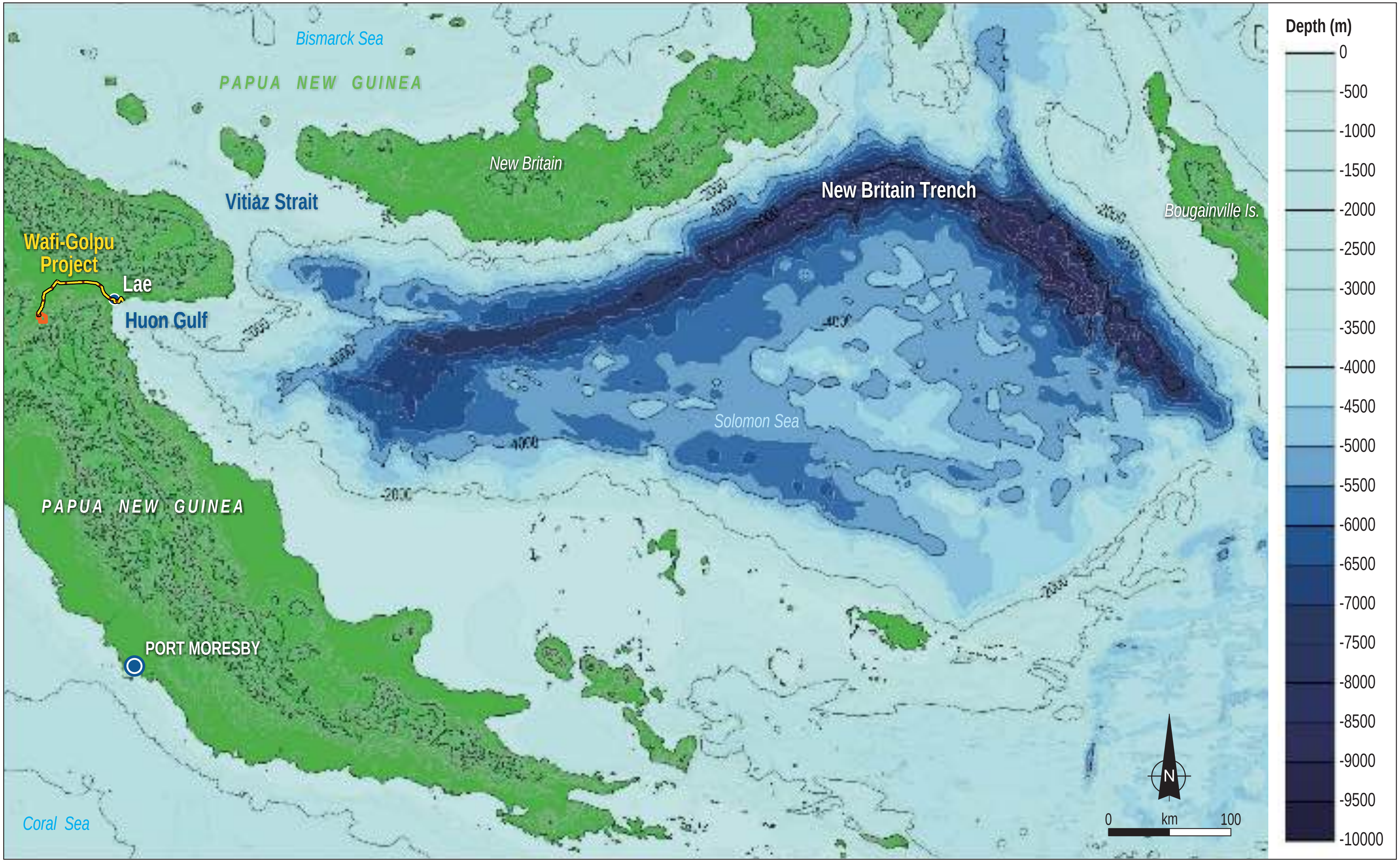

Source: GEBCO 2014

coffey A TETRA TECH COMPANY

Date: 22.05.2018	WAFI-GOLPU JOINT VENTURE	New Britain Trench	Figure No: 11.1
Project: 754-ENAUABTF100520DD			
File Name: 0520DD_10_F11.01_GRA	Wafi-Golpu Project		

INDD Reference: 0520DD_10_GRA068.indd 4

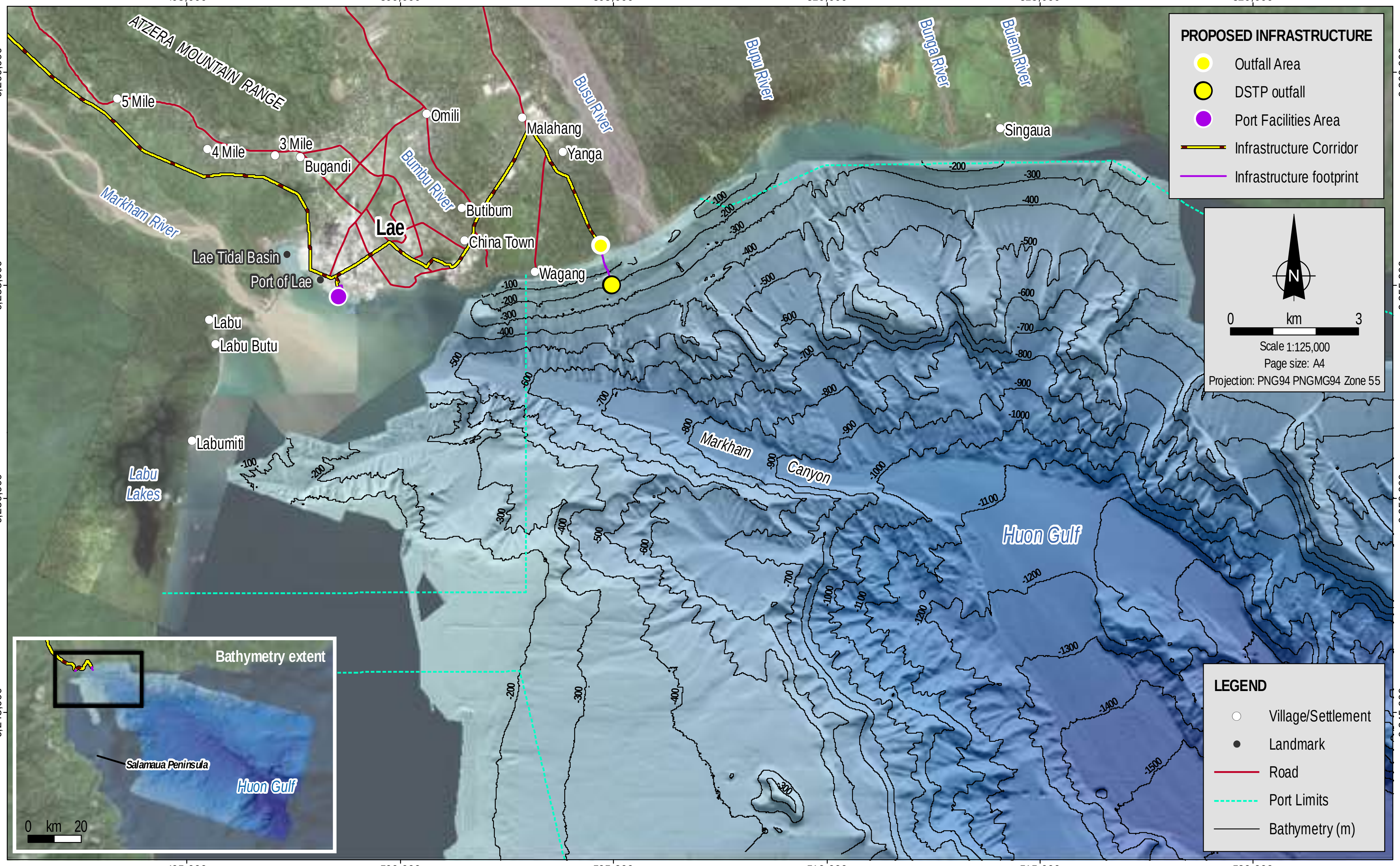

Source:
Villages/Settlements, landmarks and infrastructure from WGJV and Coffey.
Roads and Port Limits from Coffey (Port Limits indicative only).
Bathymetry from WGJV survey.
Imagery from WGJV (capture date 2016) and ArcGIS Online (capture date unknown).

coffey
A TETRA TECH COMPANY

Date: 18.01.2018
Project: 754-ENAUABTF100520DD
File Name: 0520DD_10_F11.02_GIS

WAFI-GOLPU JOINT VENTURE
Wafi-Golpu Project

Bathymetry of the western Huon Gulf

Figure No: 11.2

MXD Reference: 0520DD_10_GIS021_v0_5

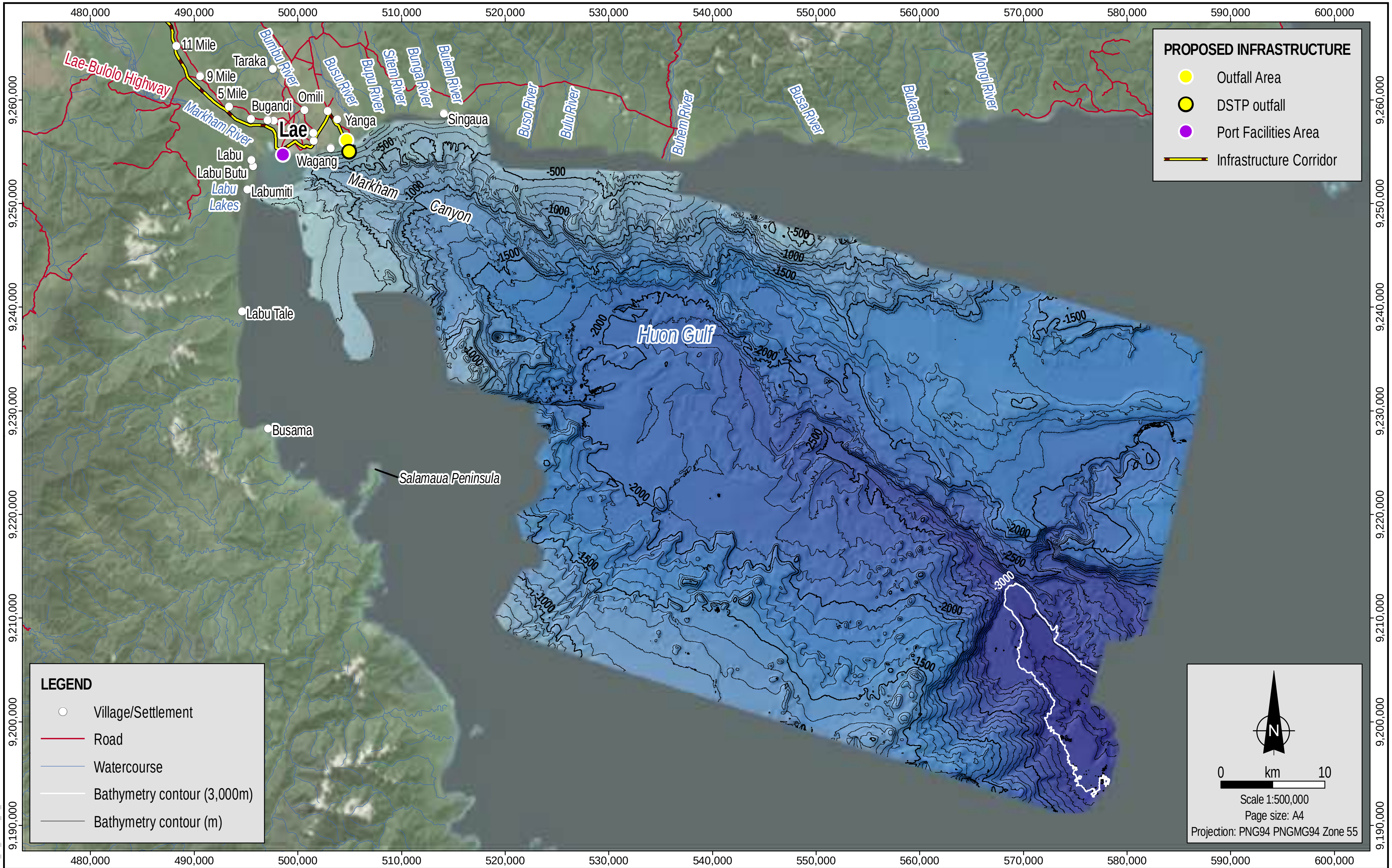

Source:
Villages/Settlements and infrastructure from WGJV and Coffey.
Roads and watercourses from NSO.
Bathymetry from WGJV survey.
Imagery from ArcGIS Online (capture date unknown).

coffey A TETRA TECH COMPANY

Date: 28.03.2018
Project: 754-ENAUABTF100520DD
File Name: 0520DD_10_F11.03_GIS

WAFI-GOLPU JOINT VENTURE

Wafi-Golpu Project

Huon Gulf deep water bathymetry to over 3,000m

Figure No: 11.3

Where the Markham Canyon emerges from the mouth of the Markham River, the floor of the canyon has a slope of approximately 6 degrees (°) for the initial 2km of the canyon, reducing to an approximately 3° slope until a depth of about 1,700m some 35km from the Markham River mouth (Appendix K, Oceanographic Investigations of the Huon Gulf). The proposed DSTP outfall is located on the north canyon wall immediately to the west of Busu River (see Figure 11.2).

The seabed in the Outfall Area is steeply sloping, with an average gradient around 20° until it reaches the Markham Canyon floor. Figure 11.4 is a three-dimensional representation of the north canyon wall showing the proposed DSTP outfall location with the Markham Canyon at the foot of the slope. Down to about 350m, the canyon wall is characterised by subparallel channels or chutes with smooth and featureless surface texture, bounded by low relief (<3m) ridges aligned perpendicular to the shoreline. Below a depth of approximately 350m, most chute channels narrow, along with an increase in the vertical relief of the bounding ridges. Numerous erosional knickpoint features (i.e., a sharp change in channel slope) occur on the lower parts of the chute channels.

Below the Outfall Area, the floor of the Markham Canyon continues its downward slope to a depth of over 3,000m, some 120km from the mouth of the Markham River (see Figure 11.3).

11.2. Upper Ocean Profiling

Profiling of the upper ocean in the Huon Gulf is a key component of the Project's oceanographic investigations.

Measurements spanning at least 12 months of the following upper ocean characteristics have been used to determine the depth of the proposed DSTP outfall in accordance with PNG's Draft General Guidelines for DSTP (SAMS, 2010a):

- Surface mixed layer depth (MLD)
- Euphotic zone thickness (EZ)
- The occurrence, or otherwise, of coastal upwelling

Mixing of surface waters primarily occurs via surface waves and wind-driven currents, and the MLD can vary diurnally and seasonally, as wind and wave conditions change. The MLD is formed through vertical mixing of waters and is defined as the lowest point where there is a near-homogeneous distribution of temperature and salinity, and little variation in temperature or density with depth (Kara et al., 2000). The MLD is usually determined either by defining a depth at which a specific temperature or density difference relative to a reference value (usually near surface) occurs, or where the density gradient exceeds a critical value. Numerous methods for determining the MLD are discussed in Appendix K, Oceanographic Investigations of the Huon Gulf. The Project has adopted the most conservative method, which estimates the deepest MLD as the depth at which the temperature is 1 degree Celsius (1°C) less than the temperature at 10m depth, as recommended by Cresswell (2001).

The euphotic zone of the ocean is the upper water layer where most photosynthesis by phytoplankton occurs, and is therefore, the zone of primary productivity. Profiling measurements of photosynthetically active radiation (PAR)[1] in the upper waters are used to estimate the base of the euphotic zone, which is defined as the depth where sunlight irradiance has diminished to 1% of levels found at the sea surface.

[1] A PAR sensor measures downwelling irradiance of sunlight through the upper ocean, over the spectral range of photosynthetically active radiation.

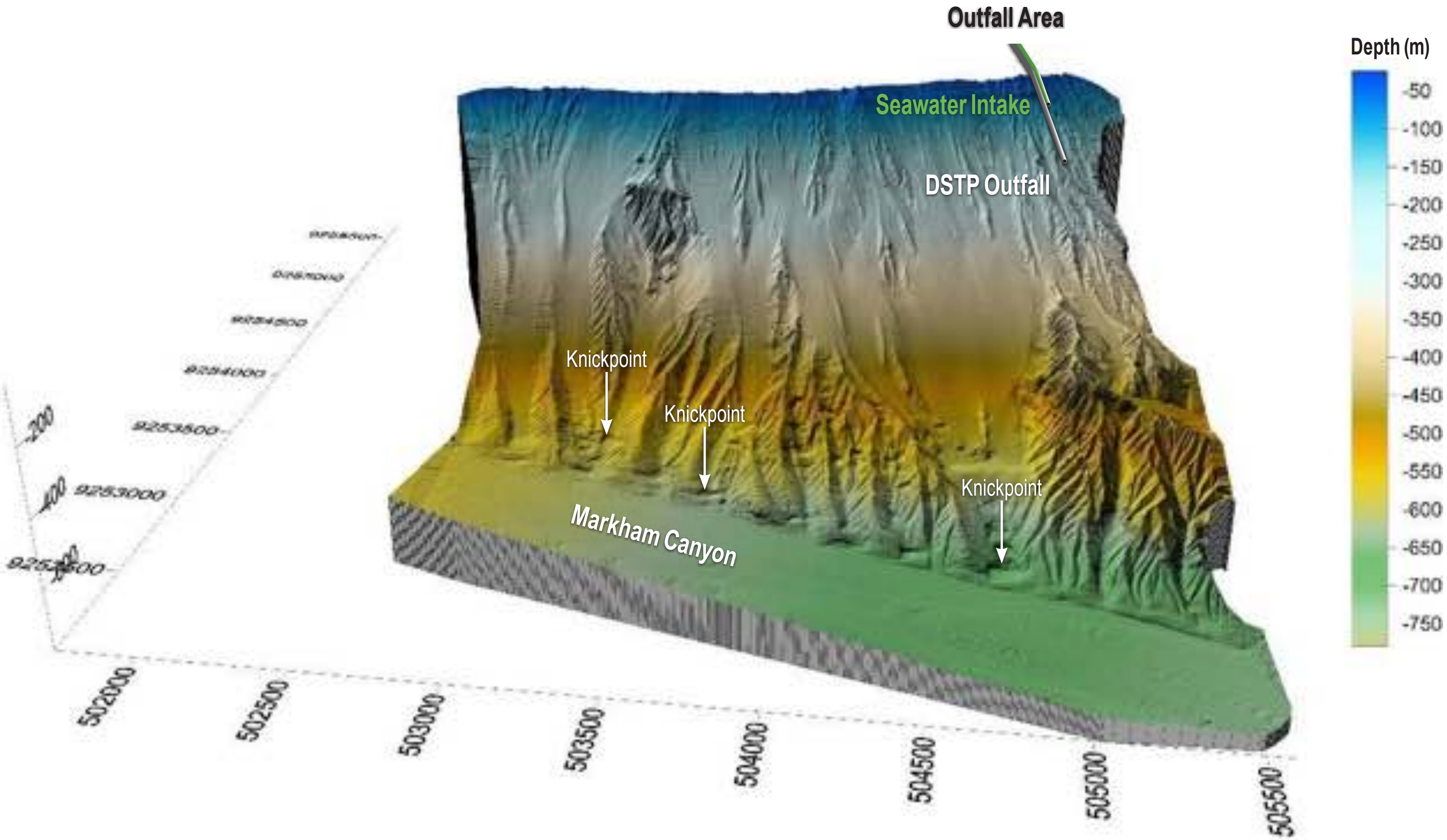

Source:
IHA Consult, 532-1104-FS-REP-0001 Rev0, Figure 2-5

coffey
A TETRA TECH COMPANY

Date: 22.05.2018
Project: 754-ENAUABTF100520DD
File Name: 0520DD_10_F11.04_GRA

WAFI-GOLPU JOINT VENTURE

Wafi-Golpu Project

Outfall Area high-resolution bathymetry

Figure No: 11.4

INDD Reference: 0520DD_10_GRA069.indd_5

Results of investigations into the occurrence, or otherwise, of coastal upwelling are described in Section 11.3.

Upper ocean profiling measurements commenced during October 2016 using a conductivity, temperature, density (CTD) instrument lowered through the ocean water column at five stations along two offshore transects (transects A and B). Transect A is to the west of the Busu River in the vicinity of the potential Outfall Area, and Transect B is to the east of the Busu River (Figure 11.5).

The CTD instrument was also equipped with a PAR sensor to determine the euphotic zone thickness, and a turbidity sensor to detect any suspended sediment plumes in the ocean water column. Profiling was undertaken at each of the ten stations at approximately fortnightly intervals from October 2016 until December 2017.

Over more than a year of measurements, the oceanographic profile data shows no obvious or persistent formation of well-mixed homogeneous surface layers, which are usually typical of PNG ocean waters (Appendix K, Oceanographic Investigations of the Huon Gulf). This may reflect the major influence of unusually high rates of freshwater inflow on the physical characteristics of the upper ocean waters of the western Huon Gulf.

Figure 11.6 (upper panel) shows the depth ranges for the surface mixed layer depths and euphotic zone thicknesses as a box and whisker plot[2] for the range of values for each set of data measured to date. Each box and whisker plot represents a different day of measurement. The surface mixed layer values are shown in blue and the euphotic zone values are shown in green.

From October 2016 to April 2017, surface MLDs were relatively shallow, ranging from 17 to 49m depth. However, over the development of the southeasterly wind season a more pronounced mixed layer deepened to a maximum observed depth of 96m during August 2017, which is more typical of what has been measured at other DSTP sites in PNG. Profiling between August and December 2017 showed a variable MLD of between 18 to 78m.

Over the same period, the base of the euphotic zone varied from 5 to 60m, which is shallower relative to other DSTP sites in PNG as a result of the large riverine sediment input to the western Huon Gulf.

Figure 11.6 (lower panel) presents box and whisker plots for each station with values showing the range of measurements obtained over the duration of profiling. There is a clear relationship of increasingly deeper euphotic zone thickness from inshore to offshore along both CTD transects, almost certainly reflecting the influence of nearshore surface buoyant plumes of suspended sediment from river inflows into the gulf. Conversely, the surface mixed layer depths show no consistent spatial variation between nearshore and offshore sites.

[2] For a box and whisker plot, the caps or whiskers at the end of each box indicate the minimum and maximum values. The box is defined by the lower 25% and upper 75% quartiles, and the horizontal line within the box is the median value whereas an “x” represents the mean value.

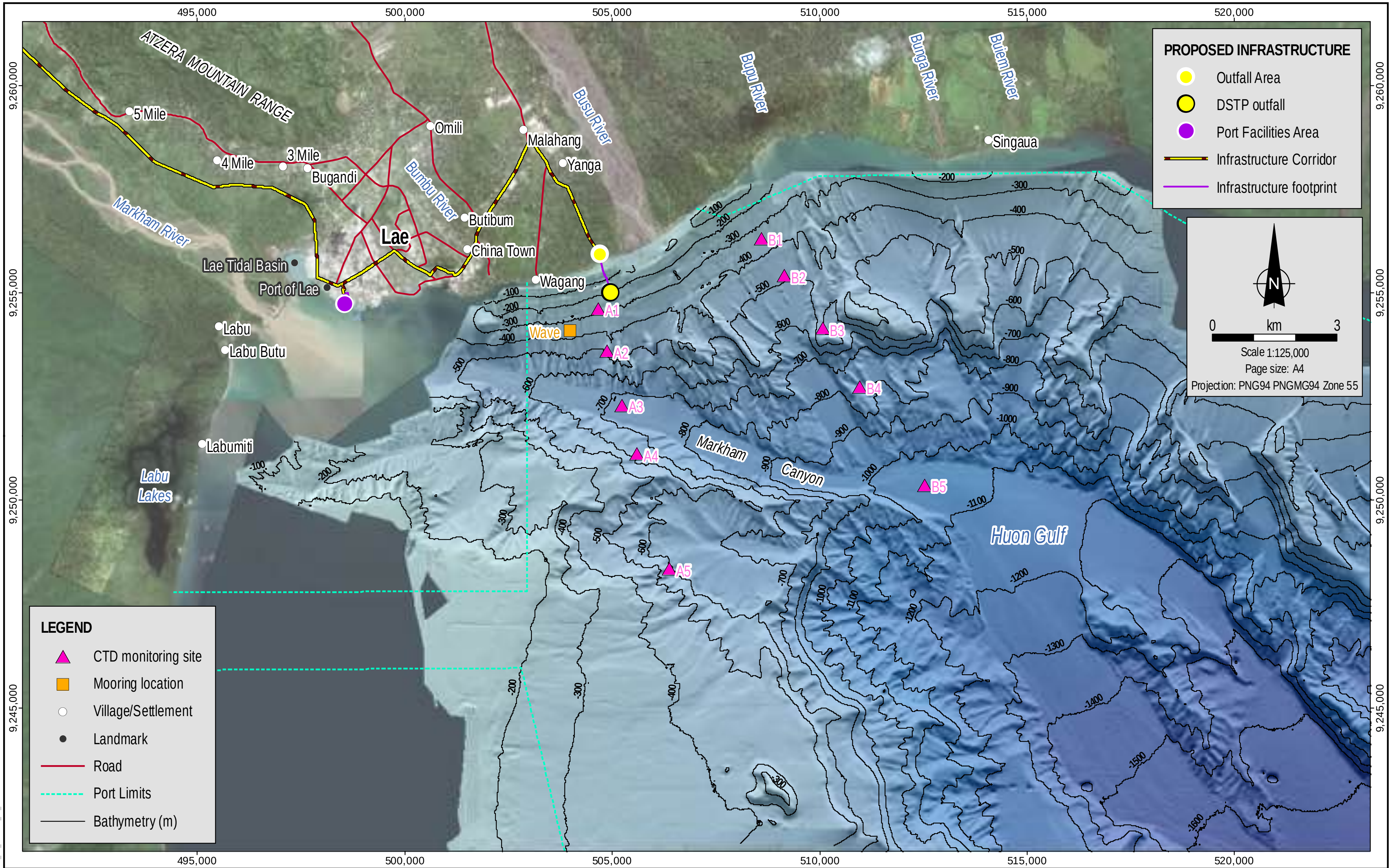

Source:
CTD monitoring sites, mooring locations, roads and Port Limits from Coffey (Port Limits indicative only).
Villages/Settlements, landmarks and infrastructure from WGJV and Coffey.
Bathymetry from WGJV survey.
Imagery from WGJV (capture date 2016) and ArcGIS Online (capture date unknown).

coffey
A TETRA TECH COMPANY

Date: 07.02.2018
Project: 754-ENAUABTF100520DD
File Name: 0520DD_10_F11.05_GIS

WAFI-GOLPU JOINT VENTURE

Wafi-Golpu Project

Upper ocean profiling locations

Figure No: 11.5

MXD Reference: 0520DD_10_GIS034_v0_3

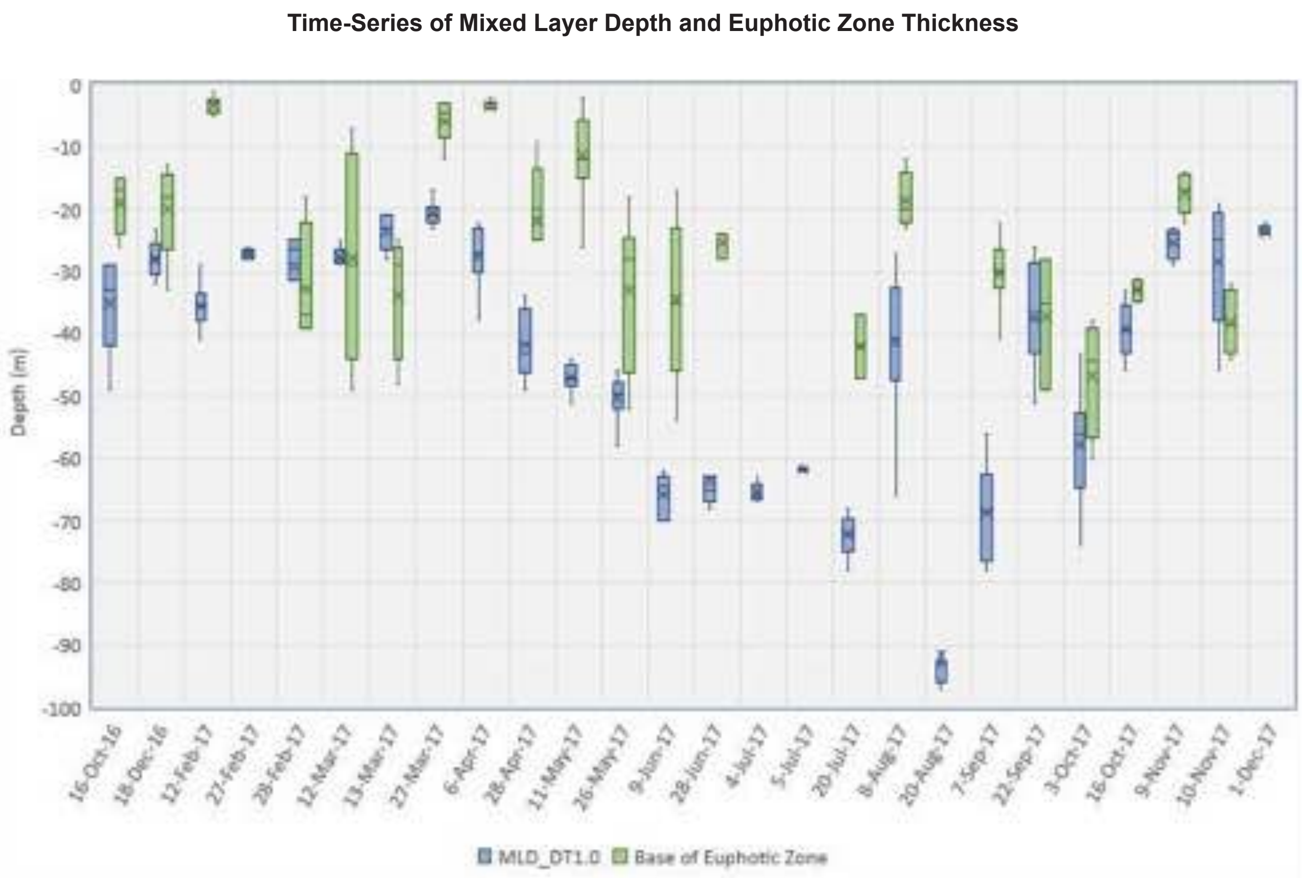

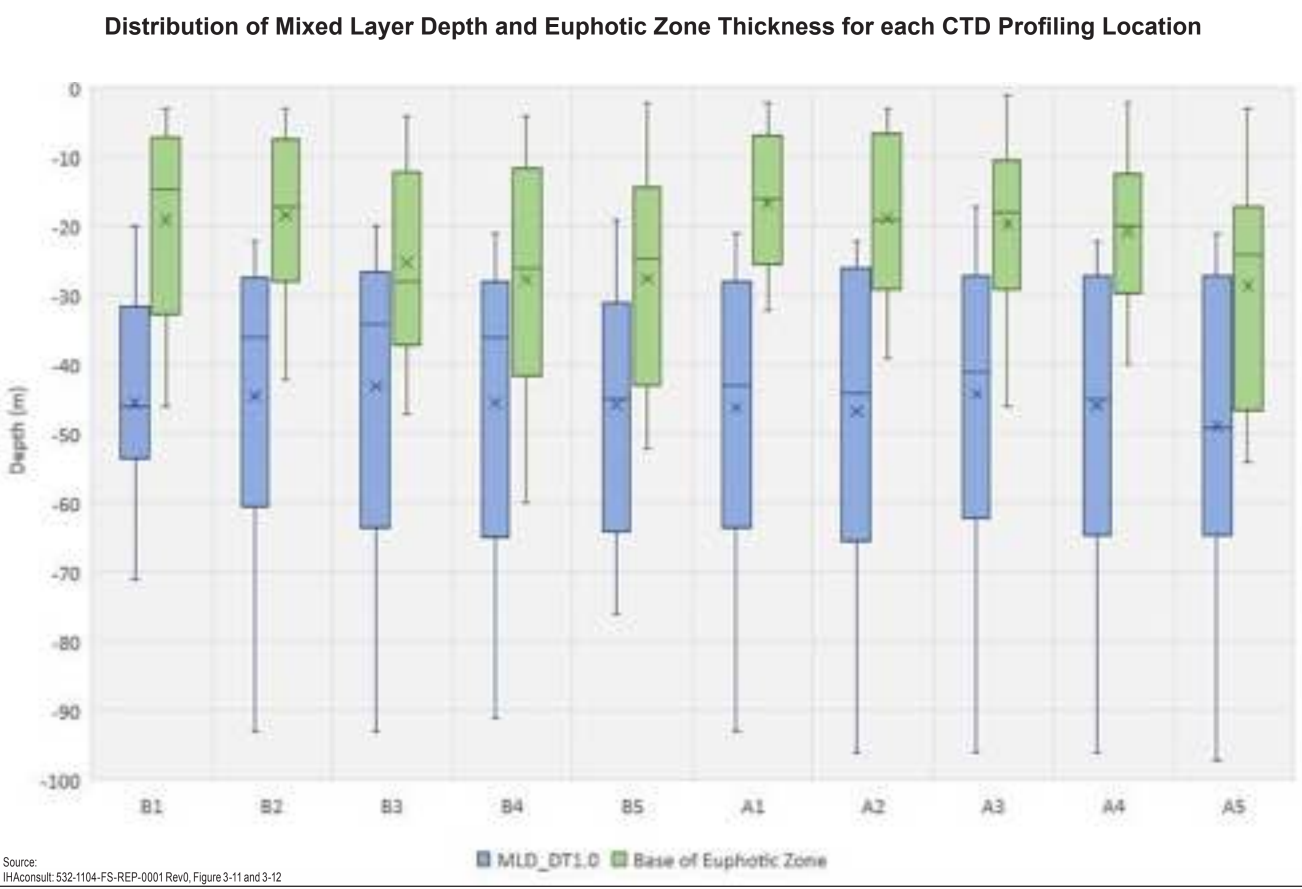

Source:
IHAconsult: 532-1104-FS-REP-0001 Rev0, Figure 3-11 and 3-12

INDD Reference: 0520DD_10_GRA055.indd_4

coffey
A TETRA TECH COMPANY

Date: 05.02.2018
Project: 754-ENAUABTF100520DD
File Name: 0520DD_10_F11.06_GRA

WAFI-GOLPU JOINT VENTURE

Wafi-Golpu Project

Surface mixed layer depth and euphotic zone thickness measured to date

Figure No: 11.6

11.3. Potential for Coastal Upwelling

Coastal upwelling occurs when a drift current transports water away from the coast, and is replaced by water from deeper layers under the influence of the pressure gradient that develops. Within the Huon Gulf (approximately latitude 7°S), upwelling could possibly occur along the west to east coastline to the east of Lae under the influence of winds with a strong and persistent easterly component, or along the north to south coastline to the south of Lae under the influence of persistent northerly winds.

A specialist review by Cresswell (2012) of the physical oceanography of the Huon Gulf included consideration of the likelihood for coastal upwelling to occur. Cresswell assessed wind stresses[3], satellite sea surface temperature (SST) imagery, and unpublished CSIRO cruise data. The dominant wind direction during the southeasterly trade wind season crosses the north coast of the gulf at an angle of about 55°. Estimated wind stress values resolved to be parallel to the west-east coastline of the Huon Gulf are mostly less than 0.025 Newton per square metre (N/m^2). A study off western New Caledonia, using the same wind stress dataset, found that wind stress values of $0.1N/m^2$ (i.e., four times higher) were required to drive coastal upwelling (Henin and Cresswell, 2005). Therefore, wind stress values in the Huon Gulf were considered to be probably too low to drive coastal upwelling (Appendix K, Oceanographic Investigations of the Huon Gulf).

Further to this, Cresswell (2012) reviewed satellite SST images, and for the southeasterly trade wind season the images showed no evidence of upwelling in the Huon Gulf. Cloud cover obscured most of the available SST images for the northwest wind season. However, one image for this season did show a cool structure in the surface waters of the gulf, but without simultaneous *in situ* measurements Cresswell was unable to assess its source.

Cresswell (2012) suggested that to determine unambiguously if and when upwelling occurs, and from what depth, a program of current and temperature measurement with moored instruments, combined with regular CTD transects perpendicular to the shoreline, would be required.

To address the Cresswell (2012) recommendation, all temperature data from the CTD transects described in the previous section were individually gridded in the Y-Z plane for each day of profile measurement, and contours of temperature, salinity and density were examined for any influence of coastal upwelling processes. Coastal upwelling, if it occurs, typically results in isotherms[4] curving upwards close to shore, as deeper and cooler water upwells.

Figure 11.7 shows examples of temperature profiles from transects A and B during February, July and August 2017, and indicates no evidence of upward incursion of colder water near the shore (on the left side of each temperature profile). Appendix K, Oceanographic Investigations of the Huon Gulf, contains cross sections for CTD transects undertaken between 15 August 2016 until 3 October 2017 and none shows any evidence of upwelling occurring along the shoreline of the Huon Gulf immediately to the east and west of the Busu River (i.e., including the Outfall Area).

---

[3] Derived from a global grid dataset of wind stress records, covering the period from 1982 to 2005.

[4] Contours of equal temperature.

Transect A

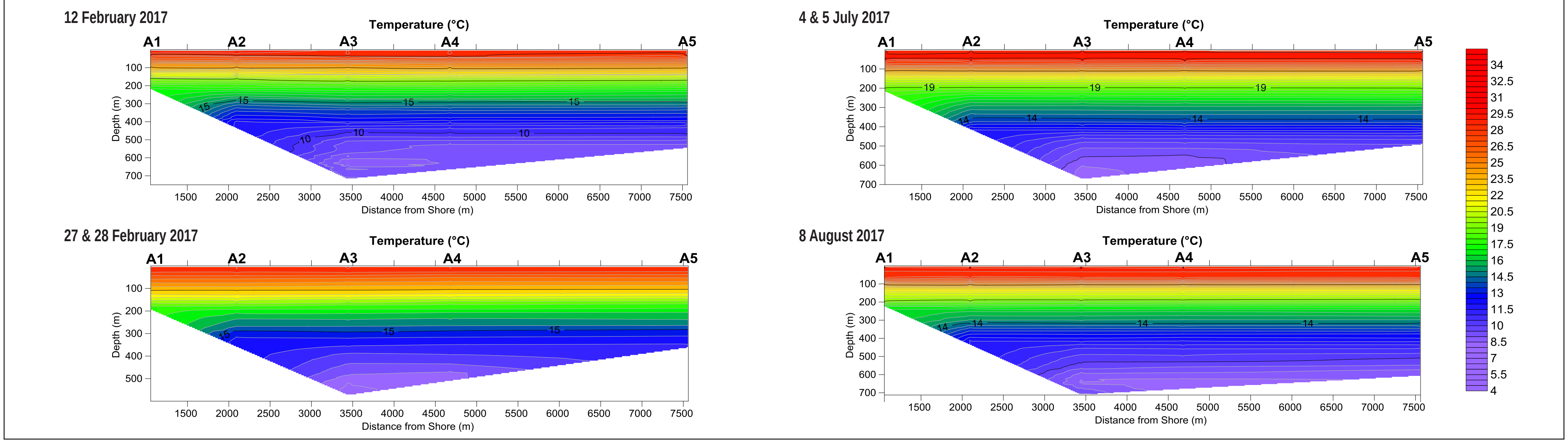

Transect B

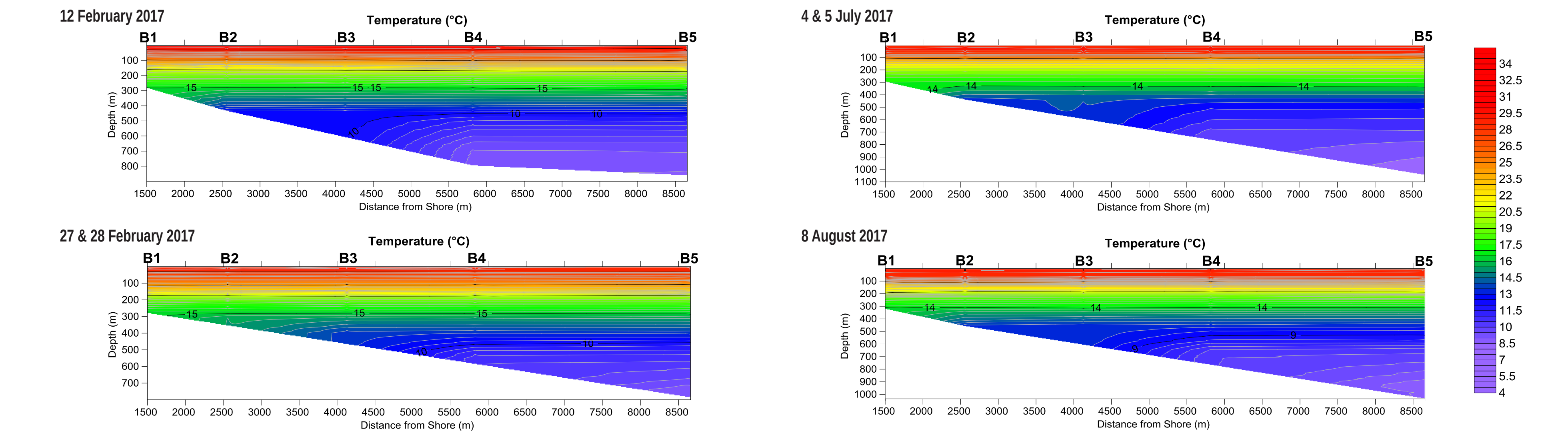

Source:
IHAconsult: 532-1104-FS-REP-0001 Rev0

coffey
A TETRA TECH COMPANY

Date: 22.05.2018
Project: 754-ENAUABTF100520DD
File Name: 0520DD_10_F11.07_GRA

WAFI-GOLPU JOINT VENTURE

Wafi-Golpu Project

Temperature profiles at transects A and B from February, July and August 2017

Figure No: 11.7

INDD Reference: 0520DD_10_GRA056.indd 4

The possible occurrence of upwelling was further investigated by placing data loggers fitted with temperature and pressure sensors along the Wave Mooring located to the west of the Busu River (Figure 11.5) in water depth of 350m and near the proposed DSTP outfall location. The temperature and pressure data loggers were set on the mooring string to be at nominal depths of 60, 150 and 225m depth, but the actual depth for the sensors varied slightly between deployments and is dependent on where the mooring for each deployment was placed on the steep canyon wall.

If coastal upwelling were to occur, then the water column close to shore at the Wave Mooring should show cooler temperatures over a sustained period of days to weeks.

While the temperature sensors were not installed until March 2017, the six months of temperature data as presented in Appendix K, Oceanographic Investigations of the Huon Gulf, shows:

- The maximum variability at each measurement depth is over the range of about 2 to 3°C for each of the deployments.
- There is no evidence of cooler water rising from the deepest to shallowest depths in any of the temperature recordings.
- There is no overlap in temperatures from the deep, mid water and shallow recording depths as would be expected if coastal upwelling was occurring.

The current meter deployed at the Outfall A Mooring for over 12 months also recorded vertical currents, and if upwelling were to occur then sustained periods of upward flow through the water column would likely be apparent. In general, the vertical current speeds (both upwards and downwards) were low and ranged from 1 to 2 centimetres per second (cm/s). From the surface waters to at least 150m water depth, diel migrations have been recorded, but these do not represent vertical motions of water but rather the movement of zooplankton as recorded by the echo returns from the Acoustic Doppler Current Profiler (ADCP) pings. In the lower part of the water column, most ADCP-measured vertical velocities were downwards, probably representing settling of sediment towards the bed.

Hence it can be concluded from the results of Cresswell (2012), the year-long CTD transect data collected either side of the proposed DSTP outfall, the thermistor string data at the Wave Mooring and the year-long ocean vertical current measurements at the Outfall A mooring that there is no evidence from the data analysed of coastal upwelling in the vicinity of the proposed DSTP outfall.

11.4. Ocean Currents

11.4.1. Ocean Current Data Collection

A program of ocean current data collection was undertaken at numerous sites in the Huon Gulf spanning a period of at least 12 months in accordance with PNG's Draft General Guidelines for DSTP (SAMS, 2010a).

The current measurements have been used both to describe the circulation patterns within the Huon Gulf and also to calibrate the currents simulated by three-dimensional hydrodynamic modelling that has been developed to predict DSTP plume dispersion and deposition of tailing solids.

Ocean current measurement commenced in October 2016 and continued until November 2017. This involved the initial deployment of oceanographic mooring arrays using upward and downward facing ADCP (Appendix K, Oceanographic Investigations of the Huon Gulf).

Since October 2016, ocean current measurements have been conducted at a total of eight sites (Figure 11.8), and include current velocity measurements which are discussed below, from the following general areas:

- On the north wall of the Markham Canyon near the proposed DSTP outfall location
- From within the Markham Canyon, including close to the seafloor
- From the wider Huon Gulf (not within the Markham Canyon)

11.4.2. Ocean Floor Mass Movement Events

Both the Canyon and Basin moorings located on the floor of the Markham Canyon were affected by periodic, highly energetic mass movement events along the floor of the canyon, that have caused the down-canyon displacement and relocation of the mooring strings some 2 to 15km from their original deployment locations. The mass movement events were accompanied by very high turbidities in the near-bed flow and are interpreted to have been caused by submarine slope failures along the sidewalls of the Markham Canyon leading to the formation of turbidity current[5] events that transport a high sediment load through the Markham Canyon towards the deeper waters of the New Britain Trench.

The rationale for the multiple current meter measurement sites in Figure 11.8 (Canyon A, B and C and Basin A and B) was a number of high-energy mass movement events that displaced the canyon and basin moorings downslope. The current measuring arrays were initially deployed at three locations: one at Outfall in 300m depth below the proposed DSTP Outfall, the second at Canyon A in 830m water depth on the Markham Canyon floor, and the third at Basin A, in about 1,660m water depth, further down the canyon. However, both the canyon and basin moorings were significantly affected by episodic but highly energetic turbidity current flow events along the floor of the canyon that, in the first instance, sheared the Canyon A array from its anchor and displaced the entire Basin A mooring, together with its anchor, some 15km further down the canyon.

Following this event the focus was changed to measurement of near-bed currents and both the canyon and basin moorings were relocated. New moorings were established at the Far Field mooring at 2,100m water depth, located on a berm about 150m above the canyon floor, and a Trench mooring (which did not collect near-bed current data during the current campaign) located approximately 85km to the southeast of the DSTP Outfall in 3,270m water depth.

Over the year-long period of measurement, five major turbidity current events (8 January 2017, 3 June 2017, 1 August 2017, 2 September 2017 and 15 November 2017) and a number of lesser magnitude mass flow events were measured at various moorings.

The speed of the front of each of the major turbidity current events has been estimated by extracting the time that high current speeds were first recorded at two locations and measuring the distance along the canyon thalweg, as is summarised in Table 11.1. The speed estimates are high, varying from 1.6 to 8.4 metres per second (m/s) (3.1 to 16.3 knots (kn)) and have the capacity to entrain and transport large quantities of sediment, and likely account for the scoured appearance of the canyon floor and the coarse material on its bed.

[5] A turbidity current is the coherent movement of a mixture of seawater and suspended solids which, due to the high suspended solids concentration entrained in the mixture, is denser than the surrounding seawater. This density differential causes the density current to flow along the seafloor as a bottom-attached flow.

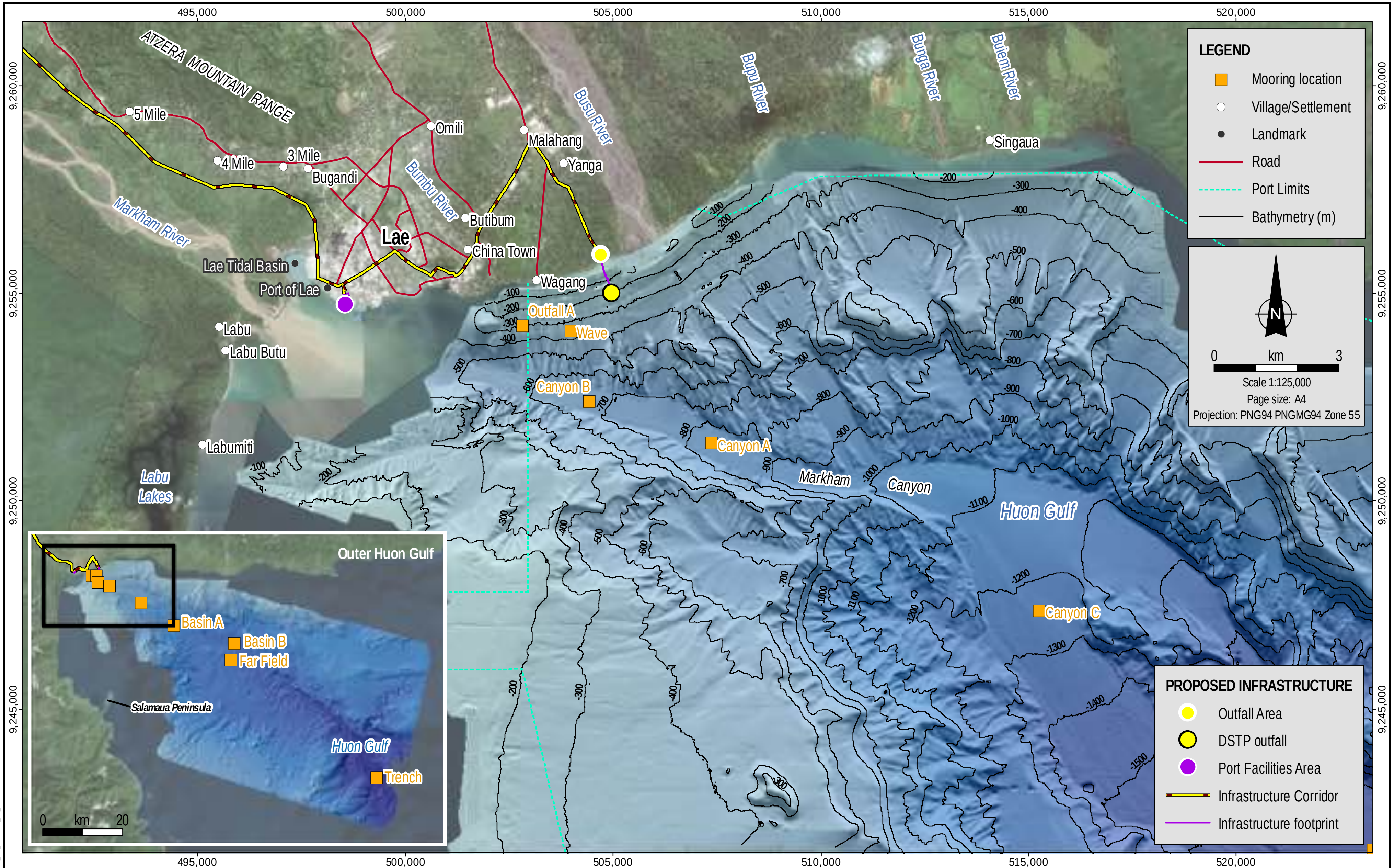

Source:
Mooring sites, roads and Port Limits from Coffey (Port Limits indicative only).
Villages/Settlements, landmarks and infrastructure from WGJV and Coffey.
Bathymetry from WGJV survey.
Imagery from WGJV (capture date 2016) and ArcGIS Online (capture date unknown).

coffey
A TETRA TECH COMPANY

Date: 26.03.2018
Project: 754-ENAUABTF100520DD
File Name: 0520DD_10_F11.08_GIS

WAFI-GOLPU JOINT VENTURE

Wafi-Golpu Project

Huon Gulf ADCP oceanographic instrument mooring locations

Figure No: 11.8

MXD Reference: 0520DD_10_GIS035_v0_5

Table 11.1: Estimated Speed of Turbidity Current Fronts

Date	Canyon Section	Time of Travel (min)	Distance (km)	Estimated Turbidity Current Speed (m/s)
8 Jan 17	Canyon A to Basin A	40	18.7	7.8
3 Jun 17	Canyon B to Basin B	87	43.9	8.4
1 Aug 17	Canyon C to Basin B	302	32.8	1.8
2 Sep 17	Canyon C to Basin B	188	32.6	2.9
15 Nov 17	Canyon C to Basin B	345	32.6	1.6

11.4.3. Outfall A Currents

Current measurements from the Outfall A mooring indicate that current speeds were low, with maximum values approaching 0.20 to 0.25m/s (less than 0.5kn), though most speed values were considerably lower. Current direction oscillated at tidal frequencies, but through the water column showed complex patterns of current shearing that varied over time. Close to the bed, over the lowest 5 to 7m, current velocities were turbulent and omni-directional, reflecting frictional effects of the interaction of current flows with the bed.

Net current flows were mostly parallel to the shoreline, and mostly to the northeast. An exception was for near-bed flow, which tended to exhibit a weak net current drift oriented offshore to the south.

Continuous vector plots indicate some mid-water current velocities, occurring over the 260 to 293m depth range (dependent on deployment), had net drift currents oriented inshore to the north. The drift currents were very weak with mean values in the range of 0.002 to 0.003m/s. However, continuous vector plots at levels above the depth of inshore flow had differing directions, and were broadly parallel to the shoreline, indicating the net current flow to north at the mooring location is not a thick layer of inshore flow with association to upslope flow. The most pronounced northward flow at the mooring occurred at a depth of 260m during the period of the fourth deployment, over May to June 2017. Currents at 244m depth, just 14m above the northward flow, were directed to the northeast parallel to the shoreline. Vertical velocities recorded at 260m depth, and indeed the entire water column, showed no evidence for sustained upward flow.

There is no apparent trend suggesting seasonality in the current velocity distributions at the Outfall A location.

11.4.4. Canyon Mooring Currents

11.4.4.1. Mid-Water Currents

The initial Canyon A mooring location was located on the canyon floor, to the east of the Busu River mouth, in a water depth of 815m. The upward facing current meter measured current velocities over a depth range from 765m to 141m. Similar to the Outfall Mooring data, current speeds were low with maximum speeds rarely attaining 0.25m/s (~0.5kn), and mostly much lower than 0.10m/s. Current directions oscillated at tidal frequency, and a complex pattern of current shearing occurred through the water profile with similarity to the mid and upper water profile at the Outfall Mooring. The deepest measured currents, at an altitude of 55m above the bed (765m depth), had a net flow up-canyon to the northwest, with a net current speed of 0.03m/s, as did currents 64m higher in the water column, but at about half the net current speed. Higher in the water column current velocities were more variable with tidal oscillations and variable current drift patterns, resulting from the current shearing at different water depths.

The dominance of up-canyon flow in the mid-water was noted and was different to the preponderance of down-canyon flow for the near-bed currents. The up-canyon flow may represent a replacement current to balance the overall displacement of water through the canyon. This up canyon flow did not affect the likelihood of upwelling near the proposed outfall location as described in Section 11.3.

11.4.4.2. Near-Bed Currents

Following redeployment of the Canyon B Mooring to the west of the Busu River mouth and throughout May 2017, the measured near-bed currents in the lowest depth from 2 to 20m above the bed showed a dominant flow aligned down-canyon, with multiple short period current bursts in excess of 0.8m/s (>1.6kn). Currents had greater velocity towards the bed and showed near-continuous down-canyon flow and persistently high turbidities. This period of record was affected by another major mass movement event on 3 June 2017 when the mooring was displaced some 15km down-canyon. Prior to this event, five separate turbidity current events occurred and resulted in small displacements of the mooring along the floor of the canyon.

Following the large displacement of the Canyon B Mooring on 3 June 2017, the mooring was then relocated down-canyon and approximately adjacent to where the mooring came to rest, but positioned more centrally on the canyon floor at the Canyon C Mooring location. As for the previous deployment, the current speed record was characterised by short term current bursts; the record contained 10 current bursts where speeds exceeded 0.5m/s (~1kn). Current directions oscillated at tidal frequency with dominance of up- and down-canyon flow, especially just above the seafloor. The current burst peaks were all directed down-canyon again supporting their association to the passage of turbidity current events.

For the deployment completed at Canyon C in September 2017, there was one distinct current burst on 2 September 2017, which displaced the location of the mooring again to the northern margin of the canyon. Prior to this event, current velocities were represented by low speed tidal oscillations, typical of conditions in the central region of the canyon floor. Otherwise current speeds were very low, and less than 0.15m/s.

The current speed record from the last deployment completed at Canyon C in November 2017 contains several short-term current bursts, as for previous deployments, with the maximum recorded peak current speed of 1.2m/s (2.3kn) on 15 November 2017. The ancillary pressure and temperature records indicate the mooring was stationary over these current burst events.

Figure 11.9 presents a compilation of the near-bed current speed records from Canyon B and C moorings from May to September 2017, which highlights the frequent bursts of current speeds described above. At the Canyon B location, frequent current bursts above 0.8m/s preceded the mass movement event of 3 June that displaced the Canyon B mooring some 15km down-canyon to the Canyon C location. At the Canyon C location, background currents were generally below 0.2m/s, but nine current bursts exceeding 0.8m/s were recorded up to 2 November. Of these, the bursts on 19 July, 31 July and 2 September 2017 were strong enough to cause further movement of the mooring, although not to the extent of the January 8 and June 3 occasions.

Canyon B

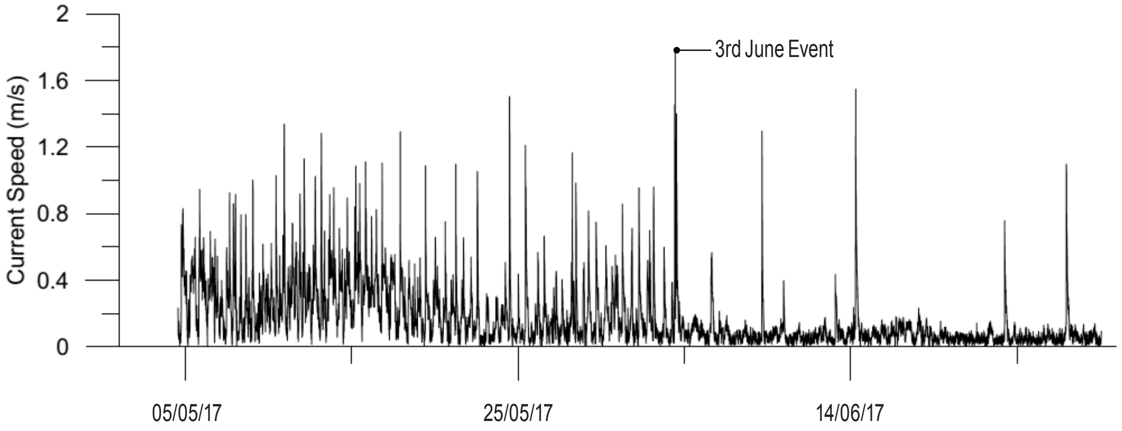

Canyon C

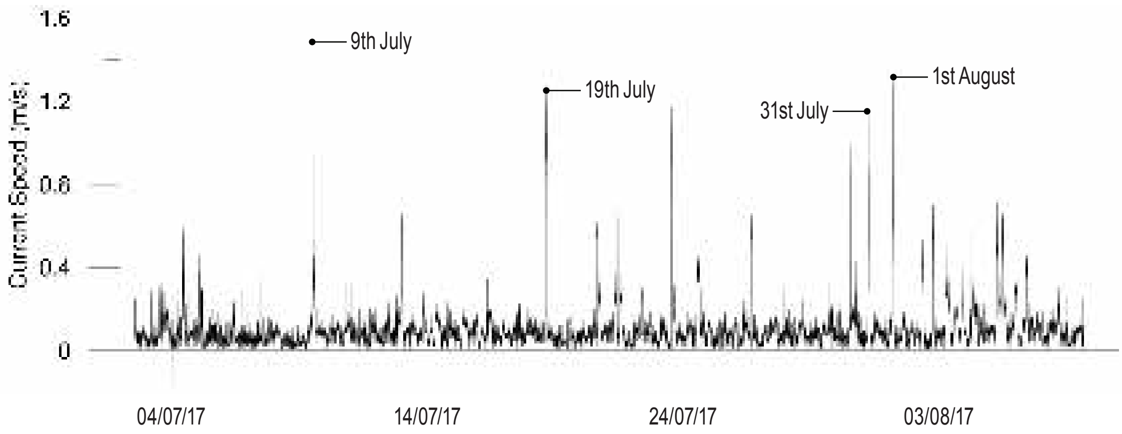

Canyon C

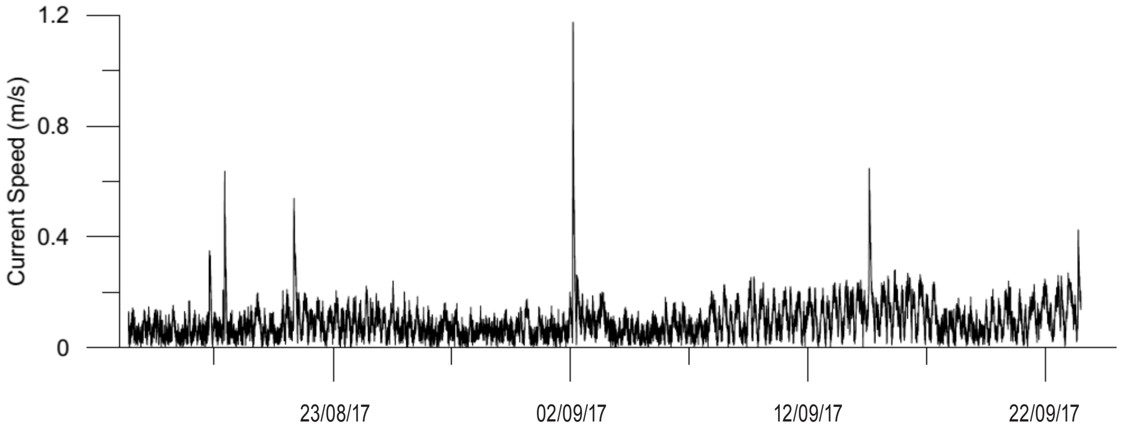

Source:
IHAconsult: 532-1104-FS-REP-0001 Rev0

Near-bed current speeds at Canyon B and Canyon C moorings from May to September 2017

11.4.4.3. Basin Mooring Currents

The Basin Mooring current measurements at the initial location of Basin A showed background currents with low speeds interspersed with short period current bursts, with the strongest burst occurring over a 4-hour period with a peak speed of 1.6m/s (~3.1kn). Currents were stronger towards the bed and the burst velocities were oriented down-canyon, and are interpreted to represent the passage of turbidity current events.

The subsequent Basin Mooring deployment at the Basin B location, at least for the period leading up to the 3 June 2017 event, again showed low velocity background currents with intermittent current bursts. Since 3 June 2017, turbidity current events occurred on 8 July, 19 July, 1 August, 2 September, and 15 November 2017. Some events have also been recorded at either the Canyon C or Basin B locations, indicating multiple sources of seabed instability initiating mass movement events with the potential to generate turbidity currents.

11.4.4.4. Far-Field Currents

The Far-Field Mooring was established during May 2017, and was located on a slightly raised region of the seabed at about 2,200m depth, to the south of the Basin B location and located about 200m shallower than the Basin B Mooring. Current velocities were characterised by tidally reversing currents with speeds mostly less than 0.12m/s. Near the bed, current velocities had a pronounced southerly component, with greater current speeds closer to the bed, which is possibly indicative of bed or near-bed transport of sediment.

11.5. Terrestrial Sediment Supply

Along the 75km of coast to the east of Lae, 11 major rivers drain a total catchment area of 4,100km^2, which are shown in Figure 11.10. These rivers discharge large quantities of fluvial sediments to the Huon Gulf. The Markham River is the fourth largest river in PNG; with a catchment area of 12,600km^2. The catchment drains the Watut and Bulolo river basins, and the Finisterre Range to the north of the Markham Valley. Other rivers discharging to the north shoreline of the Huon Gulf drain the steep and rugged topography of the Finisterre Range.

The annual suspended sediment load from the Markham River, transported directly to the head of the Markham Canyon, has been estimated as 12Mtpa by Renagi et al. (2010), based on a 6-week intensive sampling campaign during 2007, where both river discharge and suspended sediment concentrations were measured. The results were then extrapolated over a one-year period through the consideration of rainfall measurements through the Markham River catchment (personal communication Renagi, 2017).

Milliman (1995) examined the sediment load from 280 rivers across the globe discharging to the ocean and found that sediment loads are a log-linear function of basin area and maximum catchment elevation. Individual algorithms were developed for application to the Oceania region (including PNG), for categories of catchment elevations greater than 3,000m (High Mountain), 1,000 to 3,000m (Mountain), and 500 to 1,000m (Upland). Applying these algorithms to the catchments of each of the 11 rivers draining the Finisterre Range into the Huon Gulf resulted in an estimated total sediment load of 48.7Mtpa from a combined catchment area of 4,100km^2.

Combining the estimates of Renagi et al. (2010) for the Markham River and Milliman (1995) for the remaining rivers gives an estimated suspended sediment discharge to the Huon Gulf in the order of 60Mtpa. This excludes the contribution to the total load from bed sediment transport.

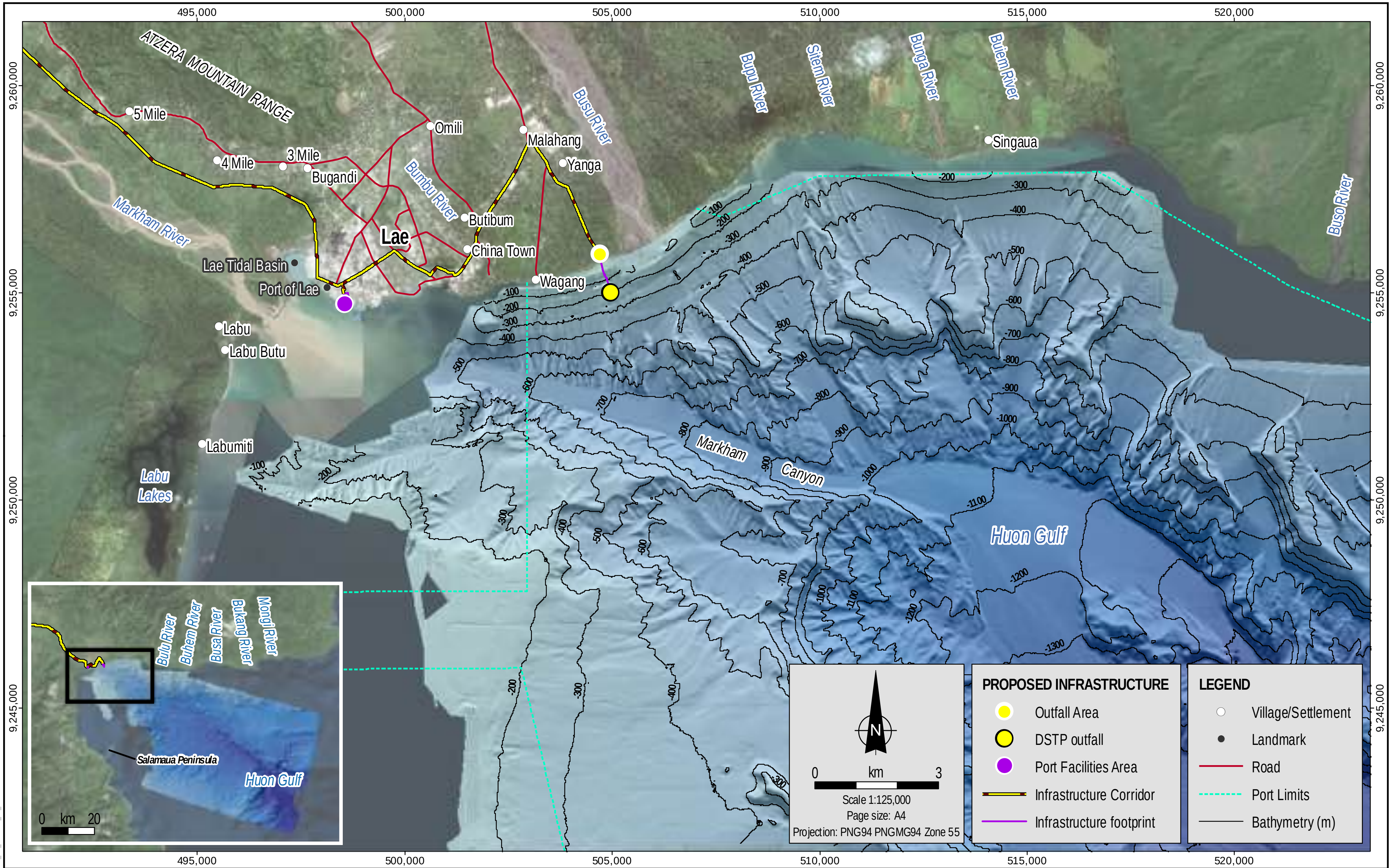

Source:
Villages/Settlements, landmarks and infrastructure from WGJV and Coffey.
Roads and Port Limits from Coffey (Port Limits indicative only).
Bathymetry from WGJV survey.
Imagery from WGJV (capture date 2016) and ArcGIS Online (capture date unknown).

coffey
A TETRA TECH COMPANY

Date: 16.02.2018
Project: 754-ENAUABTF100520DD
File Name: 0520DD_10_F11.10_GIS

WAFI-GOLPU JOINT VENTURE

Wafi-Golpu Project

Rivers draining to the northern shoreline of the Huon Gulf

Figure No: 11.10

MXD Reference: 0520DD_10_GIS036_v0_3

Further estimated annual suspended sediment loads are provided from two sets of data collected from the Markham River between 2011 and 2017, and from the Busu River between October 2016 and September 2017 (Table 11.2) (Appendix M, Physical, Chemical and Biological Sedimentology of the Huon Gulf). These annual estimates of TSS loads are based on measurements of mean flow, mean TSS concentrations and daily TSS loads. These annual estimates are approximately consistent with the overall estimate for suspended sediment input to the Huon Gulf of around 60Mtpa and are considered conservative, particularly as this data set does not include the contributions from 10 other rivers on the north coast.

Table 11.2: Estimated suspended sediment load for the Markham and Busu rivers

Period	Mean Flow (m^3/s)	Mean TSS (mg/L)	Mean Daily Load (t/d)	Estimated Annual Load (Mtpa)
Markham River				
2011-2015	503	1,164	50,800	18.6
2016-2017	545	2,492	117,970	43.1
Busu River				
October 2016 to September 2017	105	1,103	12,300	4.5

N.B: The difference in mean TSS values and estimated annual load between the two sampling periods is attributed to the results gained via the use of optical backscatter measurement methods in the 2011-2015 estimate, compared to the implementation of acoustic backscatter measurement methods in the 2016-2017 period. Acoustic backscatter measurement is recognised as a superior measurement technique.

11.6. Sediment Transport Through the Markham Canyon

The natural distribution, transport, settling and redistribution of suspended sediment through the Markham Canyon has been investigated by GDA Consult Pty Ltd and IHAconsult (Appendix M, Physical, Chemical and Biological Sedimentology of the Huon Gulf) using a combination of CTD profiling instruments fitted with an auxiliary nephelometry sensor, moored nephelometers, and moored sediment traps on the ADCP current monitoring arrays (see Figure 11.8 for locations).

Turbidity profiles measured at two CTD locations, A3 and B5 (see Figure 11.5), directly above the floor of the Markham Canyon at water depths of 720m and 1,050m, respectively, are presented in Figure 11.11 (for A3) and Figure 11.12 (for B5). Each plot shows turbidity profiles measured over a 12-month period that have been superimposed and presented on a linear scale (left panel) and on a logarithmic scale (right panel) to better illustrate the low values through most of the water column. The turbidity profiles at each location show low values of mostly less than one formazin turbidity unit[6] in the water column, typically until about 250m above the canyon bed where turbidity gradients increase markedly.

[6] Formazin turbidity units are roughly equivalent to nephelometric turbidity units (US Geological Survey, 2006). These are both measures of turbidity but use different wavelengths of light.

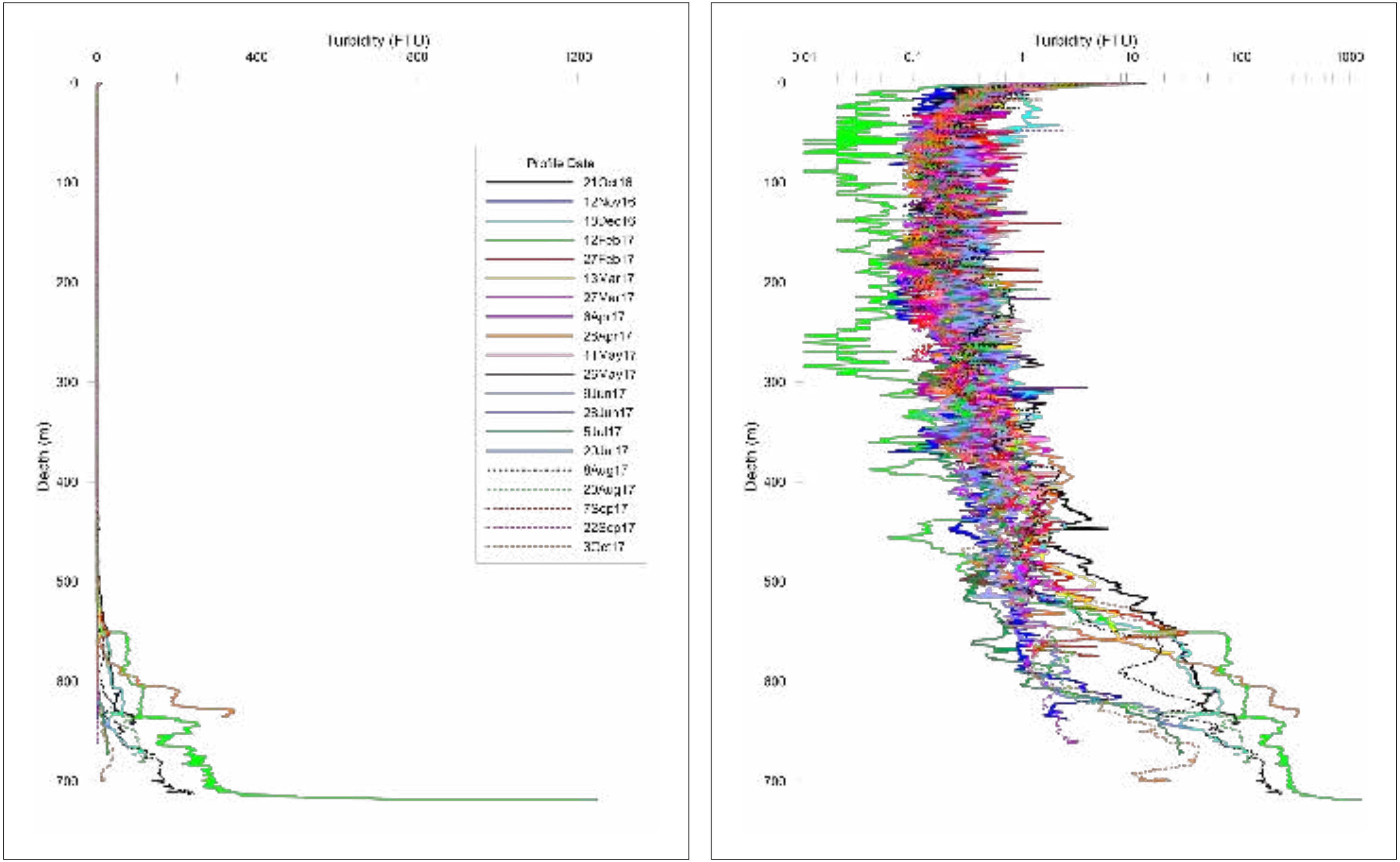

Source:
IHAconsult: 532-1104-FS-REP-0003 Sedimentology_Rev B-2_8, Figure 4-7

coffey
A TETRA TECH COMPANY

Date: 16.02.2018
Project: 754-ENAUABTF100520DD
File Name: 0520DD_10_F11.11_GRA

WAFI-GOLPU JOINT VENTURE

Wafi-Golpu Project

Turbidity profiles from CTD location A3

Figure No: 11.11

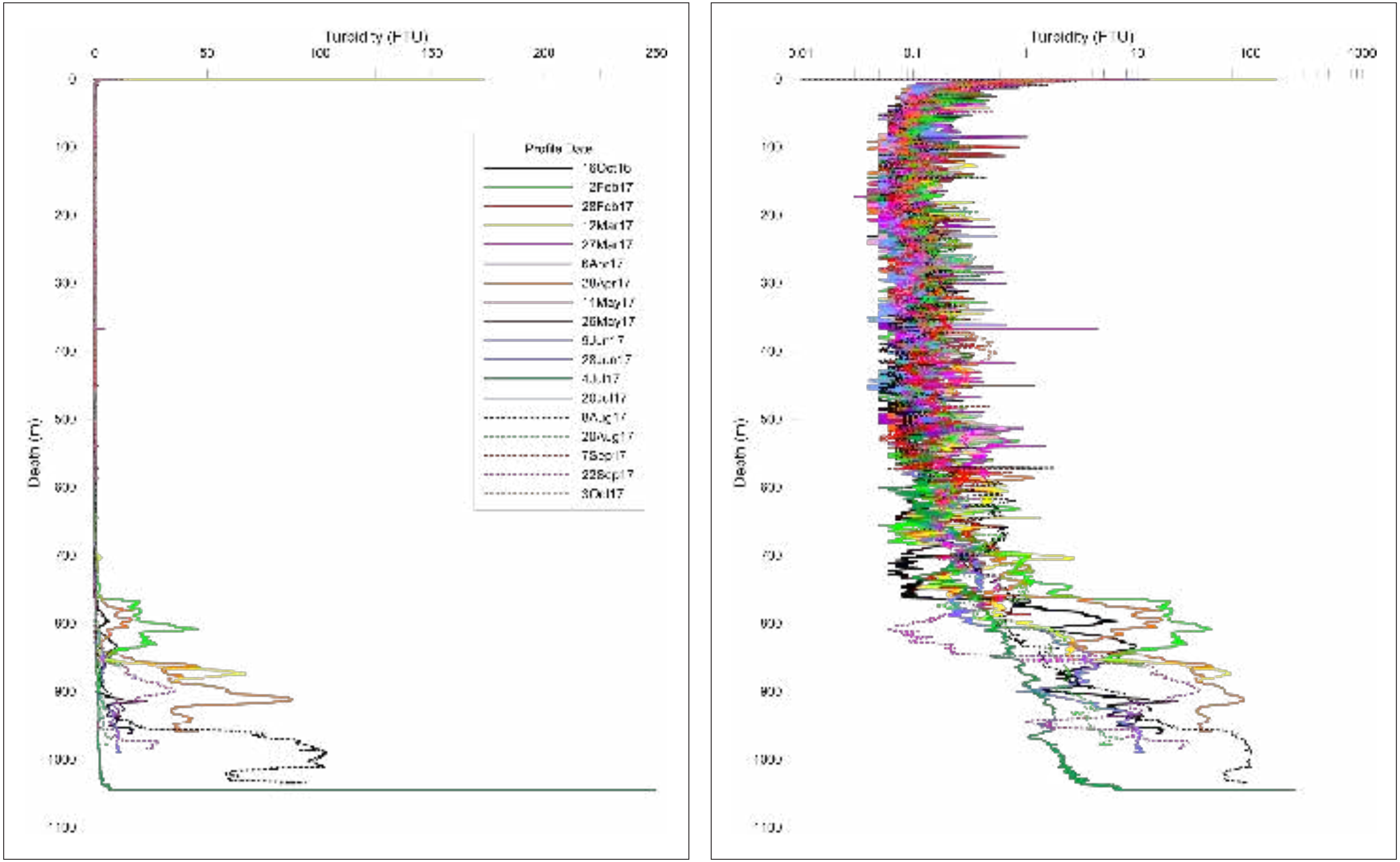

Source:
IHAconsult: 532-1104-FS-REP-0003 Sedimentology_Rev B-2_8, Figure 4-8

coffey
A TETRA TECH COMPANY

Date: 16.02.2018
Project: 754-ENAUABTF100520DD
File Name: 0520DD_10_F11.12_GRA

WAFI-GOLPU JOINT VENTURE

Wafi-Golpu Project

Turbidity profiles from CTD location B5

Figure No: 11.12

This indicates the almost continual occurrence of bottom-attached plumes of suspended sediment of variable thickness near the canyon floor. Apart from the persistent occurrence of thin surface buoyant plumes, there was no incidence of any well-defined mid-water subsurface plumes, which is consistent with the density profiles measured to date not showing strong stratification with clearly defined pycnoclines. This is also consistent with opportunistic deep-sea video footage collected in the water column during the benthic video characterisation study (Appendix O, Benthic Video Characterisation). That study found that with the exception of a site close to the Markham River mouth, the mid-water column above the Markham Canyon was generally devoid of suspended sediment plumes but closer to the bed, bottom-attached sediment plumes occurred that were between about 50m to 300m thick.

Time-series of turbidity data from 13m above the bed at the Outfall, Canyon and Basin moorings typically show relatively frequent short-term bursts of turbidity of varying strength and duration in excess of 1,000 formazin turbidity units (greatest nearest the seafloor), being most frequent at the Basin and Canyon mooring locations. With the exception of the turbidity current events through the Canyon and Basin Moorings on the 3 June 2017, 7 July 2017 and 15 November 2017 as described in Appendix M, Physical, Chemical and Biological Sedimentology of the Huon Gulf, there is no evident correlation of elevated turbidity levels between the mooring locations or with flood events in the Markham and Busu rivers.

Sediment traps were installed on all oceanographic moorings, with the exception of the Wave Mooring and the results are reported in Appendix M, Physical, Chemical and Biological Sedimentology of the Huon Gulf. Sediment trap data showed an increase in deposition rates with down-gradient distance along the Markham Canyon at least as far as the Basin Mooring. At the Trench Mooring, deposition rates in the sediment traps were more than an order of magnitude lower than at the Canyon and Basin moorings locations. Similarly, at the Far-Field Mooring, which is located on the southern flank of the Markham Canyon but outside the main canyon thalweg, sediment traps had the lowest deposition rates of all the sediment trap monitoring sites. Based on the median results presented in Appendix M, Physical, Chemical and Biological Sedimentology of the Huon Gulf, the amount of suspended sediment deposited on the floor of the Huon Gulf would equate to annual deposition of approximately 5,000 to 10,000 tonnes per square kilometre. However, these figures do not necessarily represent net aggradation of the bed, but more likely reflect two different mechanisms of sediment transport. The data from the Markham Canyon moorings likely represents a greater contribution from bottom-attached turbidity currents, including turbidity current events through the canyon, while the Outfall site likely represents settling from the extensive surface plumes of suspended sediment originating from the Markham and Busu rivers in particular.

The sediment trap settling rate data show the dominance of the Markham Canyon in the transport of sediment through the Huon Gulf, with settling rate and particle size being higher at the Markham Canyon mooring locations compared to both the Far Field and Outfall mooring locations, which lie outside the thalweg of the Markham Canyon. The maximum sediment deposition rate occurred at the Canyon Mooring site; the lowest was at the Far Field location. The occasional, but less frequent, elevated concentrations of sediment collected in the Far Field sediment trap demonstrates the ability of larger, less frequent turbidity current events to extend beyond the confines of the Markham Canyon.

Measurements of bed fluctuations underneath each of the moorings from the altimeter recordings show highly irregular bedforms spatially and temporally, possibly reflecting highly localised currents and transport processes (see Appendix M, Physical, Chemical and Biological Sedimentology of the Huon Gulf, for details). However, data from the regular bathymetric profiles during the oceanographic surveys suggests bedforms also exist on a completely different spatial scale to those recorded by the altimeters. A bathymetric profile of the bed of the Markham Canyon along one of the regular profile lines along the floor of the canyon is shown in Figure 11.13, and was recorded up-canyon of the Trench mooring, displaying what appears to be bed-waves with amplitudes of over 80m high and wavelengths of 500 to 700m.

11.7. Benthic Sediment Characteristics

Seafloor sediments in the Huon Gulf have been characterised by GDA Consult Pty Ltd and IHAconsult. Samples were collected during two surveys; the first using a box corer at 14 sampling sites in 2017, and the second using a box corer and a multi-corer at 25 sampling sites in 2018 (Figure 11.14) (Appendix M, Physical, Chemical and Biological Sedimentology of the Huon Gulf).

Samples were analysed for[7]:

- Particle size distribution
- Total metals
- Ethylenediaminetetraacetic acid (EDTA) extracted metals. This method provides indication of the proportion of metals likely to be bioavailable to organisms.
- Alkalinity
- Total organic carbon (TOC)
- Infauna (see Section 11.8.3, Deep Sea Benthic Ecology)

Sediment metals concentrations were compared to the Australian and New Zealand Environment and Conservation Council/Agriculture and Resource Management Council of Australia and New Zealand ANZECC/ARMCANZ (2000) international sediment quality guideline values (SQGV). These guidelines were adopted for comparison as per Long et al. (1995), as there are no PNG sediment quality guidelines and also incorporate the more recent revision to the guidelines (Simpson et al., 2013). The sediment quality guidelines in Simpson, et al. (2013) are presented as two guideline values:

- Guideline Value: threshold concentration level below which there is a low probability that biological effects could occur.
- Guideline Value-High: threshold concentration level above which there is a high probability that biological effects could occur.

These guidelines were developed for assessing potential risks to organisms in contact with benthic sediment rather than suspended solids.

[7] Sediment geochemistry data presented in this EIS is based on 2017 samples, while benthic ecology data for 2017 and 2018 samples is presented in this EIS.

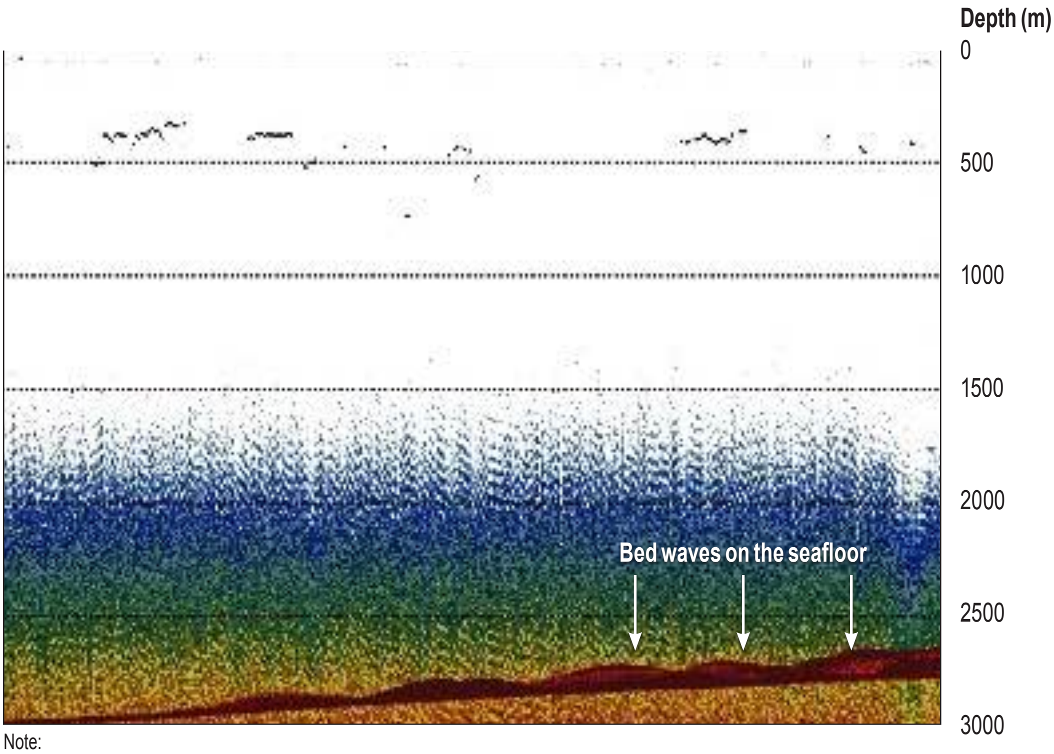

Note:
The colouring represents intensity of acoustic backscatter with red being the highest and blue being lowest.

Source:
IHAconsult: 532-1104-FS-REP-0003 Sedimentology_Rev B-2_8, Figure 5-8

INDD Reference: 0520DD_10_GRA059.indd_4

coffey A TETRA TECH COMPANY	Date: 23.05.2018 Project: 754-ENAUABTF100520DD File Name: 0520DD_10_F11.13_GRA	WAFI-GOLPU JOINT VENTURE Wafi-Golpu Project	Echo-sounder trace of acoustic backscatter indicating the presence of large bed waves along the floor of the Markham Canyon up canyon of the Trench Mooring	Figure No: 11.13

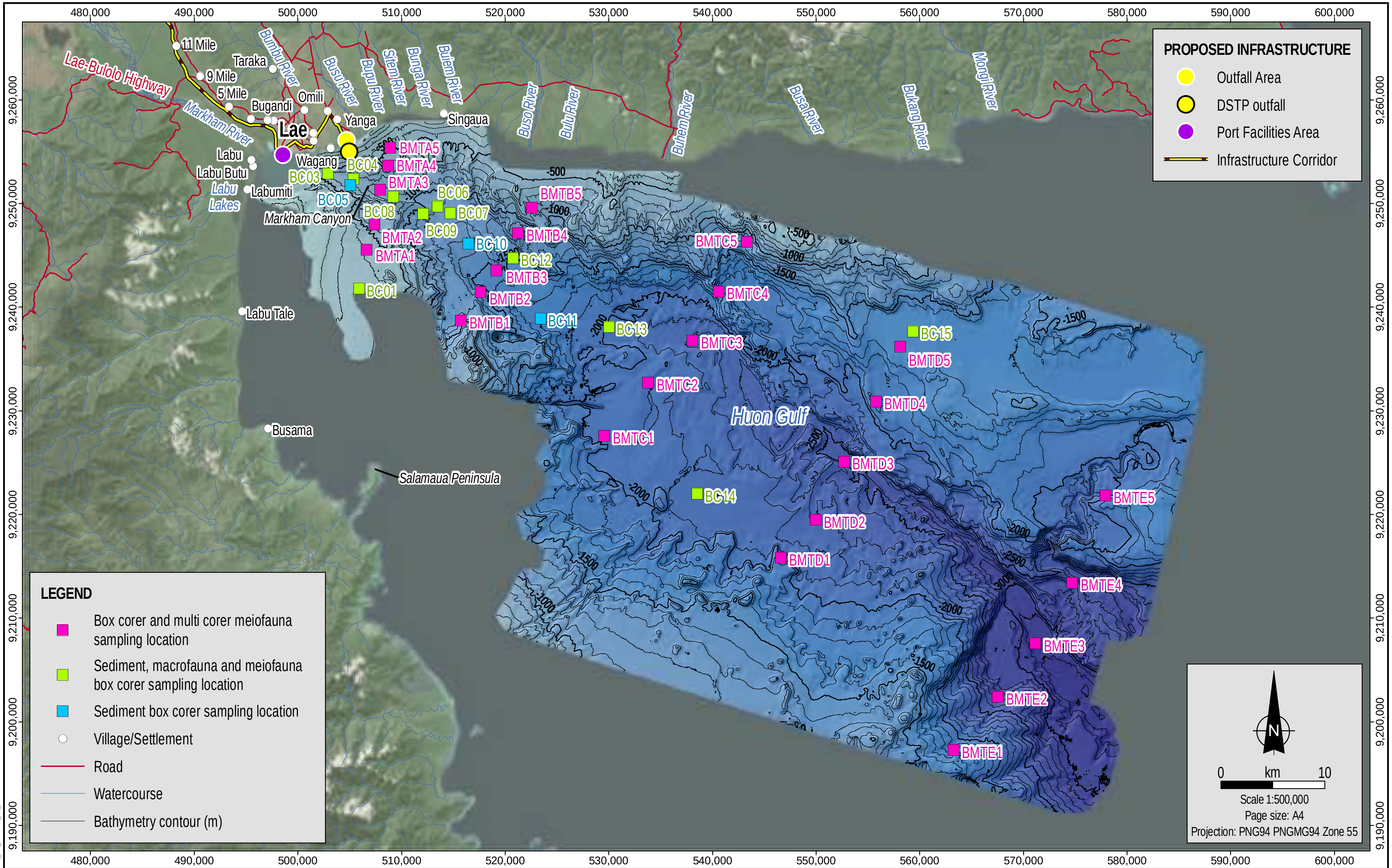

MXD Reference: 0520DD_10_GIS049_v0_4

Source:
Box core and bentic fauna sites from Coffey.
Villages/Settlements and infrastructure from WGJV and Coffey.
Roads and watercourses from NSO.
Bathymetry from WGJV survey.
Imagery from ArcGIS Online (capture date unknown).

coffey
A TETRA TECH COMPANY

Date: 07.03.2018
Project: 754-ENAUABTF100520DD
File Name: 0520DD_10_F11.14_GIS

WAFI-GOLPU JOINT VENTURE

Wafi-Golpu Project

Benthic sediment and infauna box corer and multi corer sampling locations

Figure No: 11.14

11.7.1. Particle Size Distribution

Table 11.3 shows the particle size distribution data from the box core samples and demonstrates the substantial differences between sites. The sediment grain size was coarsest at locations within the confines of the main structure of the Markham Canyon (i.e., sites BC03, BC04, BC06, BC07, BC08, BC09, BC10, BC12 and BC13). For the off-canyon sites (i.e., sites BC01, BC05, BC11, BC14 and BC15), where there are lower current velocities and a lower incidence of turbidity current events, bed sediments had finer grain sizes. This distinction between the coarse material on the main canyon floor and fine material on the canyon walls is consistent with scouring action of the periodic turbidity current flows recorded from the current meters, as well as the evidence from the considerable down canyon displacement of the canyon and basin moorings that occurred in January 2017 and June 2017.

Table 11.3: Particle size distribution in bed sediments from box core samples – February 2017

Site	Depth (m)	D_{10} (µm)	D_{50} (µm)	D_{90} (µm)	Sediment classification
BC01	355	2.38	8.5	37.3	Silt
BC03	589	4.01	45.8	195	Silt to fine sand
BC04	721	52.6	141	291	Silt to fine sand
BC05	654	2.16	10.1	42.4	Silt
BC06	1,098	17.6	220	733	Silt to sand
BC07	1,143	3.28	28.2	108	Silt to fine sand
BC08	915	51.6	128	564	Silt to sand
BC09	1,022	2.38	10.9	44	Silt
BC10	1,341	83.8	273	553	Sand
BC11	1,781	2.77	12.1	211	Silt to fine sand
BC12	1,489	3.53	31.6	441	Silt to sand
BC13	2,001	3.56	30.9	199	Silt to fine sand
BC14	2,121	3.17	16.4	87	Silt to fine sand
BC15	1,656	2.57	9.86	67.1	Silt to fine sand

D_{10} denotes the 10^{th} percentile particle size.
D_{50} denotes the median particle size.
D_{90} denotes the 90^{th} percentile particle size.

11.7.2. Metals

Table 11.4 and Table 11.5 show the total and EDTA sediment metals concentrations, respectively, and compares these to sediment quality guidelines and literature values for deep-sea clays (Salomons and Förstner, 1984). Results for TOC are also presented in Table 11.4.

Sediment geochemistry was relatively uniform across the study area with no clear delineation of metals chemistry with distance from the shore or depth. This is indicative of the highly dynamic nature of the Markham Canyon and thorough mixing of sediments via episodic but frequent turbidity current events and bedload transport processes.

The concentrations of particulate metals in the Huon Gulf box core samples are mostly lower than or similar to global averages for deep sea clays reported in Salomons and Förstner (1984).

Table 11.4: Total sediment metals (mg/kg) concentrations from box core samples – February 2017

Site	Al	Ag	As	Cd	Co	Cr	Cu	Fe	Hg	Mn	Ni	Pb	Se	Sb	V	Zn	Ba	Mo	Sn	TOC %
BC01	40,500	<2	13	<1	28	52	74	52,600	-	1,600	71	11	<5	<5	130	79	30	<2	<5	0.62
BC03	29,600	<2	6	<1	18	35	60	42,800	<0.1	799	37	6	7	<5	134	69	70	<2	<5	0.34
BC04	41,900	<2	11	<1	27	54	95	57,800	<0.1	1,180	60	11	<5	<5	146	94	60	<2	<5	0.08
BC05	28,600	<2	6	<1	15	29	48	35,600	<0.1	664	34	5	5	<5	111	59	60	<2	<5	0.45
BC06	29,800	<2	<5	<1	16	21	54	37,900	<0.1	766	33	<5	5	<5	118	62	60	<2	<5	0.10
BC07	38,200	<2	10	<1	24	48	85	52,200	<0.1	1,040	56	10	<5	<5	134	91	60	<2	<5	0.44
BC08	39,700	<2	14	<1	26	53	91	57,600	<0.1	1,250	63	13	<5	<5	140	100	60	<2	<5	0.05
BC09	28,700	<2	5	<1	16	23	51	35,500	<0.1	732	32	5	<5	<5	99	61	60	<2	<5	0.41
BC10	35,100	<2	10	<1	20	49	66	46,400	<0.1	1,140	50	9	<5	<5	119	81	70	<2	<5	0.04
BC12	35,300	<2	7	<1	20	37	66	43,300	<0.1	823	46	7	<5	<5	121	69	60	<2	<5	0.09
BC13	33,400	<2	5	<1	19	30	63	42,500	<0.1	808	40	5	<5	<5	128	64	60	<2	<5	0.29
BC14	34,400	<2	<5	<1	16	25	55	37,600	<0.1	727	35	5	<5	<5	120	59	60	<2	<5	0.58
BC15	43,600	<2	9	<1	32	55	92	50,900	<0.1	5,520	103	8	<5	<5	143	79	120	3	<5	0.54
Global average: deep sea clays[a]	84,000	0.11	13	0.42	74	90	250	65,000	0.08	6,700	250	80	0.17	1.0	120	165	2,300	27	1.5	-
SQGV[b]	-	1	20	1.5	-	80	65	-	0.15	-	21	50	200	-	-	200	-	-	-	-
SQGV-high[c]	-	3.7	70	10	-	370	270	-	1	-	52	200	410	-	-	410	-	-	-	-

[a] Salomons and Förstner, 1984 (p. 149).
[b] Sediment quality guideline value: threshold concentration level below which there is a low probability that biological effects could occur.
[c] Sediment quality guideline value-high: threshold concentration level above which there is a high probability that biological effects could occur.

Table 11.5: EDTA sediment metals concentrations (mg/kg) from box core samples – February 2017

Site	Al	Ag	As	Cd	Co	Cr	Cu	Fe	Hg	Mn	Ni	Pb	Se	Sb	V	Zn	Ba
BC01	-	-	-	-	-	-	-	-	-	-	-	-	-	-	-	-	-
BC03	<50	<0.2	<1.0	<0.2	<0.5	<1.0	4.1	60	<0.10	51	<1.0	<1.0	<0.5	<0.50	<2.0	<5.0	<5
BC04	<50	<0.2	<1.0	<0.2	<0.5	<1.0	<0.5	70	<0.10	58	<1.0	<1.0	<0.5	<0.50	<2.0	<5.0	<5
BC05	60	<0.2	<1.0	<0.2	0.6	<1.0	17.0	180	<0.10	200	<1.0	2.4	1.0	<0.50	2.3	<5.0	<5
BC06	<50	<0.2	<1.0	<0.2	<0.5	<1.0	<0.5	60	<0.10	44	<1.0	<1.0	<0.5	<0.50	<2.0	<5.0	<5
BC07	<50	<0.2	<1.0	<0.2	0.8	<1.0	10.2	140	<0.10	121	<1.0	1.6	<0.5	<0.50	<2.0	<5.0	<5
BC08	<50	<0.2	<1.0	<0.2	<0.5	<1.0	3.0	<50	<0.10	39	<1.0	<1.0	<0.5	<0.50	<2.0	<5.0	<5
BC09	70	<0.2	<1.0	<0.2	0.9	<1.0	16.3	210	<0.10	194	<1.0	3.0	<0.5	<0.50	2.0	<5.0	<5
BC10	<50	<0.2	<1.0	<0.2	<0.5	<1.0	3.4	<50	<0.10	40	<1.0	<1.0	<0.5	<0.50	<2.0	<5.0	<5
BC12	<50	<0.2	<1.0	<0.2	<0.5	<1.0	4.5	60	<0.10	47	<1.0	<1.0	<0.5	<0.50	<2.0	<5.0	<5
BC13	<50	<0.2	<1.0	<0.2	0.9	<1.0	12.3	160	<0.10	112	<1.0	1.6	<0.5	<0.50	<2.0	<5.0	<5
BC14	80	<0.2	<1.0	<0.2	1.3	<1.0	16.1	330	<0.10	370	<1.0	3.0	0.6	<0.50	2.7	<5.0	<5
BC15	<50	<0.2	<1.0	<0.2	2.0	<1.0	13.6	260	<0.10	1520	6.0	1.9	<0.5	<0.50	5.2	6.8	<5
SQGV[b]	-	1	20	1.5	-	80	65	-	0.15	-	21	50	200	-	-	200	-
SQGV-high[c]	-	3.7	70	10	-	370	270	-	1	-	52	200	410	-	-	410	-

[b] Sediment quality guideline value: threshold concentration level below which there is a low probability that biological effects could occur.
[c] Sediment quality guideline value-high: threshold concentration level above which there is a high probability that biological effects could occur.

Except for copper, manganese, and lead, EDTA extractable metals were all at least an order of magnitude lower than the total metals concentrations. However, for copper, manganese, and lead, the EDTA extractable fraction ranged from only 5 to 30% of the total metals concentration (where the latter was above the detection limit).

Table 11.4 shows that concentrations of seven of the 13 box core samples exceeded the lower SQGV for total copper but all remained well below the Guideline Value-high guideline value. For total nickel, all 13 samples exceeded the Guideline Value and five of the 13 samples exceeded the Guideline Value-high trigger value. The literature values reported for copper and nickel (Salomons and Förstner, 1984) in deep sea clays also exceed the Guideline Value and Guideline Value-high for copper and nickel, respectively. All other metals concentrations were within Guideline Values.

When comparing the EDTA extractable fraction of each sample, all EDTA extractable metals concentrations remained below both SQGVs. To assess the potential toxicity of metals in sediment to benthic biota, it is ultimately more useful to compare the weak-acid extractable (i.e., bioavailable) portion to the SQGVs. This finding indicates that bioavailable metals in the Huon Gulf natural ocean floor sediments are unlikely to be causing adverse effects to benthic biota.

Concentrations of TOC ranged from <0.05% to a maximum of 0.62%. The maximum TOC concentration of 0.62% was recorded at the site closest to the Labu Lakes, which likely represents the additional carbon inputs from the extensive mangrove system.

11.8. Offshore Marine Ecology

In November 2016, March 2017 and May 2017 Marscco and Coffey conducted investigations into the ecology of the pelagic environment in the Huon Gulf. These investigations involved sampling deep-slope and pelagic fish (Appendix P, Deep-slope and Pelagic Fish Characterisation) and zooplankton and micronekton (Appendix Q, Zooplankton and Micronekton Characterisation). In November 2016, the Huon Gulf benthic environment was investigated by Coffey during a deep-sea video survey (Appendix O, Benthic Video Characterisation). In February 2017 and January 2018, IHAconsult conducted studies including sediment and benthic infauna analysis derived from box corer and multi-corer sampling (Appendix M, Physical, Chemical and Biological Sedimentology of the Huon Gulf). The findings of these studies are summarised in the following sections.

11.8.1. Deep-Slope and Pelagic Fish

11.8.1.1. Study Area

The deep-slope and pelagic fish study involved two field surveys, conducted in November 2016 and May 2017 in the DSTP study area and a reference study area near Salamaua Peninsula (Figure 11.15 and Figure 11.16). The sampling sites along each transect (A to E in Figure 11.15) covered depths between 100 and 800m. Combined overall fishing effort across the two surveys totaled 146 hours of systematic dropline fishing at 41 sites over 18 days (90 hours in November 2016 and 56 hours in May 2017). To supplement the caught fish samples, samples were also collected from the Department of Civil Aviation (DCA) Point fish market in Lae and notes were made on the reported catch location and depths. A complete list of species identified during the study is provided in Appendix P, Deep-slope and Pelagic Fish Characterisation.

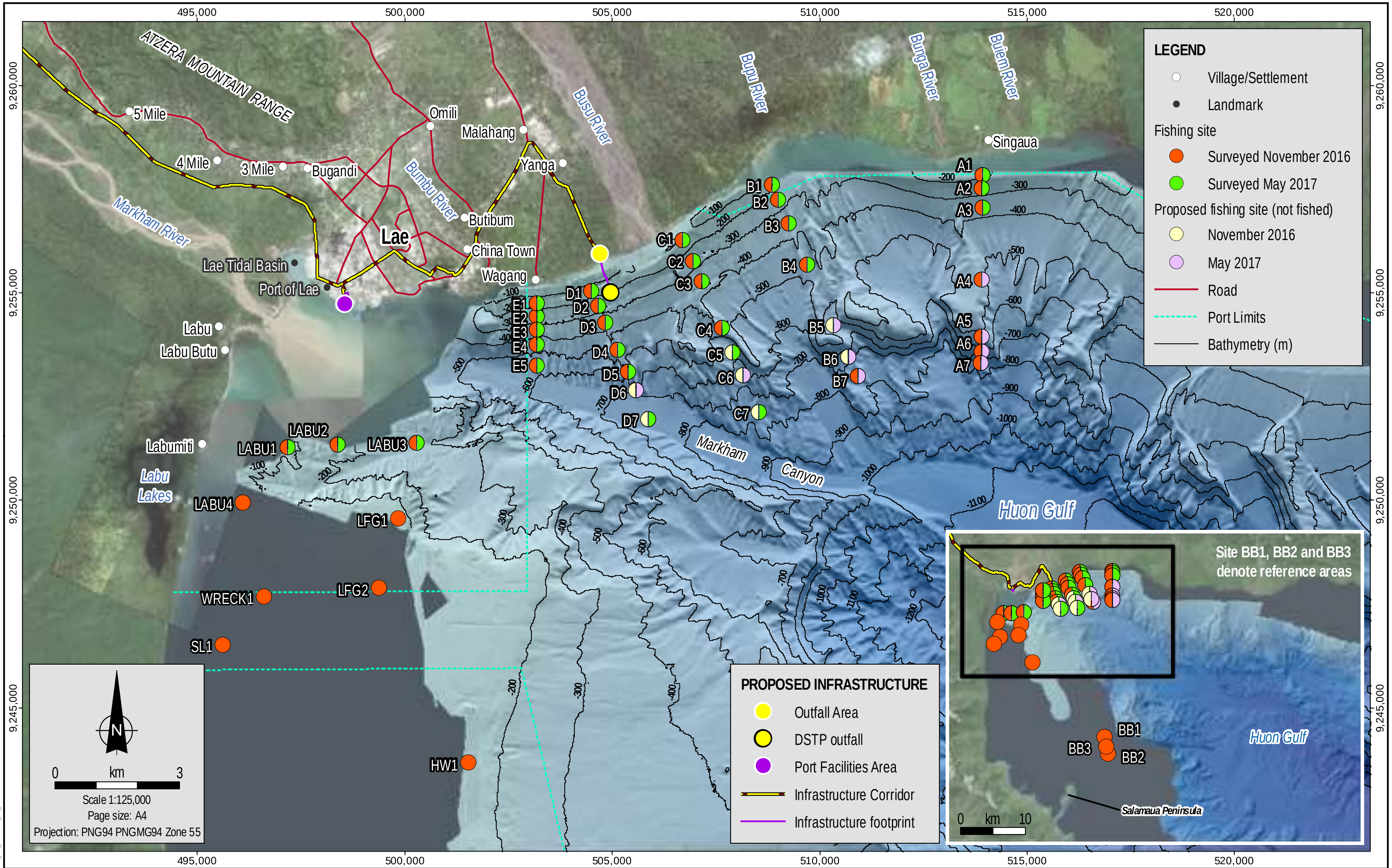

Source:
Fishing sites, roads and Port Limits from Coffey (Port Limits indicative only).
Villages/Settlements, landmarks and infrastructure from WGJV and Coffey.
Bathymetry from WGJV survey.
Imagery from WGJV (capture date 2016) and ArcGIS Online (capture date unknown).

coffey
A TETRA TECH COMPANY

Date: 19.02.2018
Project: 754-ENAUABTF100520DD
File Name: 0520DD_10_F11.15_GIS

WAFI-GOLPU JOINT VENTURE

Wafi-Golpu Project

Deep-slope and pelagic drop-line fishing locations

Figure No: 11.15

MXD Reference: 0520DD_10_GIS037_v0_4

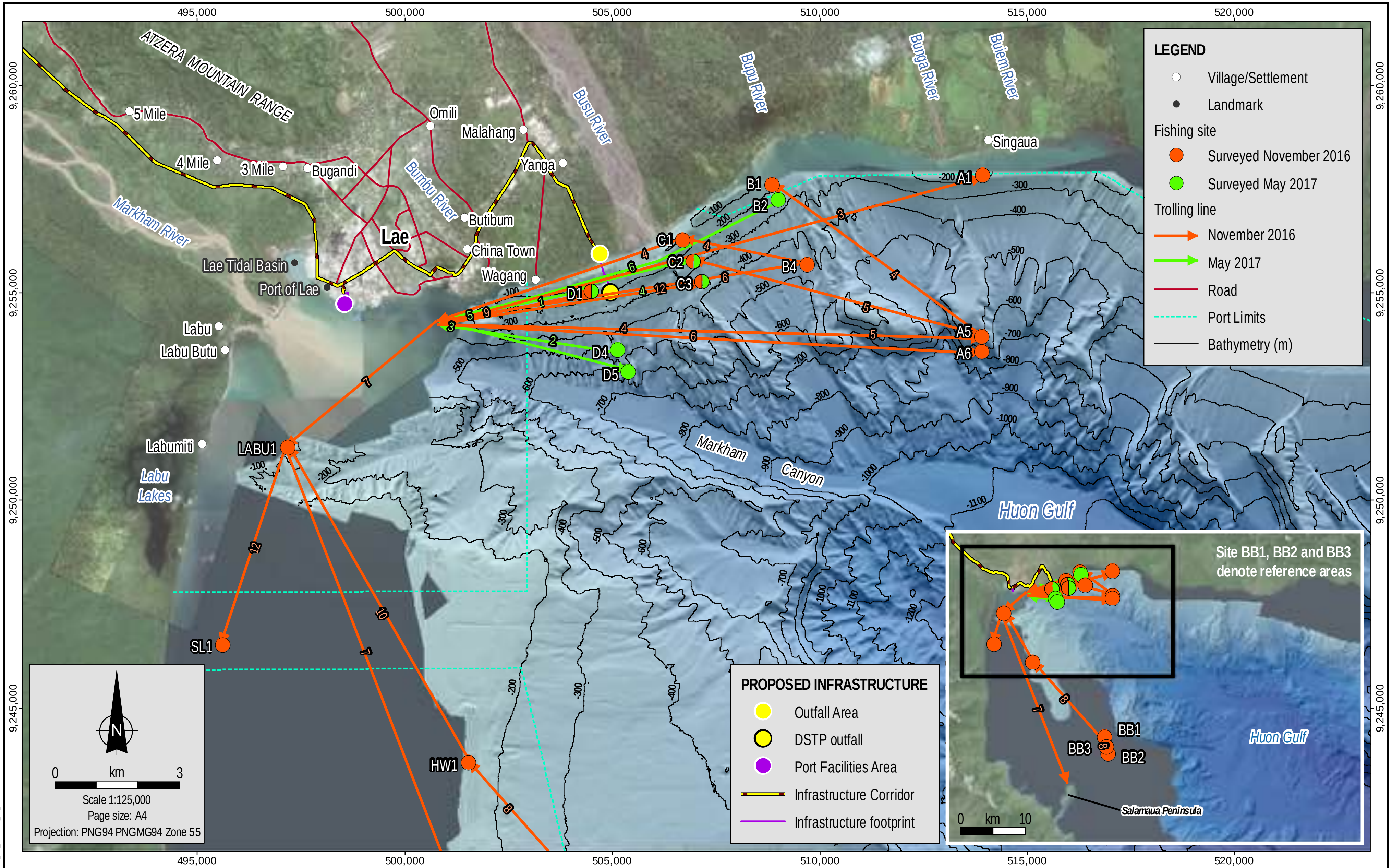

Source:
Fishing sites, trolling lines, roads and Port Limits from Coffey (Port Limits indicative only).
Villages/Settlements, landmarks and infrastructure from WGJV and Coffey.
Bathymetry from WGJV survey.
Imagery from WGJV (capture date 2016) and ArcGIS Online (capture date unknown).

coffey
A TETRA TECH COMPANY

Date: 19.02.2018
Project: 754-ENAUABTF100520DD
File Name: 0520DD_10_F11.16_GIS

WAFI-GOLPU JOINT VENTURE

Wafi-Golpu Project

Pelagic trolling transects

Figure No: 11.16

MXD Reference: 0520DD_10_GIS038_v0_4

11.8.1.2. Fish Abundance and Diversity

Results indicate that the overall diversity of deep slope fish species in the upper Huon Gulf off Lae was low for both elasmobranchs (cartilaginous fish such as sharks) and bony fishes. Diversity was also much lower than recorded from similar baseline surveys at other DSTP sites elsewhere in PNG, such as Woodlark, Misima, Ramu and Lihir (Appendix P, Deep-slope and Pelagic Fish Characterisation).

Sixty-one individuals representing eight species and five families were caught over the DSTP and reference study areas during baseline fishing in November 2016 and May 2017. Catches were dominated by sharks, and of the 58 fish that were caught below 100m depth across the two surveys, 55 were sharks (94% of the catch). The shark catch comprised:

- Forty-four dwarf gulper sharks (*Centrophorus atromarginatus*, Figure 11.17)
- Five long-finned gulper sharks (*Centrophorus longipinnis*, Figure 11.18)
- One gulper shark (*Centrophorus granulosus*, Figure 11.19)
- Five fatspine spurdogs (*Squalus crassispinis*, Figure 11.20)

All dwarf gulper sharks were captured from around the upper reaches and northern walls of the Markham Canyon at depths between 100m and 540m, with approximately 93% recorded at depths between 100m and 400m (Figure 11.21). None were caught at sites shallower than 100m outside the Markham Canyon, such as sites LABU1 and LABU4 outside Labu Lakes. The finding of three pregnant female dwarf gulper sharks suggests the presence of a resident population capable of surviving in a seemingly harsh environment with likely scarce food resources. Similarly, the capture of a pregnant female long-finned gulper shark also suggests the presence of an established population of this species.

The three non-shark species caught within the DSTP study area during the surveys comprised: one saddletail snapper (*Lutjanus malabaricus*) (Figure 11.22), caught at 100m depth; one common pike eel (*Muraenesox baggio*) (Figure 11.23), caught at 124m depth; and one blackspotted croaker (*Protonibea diacanthus*) (Figure 11.24), caught at 250m depth. In the reference study area, a mangrove jack (*Lutjanus argentimaculatus*) was caught at 100m depth and a saddletail snapper was caught at 25m depth.

The dominance of gulper sharks over bony fishes was evident at both November 2016 and May 2017 sampling periods and therefore does not suggest transitory presence of these species. Apart from the single saddletail snapper (family Lutjanidae), no other deep slope snappers or individuals from the other two most prevalent fish families recorded in comparable baseline deep slope studies elsewhere in PNG; Serranidae (sea basses and groupers) and Lethrinidae (emperors), were captured in the DSTP study area during the surveys in November 2016 or May 2017.

Fish catch per unit of effort (CPUE) across all depth strata within the DSTP and reference study areas averaged 0.09 kilograms of fish per hook per hour (kg/hook h^{-1}) during the November 2016 survey, and 0.11kg/hook h^{-1} during the May 2017 survey. These CPUE results are lower than that recorded during the baseline deep-slope fish surveys using comparable methods at Misima Island (4.0kg/hook h^{-1}), at Woodlark Island (0.5kg/hook h^{-1}) and at Niolam Island (Lihir Group) (0.19kg/hook h^{-1}). The average CPUE across all sites in the current study were also lower than that reported for the Rai Coast for the Ramu Nickel Project (0.43 to 3.08kg/hook h^{-1}) (NSR, 1998), but within the range of CPUE obtained from Astrolabe Bay and islands offshore of Madang fished during the same study (0.025 to 0.28kg/hook h^{-1}).


Photo credit: Coffey/Marscco

Figure 11.17
Dwarf gulper shark
(*Centrophorus atromarginatus*)


Photo credit: Coffey/Marscco

Figure 11.18
Long-finned gulper shark
(*Centrophorus longipinnis*)


Photo credit: Coffey/Marscco

Figure 11.19
Gulper shark
(*Centrophorus granulosus*)


Photo credit: Coffey/Marscco

Figure 11.20
Fatspine spurdog
(*Squalus crassispinis*)

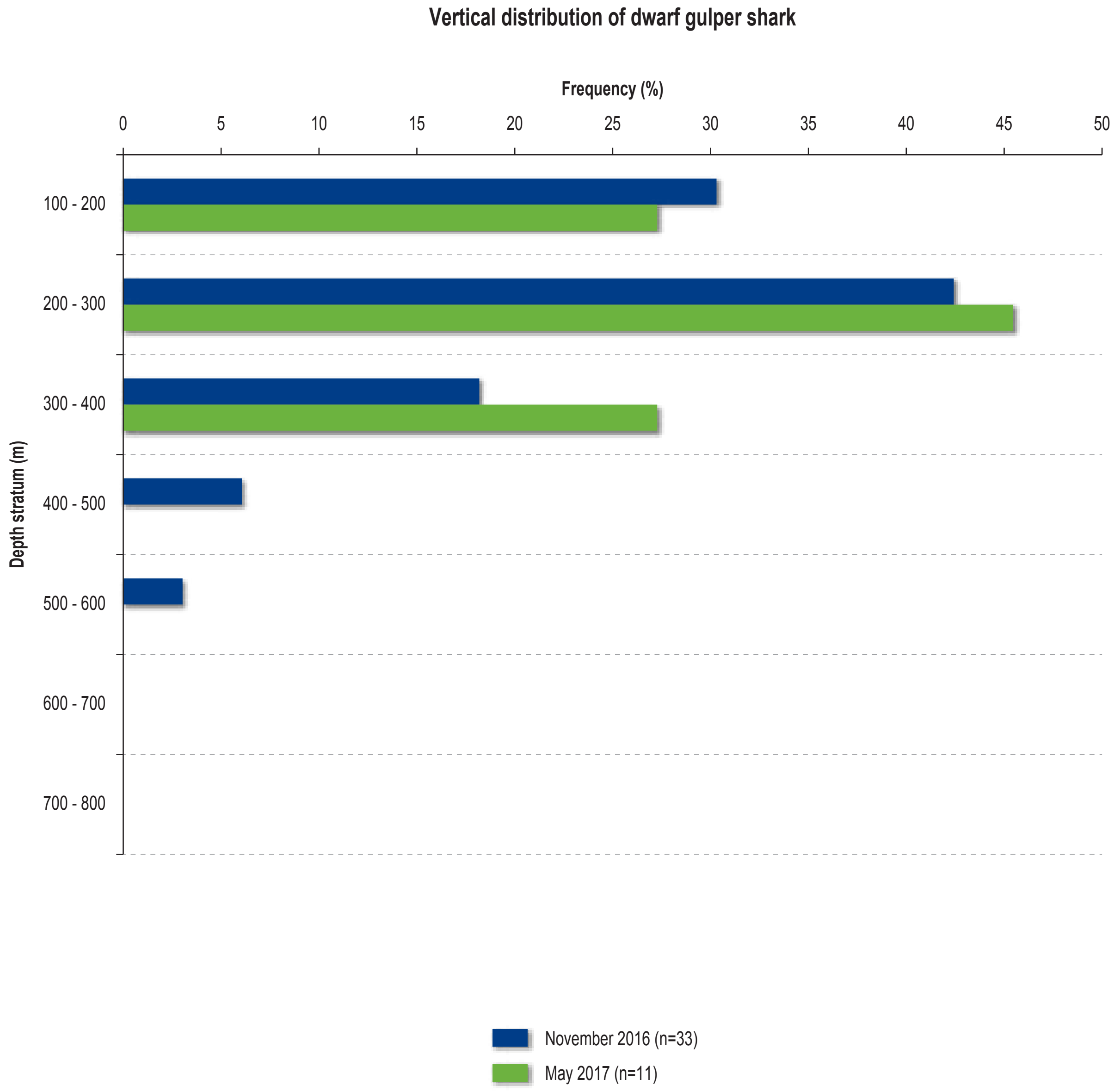

Vertical distribution of dwarf gulper sharks

Figure No: 11.21

Photo credit: Coffey/Marscco

Figure 11.22
Saddletail snapper
(*Lutjanus malabaricus*)

Photo credit: Coffey/Marscco

Figure 11.23
Common pike eel
(*Muraenesox baggio*)

Photo credit: Coffey/Marscco

Figure 11.24
Blackspotted croaker
(*Protonibea diacanthus*)

The low CPUE by weight in the Huon Gulf is likely due to the lower number of deep-slope fishes caught during the surveys in November 2016 (41 specimens caught) and May 2017 (20 specimens) compared to those reported from Misima (84 specimens), Lihir (411 specimens), Ramu (54 specimens) and Woodlark (121 specimens). While gulper sharks were somewhat common, the overall low diversity of fish fauna, combined with the low abundance of bony fish species in the areas fished during the study could be attributed to a number of factors including:

- Lack of suitable habitats such as inshore coastal reefs as well as offshore reefs and seamounts, which normally sustain a great variety of fish communities.
- Likely reduced incidence of available prey, as indicated by the very few prey remains in the stomachs of all sharks dissected.
- High rates of sediment deposition over the seafloor from the riverine discharges of the Markham River as well as the Busu and Bupu (and other) rivers, as described above.

In terms of the latter, findings from other EIS investigations showed that sediments from these rivers cover much of the seafloor in the DSTP study area, and extend as far south as the local fishing grounds to the east of the southern end of the Labu Lakes (Appendix S, Fisheries and Marine Resource Use Characterisation).

No pelagic fish species were captured within the DSTP or reference study areas after 23 trolling sessions totaling 16.5 hours of fishing during the November 2016 and May 2017 surveys. The absence of pelagic fishes was unexpected, given the substantial effort using three rods and a suite of standard lures. Factors which may have contributed to the zero catches include trolling mostly through areas of high turbidity (due to riverine sediment plumes), times of year fished, and/or species normally caught further south simply not venturing close to Lae due to absence of potential prey, i.e., schooling fishes. It is evident from market observations that local people catch mostly small pelagic species including bigeye trevally and slimy mackerel. However, local fishers have been observed to target areas of clearer waters, especially the interface between clear waters and river plumes, and/or areas with visible seabird activity (likely due to the presence of small schooling pelagic fishes). In contrast, all trolling during the two surveys was carried out with gear specifically designed to capture large pelagic fishes, and was carried out during direct transit to and from the deep slope sampling sites regardless of sea conditions.

Fourteen specimens of bony fishes were sourced from the fish market at DCA Point in Lae during the November 2016 survey. These comprised five species from two families, Lutjanidae (snappers, mangrove jack) and Carangidae (trevallies, mackerels). In terms of numbers, nine of the 14 specimens were lutjanids normally found in coastal areas with offshore reefs (e.g., *Pristipomoides typus* and *L. malabaricus*), or areas associated with coastal lagoon/lake environments (*L. argentimaculatus*). According to the market vendors, the species observed at the DCA Point fish market were captured within the upper 100m, and in coastal areas south of Lae, typically outside the influence of noticeable sediment plumes from the Markham River.

11.8.1.3. Metals in Fish Tissue

Metals were analysed (wet weight basis) from the muscle and liver tissue of 40 specimens (six species) captured in November 2016 and 14 specimens (five species) obtained at the DCA Point fish market in November 2016. Metals were also analysed from the muscle of the 20 specimens (five species) captured in May 2017.

In the absence of specific food standards in PNG, the concentrations of selected metals in muscle tissue were compared against recommended standards developed by Food Standards Australia New Zealand (FSANZ). The standards comprise the Australia New

Zealand Food Standards Code - Standard 1.4.1 - Contaminants and Natural Toxicants (FSANZ, 2016), and the Food Standards Australia New Zealand - Generally Expected Levels (GELs) for Metal Contaminants (FSANZ, 2001). The Standard 1.4.1 (Contaminants and Natural Toxicants) specifies the maximum levels of contaminants and natural toxicants that are permitted in the foods listed in the standard. The FSANZ GELs provide recommended levels that if exceeded in foods, should be further investigated. Table 11.6 outlines these standards and GELs. For simplicity, the FSANZ Food Standards Code Standard 1.4.1 is referred to in this report as 'FSANZ standard'. The FSANZ GELs are referred to as 'FSANZ GEL'. The metals concentrations outlined in the FSANZ standard and the FSANZ GEL are on a wet weight basis.

Table 11.6: Summary of food standards and guidelines

Metal	FSANZ Standard 1.4.1[a] (mg/kg)	FSANZ GEL (median)[b] (mg/kg)	FSANZ GEL (90th percentile)[b] (mg/kg)
Arsenic	2	-	-
Cadmium	-	-	-
Chromium	-	-	-
Copper	-	0.5	2
Iron	-	-	-
Lead	0.5	-	-
Mercury	1 (mean value; applies to dwarf gulper shark) 1.5 (maximum value; applies to dwarf gulper shark) 1 (maximum value; applies to gulper shark) 0.5 (mean; applies to bony fish) 1 (maximum; applies to bony fish)	0.5	2
Manganese	-	-	-
Nickel	-	-	-
Selenium	-	0.5	2
Silver	-	-	-
Zinc	-	5	15

- denotes no applicable standard or guideline

a Source: Australia New Zealand Food Standards Code - Standard 1.4.1 - Contaminants and Natural Toxicants. Canberra: Commonwealth of Australia. Standards are maximum permitted values unless otherwise noted.

b Source: Food Standards Australia New Zealand 2001. Generally Expected Levels (GELS) for Metal Contaminants - Additional guidelines to Max levels in Standard 1.4.1 - Contaminants and Natural Toxicants. The guidelines are given for median and 90th percentile values. The guidelines recommend that exceedance of the 90th percentile value should initiate further investigation into the source of the concentration.

c These criteria were calculated based on the criteria in S19-7 of the Australia New Zealand Food Standards Code - Standard 1.4.1 - Contaminants and Natural Toxicants. Limits are given for both mean concentrations in a group of sample units and maximum concentrations in any sample unit.

Figure 11.25 and Figure 11.26 present the mean metals concentrations (As, Cu, Fe, Hg, Se and Zn) of the captured fish (left side) and market-sourced fish (right side) from the study, along with the relevant FSANZ standard and FSANZ GEL for comparison, where one exists. Muscle tissue results provide a direct comparison to the FSANZ standard and GEL as this is the portion of fish commonly consumed by humans; however, for comparative purposes, metals concentrations in liver were also compared to the FSANZ standard and GEL.

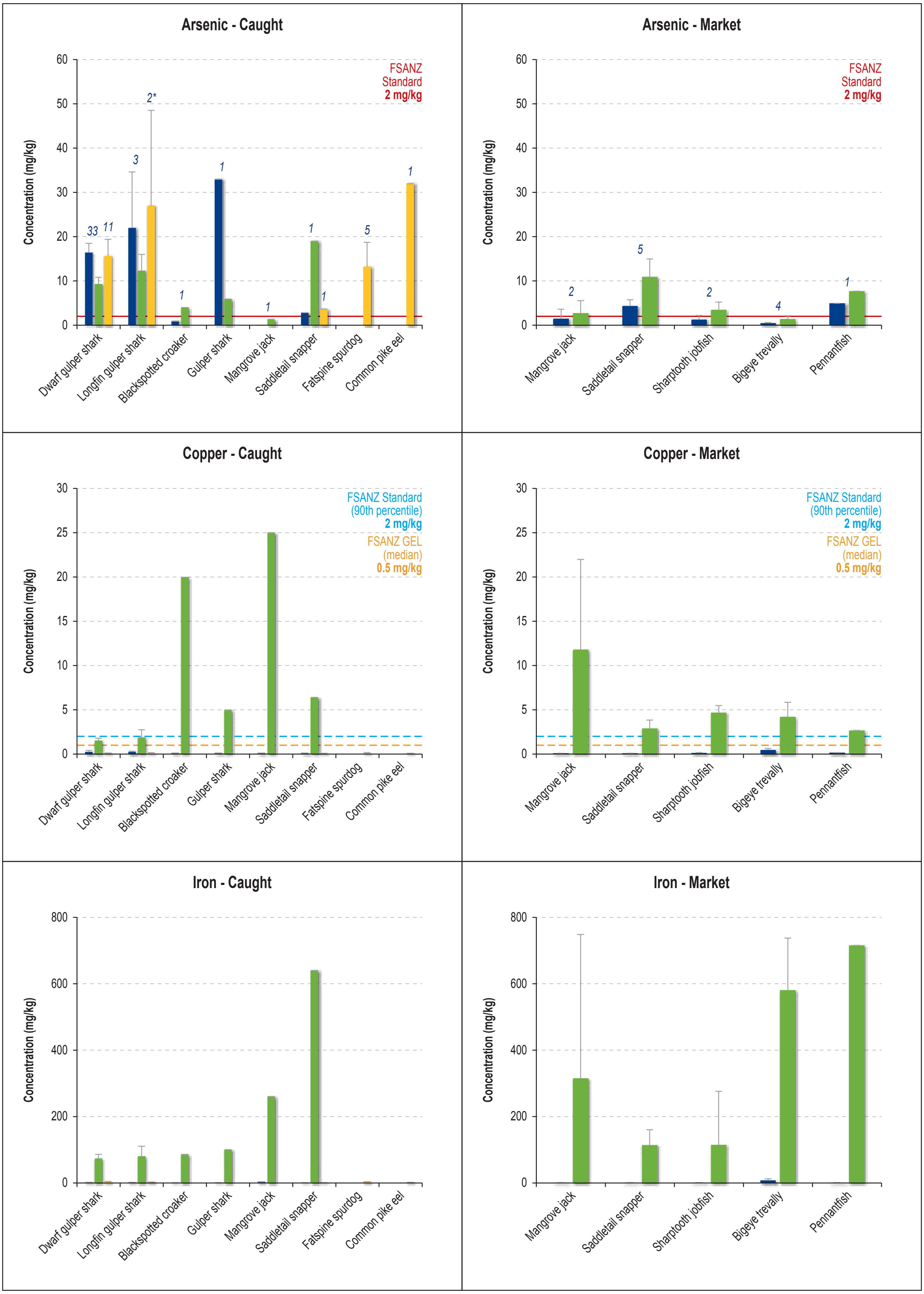

Muscle - 2016 Liver - 2016 Muscle - 2017 *Sample numbers are shown in italics above the data plots in the top graphs. These numbers are applicable for all metals.

coffey A TETRA TECH COMPANY	Date: 16.02.2018 Project: 754-ENAUABTF100520DD File Name: 0520DD_10_F11.25_GRA	WAFI-GOLPU JOINT VENTURE Wafi-Golpu Project	Mean metals concentrations (As, Cu and Fe) in liver and muscle of fishes caught (Nov 2016; May 2017) and sourced from DCA Point fish market (Nov 2016)	Figure No: 11.25

INDD Reference: 0520DD_10_GRA061.indd_3

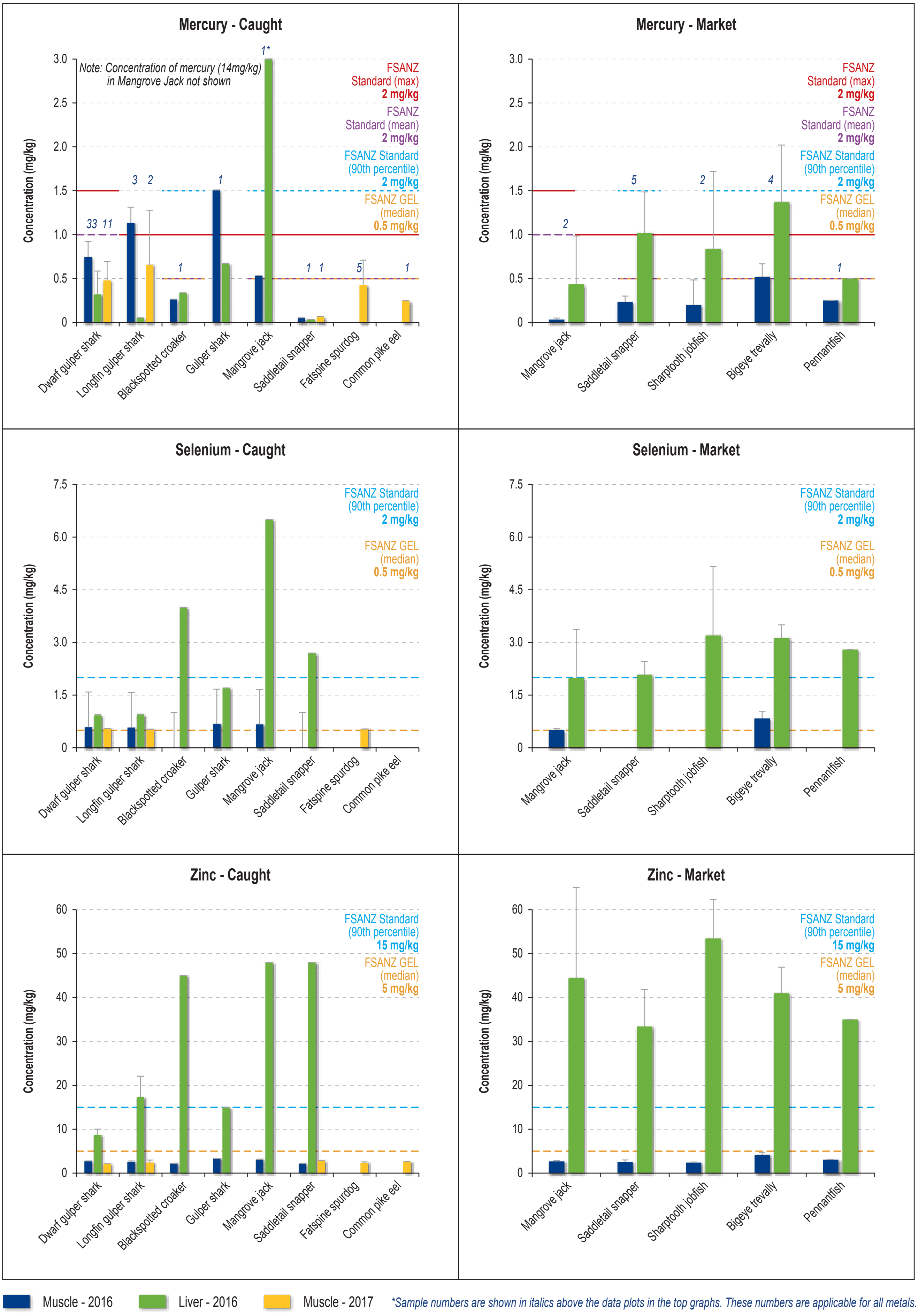

**Sample numbers are shown in italics above the data plots in the top graphs. These numbers are applicable for all metals.*

coffey
A TETRA TECH COMPANY

Date: 16.02.2018
Project: 754-ENAUABTF100520DD
File Name: 0520DD_10_F11.26_GRA

WAFI-GOLPU JOINT VENTURE

Wafi-Golpu Project

Mean metals concentrations (Hg, Se and Zn) in liver and muscle of fishes caught (Nov 2016; May 2017) and sourced from DCA Point fish market (Nov 2016)

Figure No: **11.26**

INDD Reference: 0520DD_10_GRA062.indd_3

Metals concentrations in muscle and liver of numerous bony fish and sharks exceeded the FSANZ (FSANZ, 2016) and GELs (FSANZ, 2001) for arsenic, copper, mercury, selenium and zinc in fish. Figure 11.25 and Figure 11.26 show results from all species including dwarf gulper sharks (for which values are derived from 44 individuals) as well as others for which only one or two individuals were available for analysis. Plotting of metals data was restricted to those metals with analytical results largely above the practical quantification limits and to where graphical comparisons to FSANZ standards and GELs are relevant.

The exceedances of the FSANZ standard and FSANZ GEL are summarised as follows:

Arsenic

- The FSANZ standard (maximum limit) for arsenic of 2mg/kg was exceeded in muscle tissue from all dwarf gulper sharks, as well as the liver tissue of 32 of the 33 dwarf gulper sharks (liver was only analysed in November 2016). This standard was also exceeded in muscle samples from all long-finned gulper sharks, the single gulper shark, the fatspine spurdogs, the common pike eel and all saddletail snappers. The arsenic FSANZ standard was also exceeded in the blackspotted croaker liver sample. Arsenic concentrations were higher in sharks (gulper, dwarf gulper and long-finned gulper) than in bony fishes.
- The FSANZ standard (maximum limit) for arsenic of 2mg/kg was exceeded in muscle and liver of all market-bought saddletail snapper, the pennantfish, and one of the two mangrove jacks. The arsenic FSANZ standard was also exceeded in liver of both of the market-bought sharptooth jobfish and one of the four bigeye trevallies.

Copper

- The copper FSANZ GELs (median value of 0.5mg/kg and 90th percentile value of 2mg/kg) were exceeded in liver of all caught and market-bought specimens in November 2016. There were no copper FSANZ GEL exceedances in muscle of any of the individuals tested in May 2017.

Lead

- There were no exceedances of the lead FSANZ standard (maximum limit) of 0.5mg/kg in muscle or liver from the November 2016 survey or in muscle from the May 2017 survey.

Mercury

- The mercury FSANZ standard (maximum limit) of 1.5mg/kg was exceeded in the muscle of one dwarf gulper shark and the liver from another dwarf gulper shark. The FSANZ standard (maximum limit) of 1mg/kg was exceeded in muscle from two long-finned gulper sharks and in the muscle from the single gulper shark. The FSANZ standard varies for dwarf gulper shark and the other sharks because the application of the standard is based on the number of samples caught. The mercury FSANZ standard (maximum limit) of 1mg/kg was exceeded in the liver from the mangrove jack caught in November 2016.
- The mercury FSANZ standard (maximum limit) of 1mg/kg was exceeded in the liver tissue of the following market-bought specimens: one saddletail snapper, one sharptooth jobfish and two bigeye trevallies.

Selenium

- The selenium FSANZ GEL (median value) of 0.5mg/kg was exceeded in muscle from dwarf gulper sharks, long-finned gulper sharks, and the gulper shark and mangrove jack from the November 2016 survey. This GEL was also exceeded by the dwarf gulper shark, long-finned gulper shark and fatspine spurdog from the May 2017 survey, and the market-bought mangrove jack and bigeye trevally.

- The selenium FSANZ GEL (median value) of 0.5mg/kg was exceeded by all liver samples of both the caught and market-bought specimens from the November 2016 survey. The liver samples of the caught blackspotted croaker, mangrove jack and saddletail snapper exceeded the selenium FSANZ GEL (90th percentile value) of 2mg/kg. This GEL was exceeded in the liver tissue of all the market-bought specimens.

Zinc

- The zinc FSANZ GEL (median value) of 5mg/kg and the zinc FSANZ GEL (90th percentile value) of 15mg/kg were exceeded by the liver samples of all caught and market-bought specimens, with the exception of the dwarf gulper shark, which did not exceed the FSANZ GEL (90th percentile value).

Exceedances of the FSANZ standards and GELS for these metals were also recorded in other DSTP-associated deep-slope fishing baseline studies in PNG, specifically Misima (NSR, 1988), Lihir (NSR, 1996) and Woodlark (Coffey, 2012). No metals concentrations were reported for fish catches from the NSR (1998) Ramu study. This indicates that baseline (i.e., pre-DSTP) exceedance of food standards is common in fish tissue in PNG.

Results of tissue analyses showed that most metals were significantly higher in liver tissue than muscle tissue, particularly for copper, mercury, selenium and zinc. The concentrations of arsenic were similar for muscle and liver.

Arsenic, mercury, copper, and zinc are often accumulated in the liver of fish (as well as other vertebrates), which removes these metals from the blood. The liver contains many proteins (e.g., metallothionine) that bind and/or detoxify these metals into non-toxic forms that are typically excreted unless exposure concentration and duration exceed transformation rates in the liver (or kidney in the case of mercury; Klassen et al., 1996).

Metals concentrations in muscle and liver tissues taken from 44 dwarf gulper sharks are shown against weight (left side) and total length (right side) in Figure 11.27, Figure 11.28 and Figure 11.29. Generally, the results showed no clear trends as a function of weight or total length, with the exception of the following:

- Mercury concentrations in muscle increased with increasing shark length and weight both in November 2016 and May 2017
- Cadmium concentrations in liver increased with increasing shark length and weight
- Selenium concentrations in liver decreased with increasing shark length and weight
- Zinc concentrations in liver increased with increasing shark length and weight

Metals concentrations in muscle from dwarf gulper sharks showed little variation between individuals caught in November 2016 and May 2017. This reflects the similar range in lengths and weights of dwarf gulper sharks caught over the two surveys.

Arsenic and mercury concentrations in dwarf gulper sharks caught in November 2016 were significantly greater in muscle than liver samples. Copper, iron and zinc concentrations were greater in liver than muscle samples. Metals concentrations are typically higher in the liver as a result of the detoxification role of this organ. This suggests that arsenic and mercury tend to accumulate in muscle tissue in dwarf gulper shark, while copper, iron and zinc tend to accumulate in the liver.

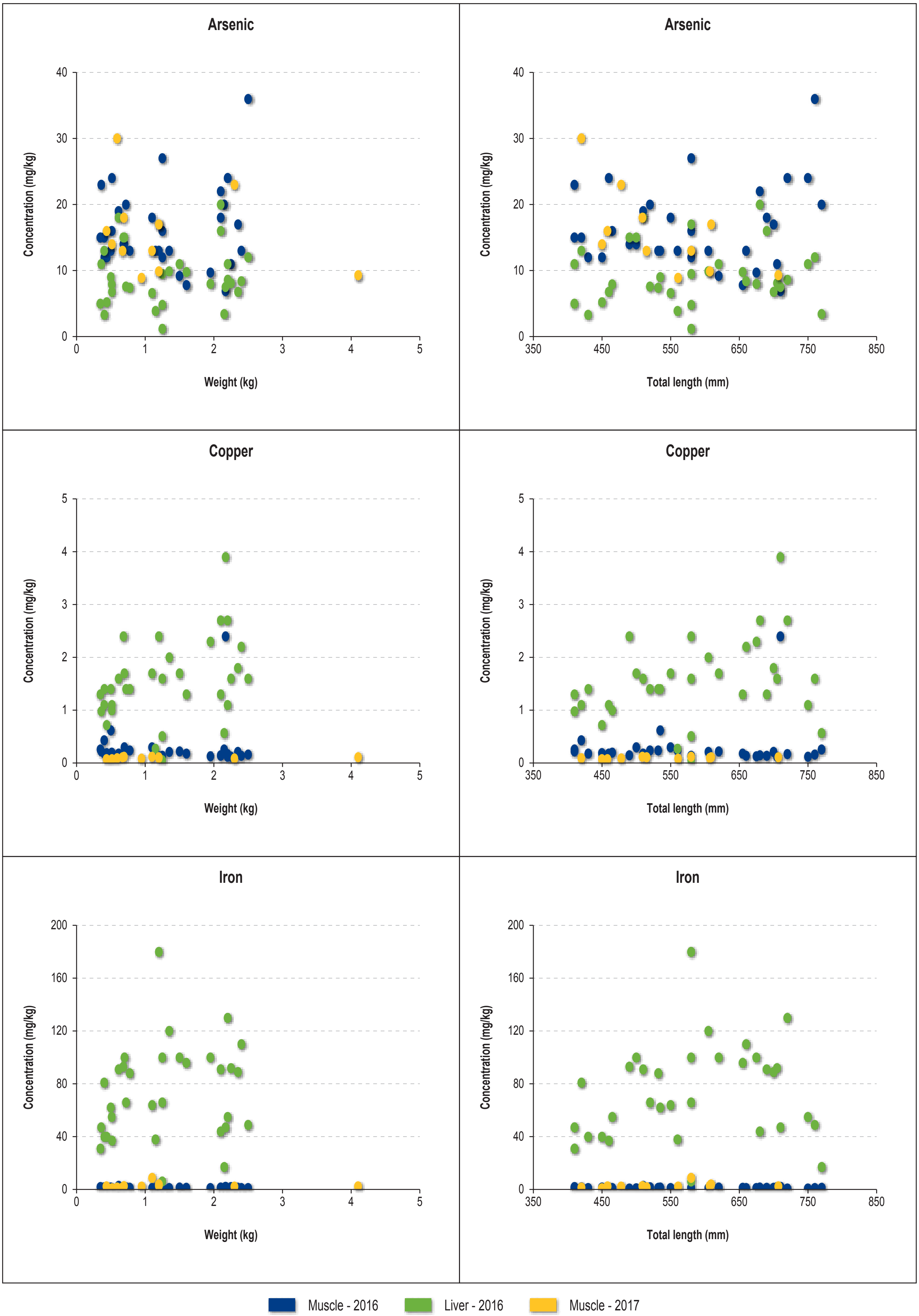

coffey
A TETRA TECH COMPANY

Date: 16.02.2018
Project: 754-ENAUABTF100520DD
File Name: 0520DD_10_F11.27_GRA

WAFI-GOLPU JOINT VENTURE

Wafi-Golpu Project

Metals concentrations (As, Cu and Fe) in liver and muscle of dwarf gulper shark by total weight and length

Figure No: 11.27

INDD Reference: 0520DD_10_GRA063.indd_3

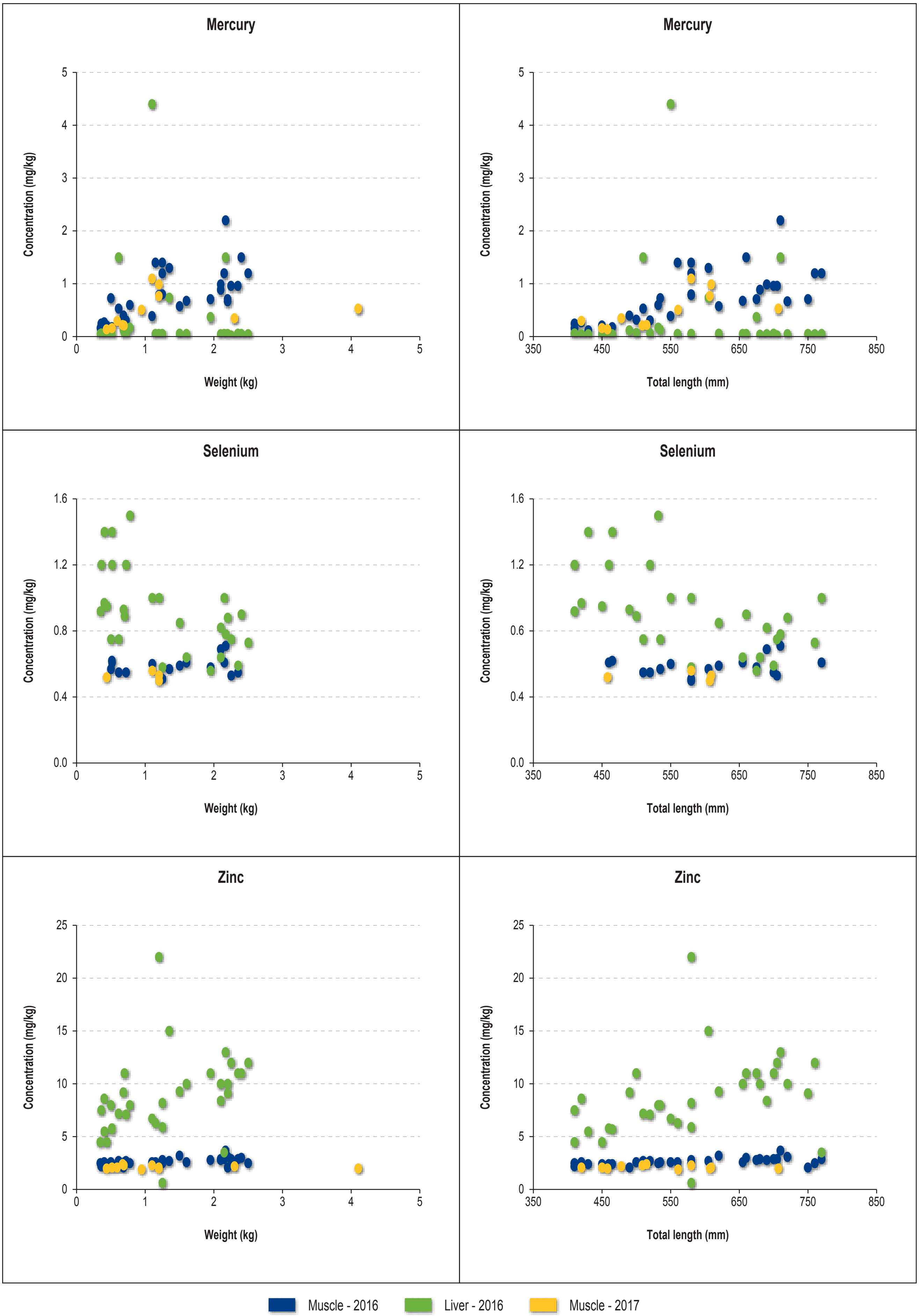

coffey A TETRA TECH COMPANY	Date: 16.02.2018 Project: 754-ENAUABTF100520DD File Name: 0520DD_10_F11.28_GRA	WAFI-GOLPU JOINT VENTURE Wafi-Golpu Project	Metals concentrations (Hg, Se and Zn) in liver and muscle of dwarf gulper shark by total weight and length	Figure No: 11.28

INDD Reference: 0520DD_10_GRA064.indd_3

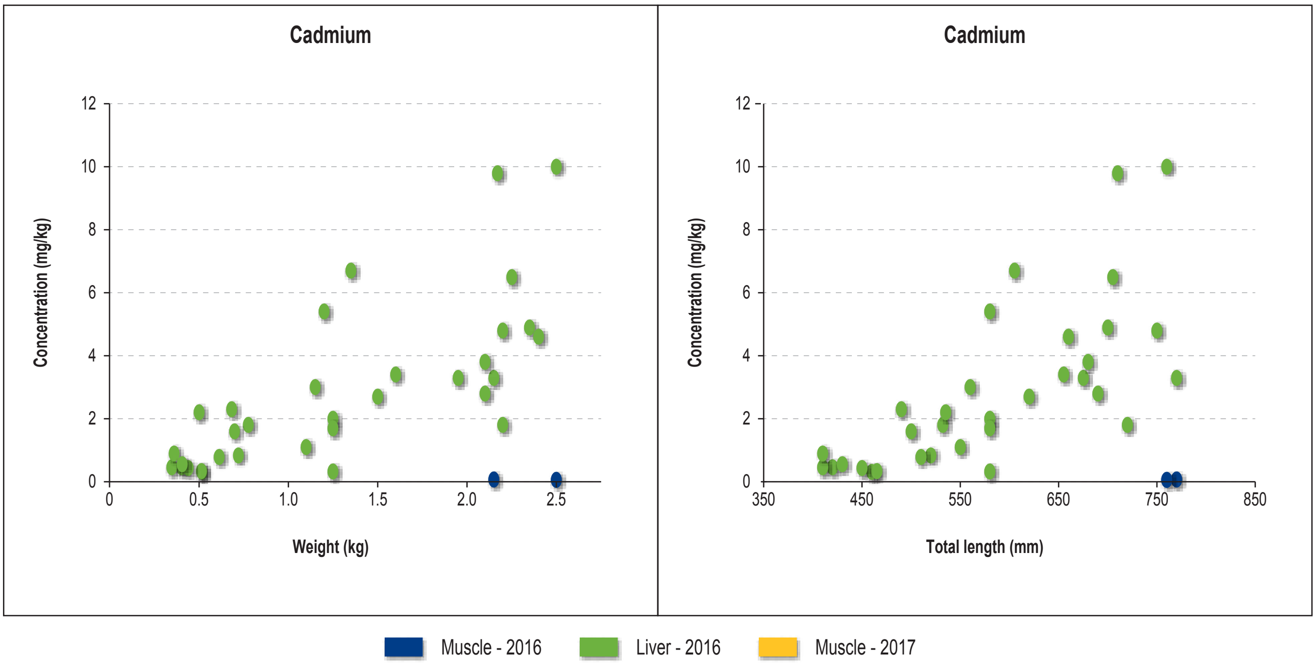

Metals concentrations (Cd) in liver and muscle of dwarf gulper shark by total weight and length

Figure No: 11.29

Arsenic concentrations were generally higher for all caught species (mostly sharks), compared with market species. However, the sharks caught during the survey are rarely consumed by local people (Appendix S, Fisheries and Marine Resource Use Characterisation). Otherwise, comparisons between caught and market sourced fish are similar, apart from individual high spikes (e.g., mercury in liver of one mangrove jack).

Metal concentrations in muscle and liver tissue samples from caught or market-sourced fish in the Project study were compared to those reported in the above-mentioned studies. Instead of intraspecific comparison, general comparisons across genera of the family Lutjanidae were made against lutjanids tested for Misima (NSR, 1988), Lihir (NSR, 1996), and Woodlark (Coffey, 2012). Notwithstanding the very high differences in mercury concentrations (in particular) between the three individuals of mangrove jack analysed in this study, metal results from this study are typical of the range observed in these other baseline studies (Appendix P, Deep-slope and Pelagic Fish Characterisation).

The exceedances of food standards for arsenic, copper, mercury, selenium and zinc in fish and tissue in this study are therefore not surprising given this has been reported in fish tissue for other DSTP sites in PNG. As none of the species tested for metals during the study have been recorded in other DSTP-associated studies in PNG, this precludes making any direct comparisons of metals concentrations between the same species.

11.8.2. Zooplankton and Micronekton

11.8.2.1. Study Area

Zooplankton was sampled in March 2017 at nine sites within the DSTP study area and at two sites within the reference study area, while micronekton was sampled in May 2017 at two sites within the DSTP study area (Figure 11.30).

Zooplankton sampling sites included inshore, mid-slope and offshore sites within the DSTP study area, and inshore and offshore sites within the reference study area. Micronekton sampling sites included inshore and offshore sites within the DSTP study area. Inshore sites were those within about 1km of the shore and/or where the water depth is about 100m and less than 200m. Mid-slope sites were those where water depths typically ranged between about 250m and 400m, while offshore sites comprised those furthest from shore, with depths around 500m or more. Zooplankton and micronekton were sampled during both day and night to allow comparison of the taxa assemblages, and obtain information on diel vertical migration.

11.8.2.2. Zooplankton

Zooplankton occurred at all offshore sites in samples taken from depths between 500m and the surface, all mid-slope sites between 250m and the surface and all inshore sites between 100m and the surface. Zooplankton abundances in the DSTP study area were highly variable across sampling sites and abundances also differed between relatively close sites. The lowest and highest average zooplankton abundances were both recorded at inshore sites, in depths of 0m to 100m.

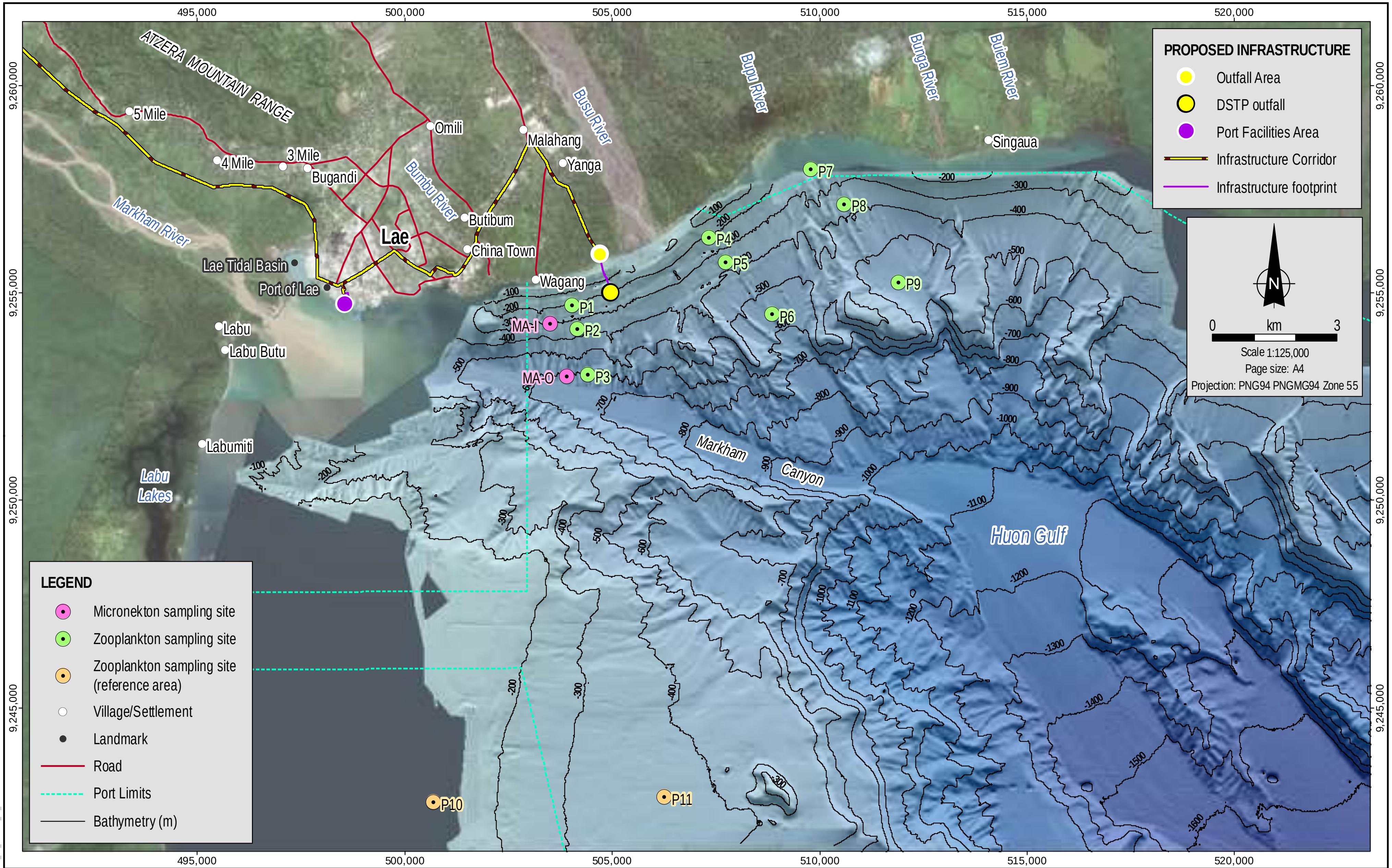

MXD Reference: 0520DD_10_GIS039_v0_5

Source:
Zooplankton and micronekton sampling sites, roads and Port Limits from Coffey (Port Limits indicative only).
Villages/Settlements, landmarks and infrastructure from WGJV and Coffey.
Bathymetry from WGJV survey.
Imagery from WGJV (capture date 2016) and ArcGIS Online (capture date unknown).

coffey — A TETRA TECH COMPANY

Date: 16.02.2018
Project: 754-ENAUABTF100520DD
File Name: 0520DD_10_F11.30_GIS

WAFI-GOLPU JOINT VENTURE

Wafi-Golpu Project

Zooplankton and micronekton sampling locations

Figure No: 11.30

Generally, no clear relationships were evident between zooplankton abundance and site location, depth, or sampling time. An exception was the vertical migration of zooplankton from deeper to shallower waters at night, which was apparent through higher zooplankton abundance at night time in shallower samples (0-100m and 0-250m), inshore sites P1 and P4 (100-0m), mid-slope sites P2 (250-0m) and P5 (100-0m and 250-0m), and offshore site P3 (250-0m). Vertical migration by zooplankton to shallower waters at night is a well-known behavior of these organisms in oceans globally and is likely due to their lower risk of being eaten by fish during their search for food in the upper water column (Hays, 2003; Ringelberg, 2010).

Water column stratification can influence the vertical distribution of zooplankton and micronekton. The absence of discrete water stratification, at least at the time of sampling, suggests that zooplankton and micronekton aggregations have limited or no restriction on movement vertically in the water column. Factors which may play a role in driving the vertical and horizontal distribution of zooplankton in the DSTP study area include daily tides, local and wind-driven ocean currents, turbidity of waters, and variable riverine discharge (and associated nutrient inputs) in the upper Huon Gulf.

Thirty-eight zooplankton taxa groups were identified across the eleven sites sampled during the March 2017 survey. Of these, 32 taxa groups (84%) were common to all sites, depths and sampling times. Taxa composition identified in zooplankton assemblages from the DSTP and reference study areas were indicative of a healthy community typical of tropical marine waters (i.e., numerous, diverse taxa with no dominant single taxa).

The zooplanktonic community of the Huon Gulf was dominated by crustaceans, including krill, copepods (Figure 11.31), ostracods (Figure 11.32) and the ghost shrimp *Lucifer* sp. (Figure 11.33), with those taxa accounting for 57% to 90% of the total numbers of taxa collected across all sampled sites.

The next most abundant zooplankton groups comprised gelatinous taxa such as siphonophores (hydrozoans of the phylum Cnidaria) (Figure 11.34) and arrow worms (chaetognaths) (Figure 11.35). Squid (cephalopod), salps and dolids (thaliaceans), and small jellyfish (cnidarians) were also collected during zooplankton sampling.

The diversity of the zooplanktonic community increased from inshore to offshore sites in the DSTP study area. However, there was considerable overlap in taxa groups across all sampled sites. In addition, similarity between the DSTP study area and reference study area was high, with at least 60% of the taxa found throughout the two areas surveyed. The latter finding indicates that, at present, the zooplankton assemblage in the Huon Gulf is likely to be similar over a wider area than that covered in this study.

11.8.2.3. Micronekton

Micronekton occurred in the offshore site from depths between the maximum sampling depth of 500m and the sea surface, and at the inshore site between 250m and the surface.

The greatest micronekton abundance, i.e., 1,564 individuals per 1,000m^3, was recorded at inshore site MA-I (between 0 to 250m depth) in the DSTP study area at night. The micronekton assemblages comprised mostly chaetognaths, copepods, siphonophores, and decapods, which were common in all four samples examined. Ostracods were abundant at offshore site MA-O, and fishes were more common in micronekton than zooplankton.

Photo credit: Kerrie Swadling

Figure 11.31
Copepod collected
during zooplankton sampling

Photo credit: Kerrie Swadling

Figure 11.32
Ostracod collected
during zooplankton sampling

Photo credit: Kerrie Swadling

Figure 11.33
Ghost shrimp 'Lucifer' collected
during zooplankton sampling

Photo credit: Kerrie Swadling

Figure 11.34
Siphonophore (hydrozoan) collected
during zooplankton sampling

Photo credit: Kerrie Swadling

Figure 11.35
Arrow worm (chaetognath) collected
during zooplankton sampling

The small number of micronekton samples available from the DSTP study area was insufficient to make detailed or comparative observations in relation to overall diversity in the Huon Gulf. Based on the microscopic analysis of the four samples, it appeared that there was a 'background' assemblage similar to that found in zooplankton samples, with groups such as Lucifer, siphonophores, and the copepods *Euchaeta* and *Eucalanus* all present in micronekton samples. Added to those groups were adults of the euphausiid genera *Stylochieron* and *Euphausia* (in the *E. sibogae* suite), large penaid prawns and fish including larvae and juvenile mesopelagic fishes including Myctophidae (lanternfishes), Trachichthyidae (slimeheads) (Figure 11.36) and Alepocephalidae (slickheads) (Figure 11.37), juvenile and adult viperfish (*Chauliodus sloani*) (Figure 11.38), and 'leptocephalus' stage larvae of anguilliform (eel) fishes (Figure 11.39). The small number of available samples could also have accounted for the fact that no adult myctophids were captured in the micronekton samples, even though these zooplanktivorous fishes comprise one of the most abundant and diverse vertebrate groups occurring in the mesopelagic zone of all oceans globally (Dypvik and Kaartvedt, 2013).

11.8.2.4. Metals in Zooplankton and Micronekton

Metals analysis (wet weight basis) was performed on bulk zooplankton samples and selected micronekton specimens comprising 21 taxa. Figure 11.40 presents the average metals concentrations in zooplankton at various depth strata, which is also a factor of distance offshore. Figure 11.41 presents the metals concentrations in selected micronekton taxa, and shows the averaged metal concentrations (plus error bars for 95th percentile values). The data presented in these two figures are restricted to analytical results above the practical quantification limits (PQL) (and therefore suitable to be shown visually).

Concentrations of most metals in bulk zooplankton samples decreased with distance from shore; i.e., were highest at inshore sites and decreased at the mid-slope and offshore sites.

Furthermore, metal concentrations in zooplankton samples collected from the reference study area (an inshore site and a mid-slope site) were lower than in samples from the DSTP study area except in the case of arsenic and cadmium, for which concentrations were similar to the lowest values detected in zooplankton samples from the DSTP study area.

The higher concentrations of metals in inshore zooplankton samples from the DSTP study area are most likely due to the influence of riverine discharges (e.g., from the Markham and Busu rivers), which are likely to discharge substantial loads of particulate metals to the DSTP study area. Other potential local sources of metals may also include anthropogenic inputs such as stormwater runoff and wastewater discharges from Lae and surrounding coastal villages. In this context, it is relevant that concentrations of metals from inshore zooplankton samples have also been reported to be markedly higher compared to open sea samples in coastal marine habitats elsewhere in the world, and have likewise been attributed both to direct river discharge (e.g., Pempkowiak et al., 2006) or a combined effect of riverine and anthropogenic sources (e.g., Ferreira et al., 2005; Wan Ying Lim et al., 2012).

It is not clear whether the higher metal concentrations of the inshore samples are due to combined bioaccumulation by individual zooplankters, or due to suspended particulate matter adhering to their body surfaces. Body surfaces include the exoskeleton in crustaceans such as copepods and ostracods, which were amongst the most abundant taxa identified in the zooplankton samples collected during the present study.

Photo credit: Francisco Neira

Photo credit: Francisco Neira

Figure 11.37
Slickhead (Family: Alepocephalidae)
collected during micronekton sampling

Photo credit: Francisco Neira

Figure 11.38
Viperfish (*Chauliodus sloani*)
collected during micronekton sampling

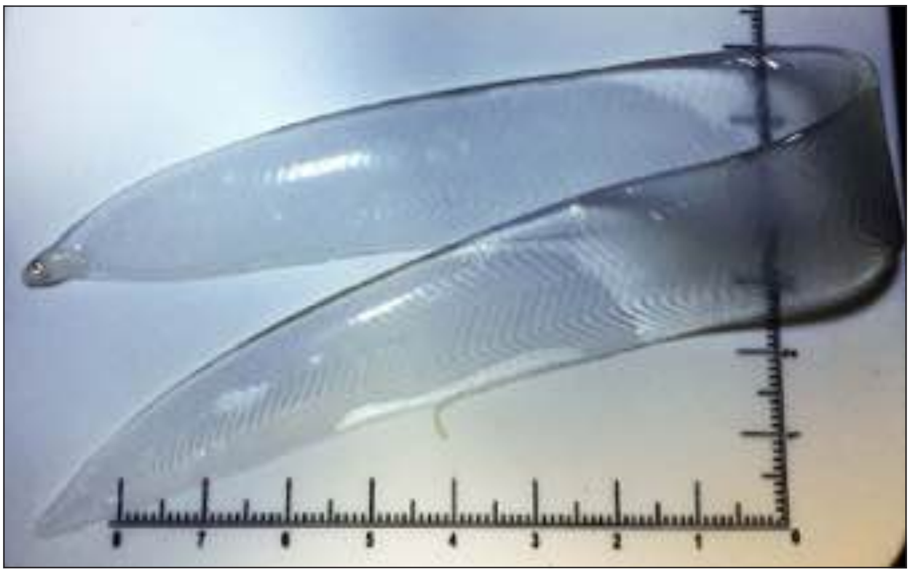

Photo credit: Francisco Neira

Figure 11.39
Leptocephalus stage larvae of anguilliform (eel)
fishes collected during micronekton sampling

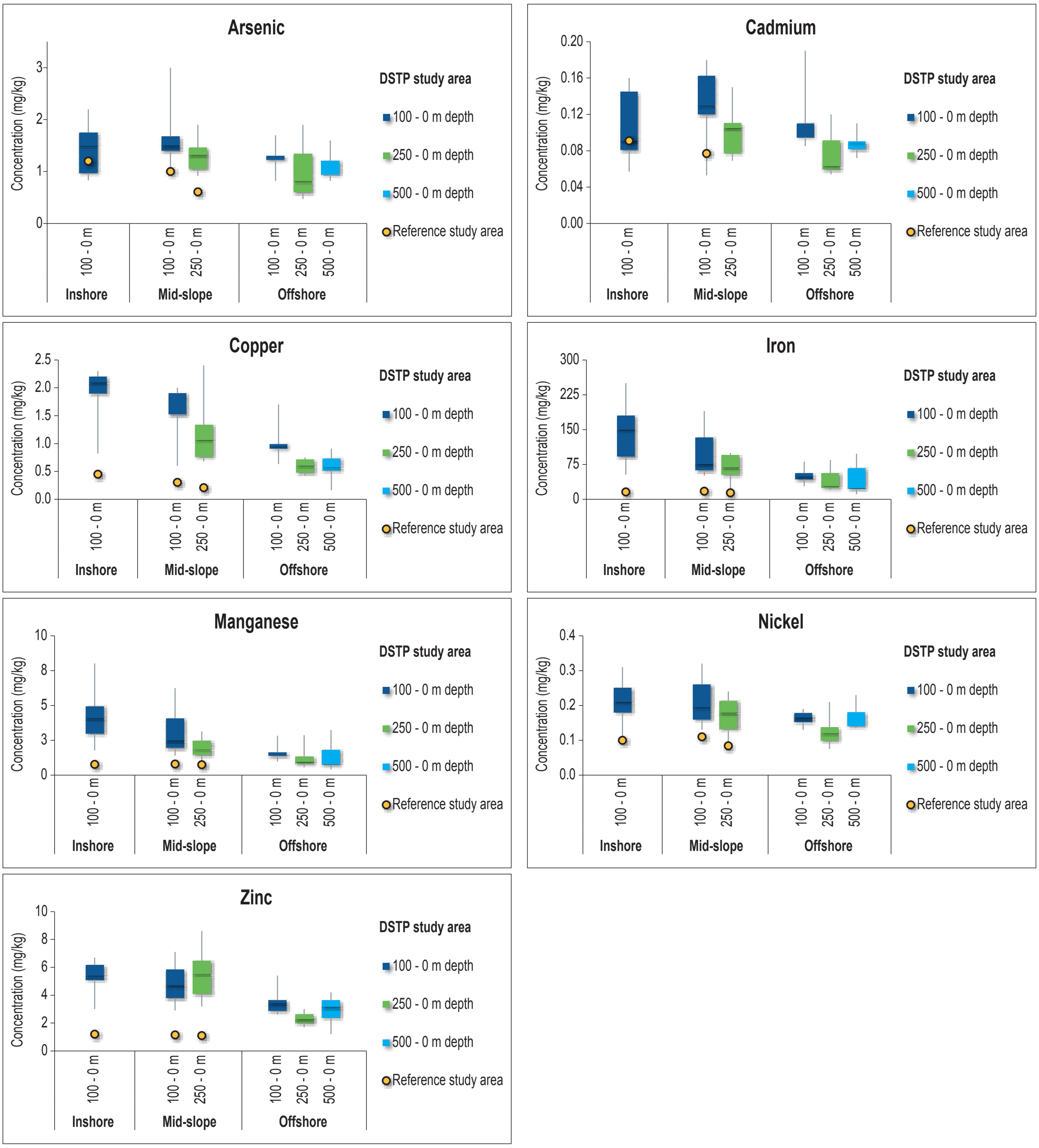

Note:
The whiskers show minimum and maximum values (bottom and top respectively), outer box borders show the 25th and 75th quartiles (bottom and top respectively), and the mid-lines denote the median values.

Average concentrations of As, Cd, Cu, Fe, Mn, Ni and Zn in zooplankton samples collected in March 2017 from the DSTP and reference study areas

Figure No: 11.40

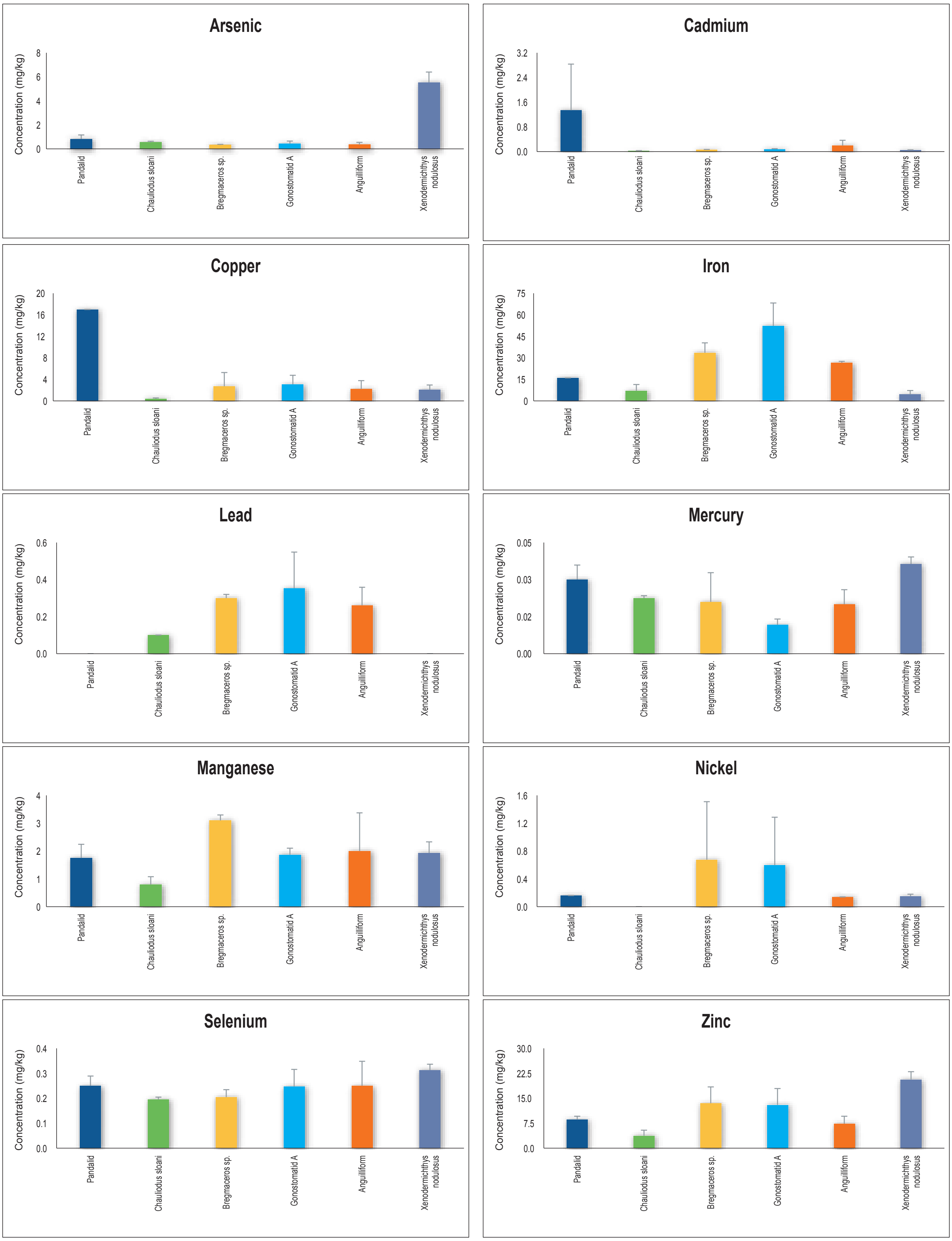

Note:
Error bars denote 95th percentile values.

coffey
A TETRA TECH COMPANY

Date: 21.03.2018
Project: 754-ENAUABTF100520DD
File Name: 0520DD_10_F11.41_GRA

WAFI-GOLPU JOINT VENTURE

Wafi-Golpu Project

Concentrations of As, Cd, Cu, Fe, Pb, Hg, Mn, Ni, Se and Zn in micronekton taxa collected in the DSTP study area in May 2017

Figure No: 11.41

INDD Reference: 0520DD_10_GRA067.indd_3

Concentrations of metals measured in micronekton taxa were highly variable across the different taxa tested. However, no single taxon consistently showed significantly higher metals concentrations than any other taxa. Pandalid shrimp had a relatively high copper concentration (17mg/kg; the next highest concentration being 5.8mg/kg in a Decapoda A) and *Xenodermichthys nodulosus* had a relatively high arsenic concentration (6.4 mg/kg; the next highest concentration being 1mg/kg in the pandalid shrimp). The reason for the elevated arsenic in this organism is not clear; however, the relatively high copper concentration in the pandalid shrimp is likely to be due to copper-based blood (haemocyanin) and the larger size of this micronekton. Metals concentrations in micronekton did not display any clear spatial differences, with generally similar concentrations recorded in the samples of various taxa, from both inshore and offshore locations.

Concentrations of most metals (i.e., arsenic, cadmium, copper, lead, mercury, nickel and zinc) were noticeably higher in micronekton taxa than in zooplankton samples, suggesting some level of bioaccumulation or biomagnification of these metals is occurring naturally from lower to higher trophic levels (i.e., zooplankters to macrozooplankters and micronekton). As with zooplankton, there may be an association between suspended particulate matter adhering to the body surfaces of micronekton and metals concentrations.

11.8.3. Deep-Sea Benthic Ecology

11.8.3.1. Study Area

The deep-sea benthic ecology was charactersied via an underwater video assessment by Coffey (Appendix O, Benthic Video Characterisation) and infauna sampling by GDA Consult Pty Ltd and IHAconsult (Appendix M, Physical, Chemical and Biological Sedimentology of the Huon Gulf). The studies investigated locations within the likely flowpath of natural sediments toward and through the Markham Canyon, the canyon slopes and seafloor, elevated features in the centre of the canyon, and locations outside of the Markham Canyon, including those further afield toward Salamaua. Macrobenthos and meiobenthos sampling was conducted concurrently with box corer sediment sampling in February 2017, and meiobenthos sampling was also conducted using a box corer and multicorer in December 2017. The latter sampling program was designed along five transects aligned perpendicularly across the Markham Canyon, with each progressively deeper from transect T1 (adjacent to the outfall site, maximum depth 700m) to transect T5 in the vicinity of the Trench mooring location (maximum depth 3,000m). Figure 11.42 shows the locations of the benthic video characterisation sites. The infauna sampling sites are shown on Figure 11.14.

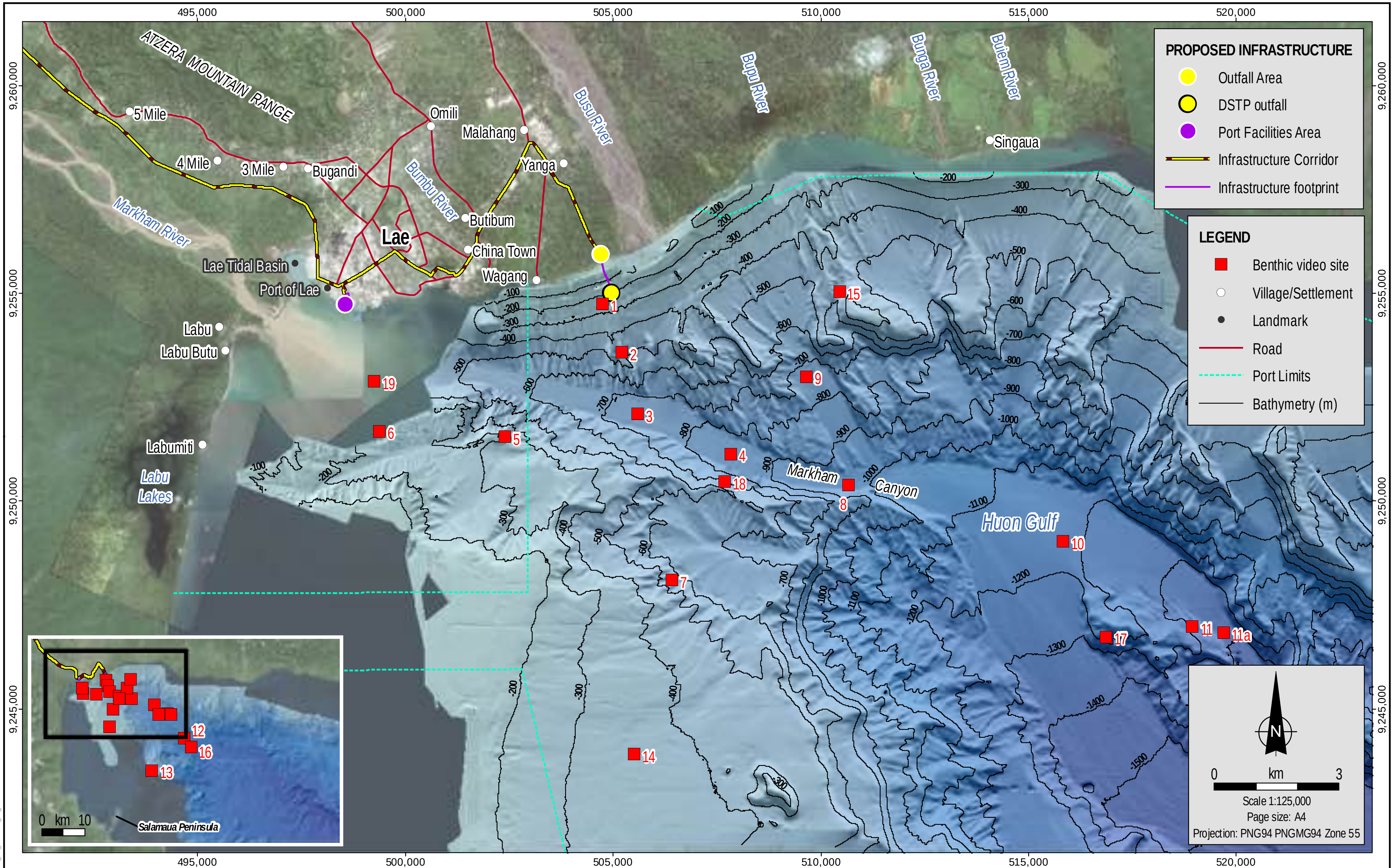

MXD Reference: 0520DD_10_GIS040_v0_3

Source:
Benthic video sites, roads and Port Limits from Coffey (Port Limits indicative only).
Villages/Settlements, landmarks and infrastructure from WGJV and Coffey.
Bathymetry from WGJV survey.
Imagery from WGJV (capture date 2016) and ArcGIS Online (capture date unknown).

coffey
A TETRA TECH COMPANY

Date: 16.02.2018
Project: 754-ENAUABTF100520DD
File Name: 0520DD_10_F11.42_GIS

WAFI-GOLPU JOINT VENTURE

Wafi-Golpu Project

Benthic video characterisation study sites

Figure No: 11.42

11.8.3.2. Deep-Sea Benthic Habitats

The benthic environment observed during the video characterisation study (Appendix O, Benthic Video Characterisation) was generally flat lying, and lacked complex three-dimensional morphology (as illustrated at Site 13 to the south of the Markham Canyon, in Figure 11.43). Rugosity, an index of surface roughness that is widely used as a measure of landscape structural complexity in studies investigating spatially explicit ecological patterns and processes, was consistently observed to be very low. At all sites, no hardstand surfaces of rock, rubble or aggregate reef habitat were observed, due to a layer of readily-mobilised sediment being present atop the underlying seafloor substrate. Benthic habitats visually assessed via video footage displayed a high degree of surface uniformity and were characterised by fine, largely homogenous sediments (as visible in Figure 11.43). Very occasionally, fragments of terrestrial vegetation, and at Site 1 cobble-sized rocks of riverine origin (Figure 11.44), were observed. During sediment sampling (Appendix M, Physical, Chemical and Biological Sedimentology of the Huon Gulf) on the floor of the Markham Canyon, the recovered benthic samples were found to contain large amounts of terrestrial sediments including fine silts, sands, gravels and cobbles.

11.8.3.3. Deep-Sea Benthic Fauna

Opportunistic fauna observations took place during the benthic video characterisation study. The presence of benthic macrofauna was visually discernible via evidence comprising mounds, burrows and faecal casts at most sites where seafloor visibility was adequate. Shrimp, sea whips, ophiuroids and other fauna were observed in very low numbers (typically solitary), and none of these could be identified to species level due to their distance from the video camera and suspended sediment adversely affecting video resolution. While no benthic fish were observed, demersal fish including a grenadier or rattail fish of the family Macrouridae, and solitary dwarf gulper sharks (probably *Centrophorus atromarginatus*), were encountered swimming just above the seafloor.

During the underwater video assessment, to varying degrees the benthic environment was visible at locations outside of the Markham Canyon or occasionally on the canyon slopes.

Seafloor water clarity was highest at Sites 1, 5, 7, 13 to 15, 17 and 18. At Sites 2, 6, 9, 11 and 16 there was typically partial and generally very poor seafloor visibility. Sites within the Markham Canyon or in the path of sediment plumes from Markham River (Sites 3, 4, 8, 10 to 12, 16 and 19) were generally highly turbid and the seafloor could not be seen at most of these sites. Fauna sightings principally occurred at locations with higher visibility, situated at greater distances from the main influences of sedimentation, such as Sites 13 and 14.

Brief, opportunistic use of a baited remote underwater video sampling technique, involving a baited bag attached to the underwater imaging system to record fauna attracted to the bait within the field of view of the camera, resulted in no observations of fish or other fauna at Sites 6, 7, 8 and 9 (total recording time less than one hour).

Diverse or abundant epibenthic faunal communities such as those associated with seamounts, deep-sea coral reefs or hydrothermal vent communities, were not observed at any sites between 220m and approximately 1,800m water depth.

Photo credit: Coffey

Figure 11.43
Sea whip (lower left of frame) at Site 13 (depth 757m). Note mounds and burrows in sediment.

Photo credit: Coffey

Figure 11.44
Cobble sized rocks of riverine origin at Site 1, 229m depth

Seafloor photography captured by SAMS (2010b) from along the Rai Coast near Basamuk, Madang Province, PNG indicated a range of biogenic features on fairly smooth, flat sediment surfaces (SAMS, 2010b). At some sites these features included biogenic traces, burrow openings, pits or depressions, faecal casts, brittle stars and occasional land-derived vegetation, and were suggestive of a relatively low-disturbance benthic environment. Other sites photographed along the Rai Coast displayed evidence of more recent seafloor disturbance and lower diversity benthos. The observations by SAMS (2010b) largely correspond with the observations made by Coffey (Appendix O, Benthic Video Characterisation) of benthic features identified in the Huon Gulf. This included evidence at most locations (such as those in the path of riverine sedimentation plumes and inside the Markham Canyon) of recent and/or ongoing disturbance and an impoverished benthic fauna, while sites south of the Markham Canyon (without obvious indications of disturbance) were characterised by similar faunal features to those observed along the Rai Coast.

11.8.3.3.1. Infauna Sampling

Subsamples taken from benthic sediment core samples were analysed by Dr John H Moverley for meiofauna and macrofauna content. A summary of meiofauna density, and macrofauna abundance and density from February 2017 sampling, is given in Table 11.7 (Appendix M, Physical, Chemical and Biological Sedimentology of the Huon Gulf). A summary of meiofauna density from December 2017 sampling is given in Table 11.8.

Table 11.7: Macrofauna abundance and density and meiofauna density in deep-sea sediment samples, February 2017

Sample	Depth	Meiofauna	Macrofauna	
		Density (number/10cm^2)	Number in Sample	Estimated Density (number/m^2)
BC01	355	114	4	267
BC03	589	12	0	0
BC04	721	3	1	83
BC06	1,098	3	0	0
BC07	1,143	44	0	0
BC08	915	6	0	0
BC09	1,022	3	0	0
BC12	1,489	19	1	83
BC13	2,001	191	0	0
BC14	2,121	94	5	333
BC15	1,656	74	2	133

Table 11.8: Density (number/10cm^2) of meiobenthic fauna collected in the Markham Canyon survey, December 2017

Site	Transect				
	1	2	3	4	5
1	35	171*	196	87*	162
2	12**	11	49	53*	472
3	93**	22	-	-	263

Site	Transect				
	1	2	3	4	5
4	235**	460	177*	-	165
5	-	219	144	265	81

- = no data
* = average of 3 replicate multi corer samples
** = box corer sample

More than half of the deep-sea infauna samples from February 2017 contained no macrofauna and, when present, total macrofauna abundance was less than five. The low Markham Canyon macrofauna sample densities most likely reflects the dominance of samples taken from coarse mobile sediments, where macrobenthic communities cannot establish. Samples with densities greater than 100 animals per square metre were only encountered in off-canyon floor samples (BC01, BC14 and BC15). Densities of macrofauna in these samples are low compared to samples collected from other PNG unimpacted deep-sea sites where similar collection and processing methods have been used (Appendix M, Physical, Chemical and Biological Sedimentology of the Huon Gulf). Macrofauna density of the canyon floor generally appears to be low and variable, with higher densities being found in the off-canyon floor sites.

For meiofauna, in general, samples from February 2017 from the seafloor at the head of the canyon comprised very low densities, compared to samples collected away from the canyon floor. The highest meiofauna density was recorded at BC13, the deepest canyon sample. The next highest density was from sample BC1 in relatively shallow water to the south of Lae. The off-canyon samples BC14 and BC15, located on the raised plateau, had the third and fourth highest densities respectively.

Bed waves, which are elongated depositional bed forms with an undulating surface located mainly transverse or with a small angle to the dominant current direction, have been identified on the floor of the Markham Canyon. It is possible that the crests of the bed waves on the canyon floor may have low meiofauna densities while the troughs have higher densities; sample variability may be naturally high over the canyon floor as a result (Appendix M, Physical, Chemical and Biological Sedimentology of the Huon Gulf).

The median meiofauna density of 19 animals per 10 square centimetres in February 2017 is low compared to that found at unimpacted sites at other locations in PNG where similar sampling methods have been used (Appendix M, Physical, Chemical and Biological Sedimentology of the Huon Gulf). In publicly available comparable data of PNG deep-sea meiofauna densities, sample BC13 exceeded the highest density by 30%.

Generally, the meiofauna analysis from February 2017 indicated high variation between canyon floor and off canyon floor areas, and this may reflect opportunistic colonisation of the floor of the canyon, given the highly dynamic seafloor environment.

Observations from the December 2017 infauna sampling showed that box core sample densities were very similar to, though generally slightly higher than, multicore sample densities (Figure 11.45), and show that the highest meiofauna densities (Table 11.8) were more than double the maximum numbers observed in February 2017. Overall, densities were variable, both between and within transects.

The low numbers of replicates and the high variability between the replicates results in these differences not being statistically significant at the 95% confidence level.

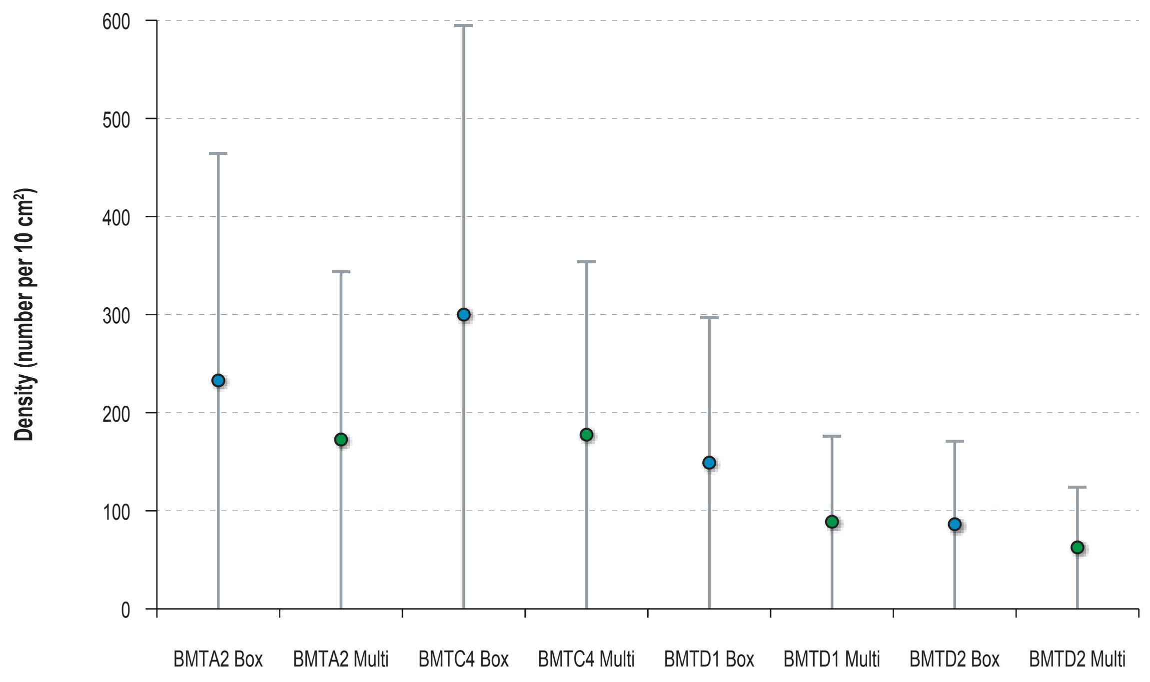

Average meiofauna density for box and multi corer replicates

Figure No:
11.45

In other comparative studies, box corer sample densities were usually less than the multicore sample densities (see Montagna et al., 2016), because of loss of surface integrity by the bow wave effect of the instrument, or loss during retrieval. Possible reasons for the comparable box corer results in this study are:

- The live-feed techniques of deployment of the box corer that have been refined over many PNG monitoring programs adequately retain intact surface sediments in these locations.
- The coarser nature of some of the sampling locations, especially those in the bottom of the canyon, were more difficult to sample by multicorer.
- The observed stickiness of the sediment in some multicore samples could result in underestimation of faunal densities during sub sampling.

While densities were higher in the December 2017 study, composition was more dominated by one group (nematodes) compared with the February 2017 study. These findings may reflect the differing number of samples and sampling areas in the December 2017 survey, however given the different sampling locations, and the high within-site variances at each transect, make comparisons between locations or physical characteristics such as particle size difficult. These results suggest a propensity for change in infauna assemblages rather than stability, indicative of the disturbances related to mass movement events observed during the oceanographic studies.

11.9. References

ANZECC/ARMCANZ. 2000. Guidelines for fresh and marine water quality, Australian and New Zealand Environment and Conservation Council, Agriculture and Resource Management Council of Australia and New Zealand.

Coffey. 2012. Slope Fishes of Wamunon Bay, Woodlark Island – Species Diversity and Biological Assessment. Report prepared by Coffey Environments Australia Pty Ltd for the Woodlark Gold Project. 1412_25. 62p.

Cresswell, G. R. 2001. Basamuk Oceanographic Study. May. Report prepared for NSR Environmental Consultants Pty Ltd.

Cresswell G. R. 2012. Aspects of the Physical Oceanography of Huon Gulf. Prepared for IHAconsult.

Dypvik, E. and Kaartvedt, S. 2013. Vertical migration and diel feeding periodicity of the skinnycheek lanternfish (*Benthosema pterotum*) in the Red Sea. Deep-Sea Research I 72: 9–16.

Ferreira A.G., Machado, A.L., and Zalmon, I.R. 2005. Temporal and spatial variation on heavy metal concentrations in the oyster *Ostrea equestris* on the northern coast of Rio De Janeiro State, Brazil. Brazilian Journal of Biology 65 (1): 67-76.

FSANZ. 2001. Generally Expected Levels (GELS) for Metal Contaminants. Food Standards Australia New Zealand. Additional guidelines to maximum levels in Standard 1.4.1 - Contaminants and Natural Toxicants. July. A WWW publication accessed on 9 February 2017 at https://www.foodstandards.gov.au/code/userguide/documents/GELs_0801.pdf

FSANZ. 2016. Australia New Zealand Food Standards Code - Standard 1.4.1 - Contaminants and Natural Toxicants. Food Standards Australia New Zealand. March (Revised). Canberra: Commonwealth of Australia. A WWW publication accessed on 9 February 2017 at http://www.foodstandards.gov.au/code/Documents/Sched%2019%20Contaminant%20MLs%20v157.pdf

General Bathymetric Chart of the Oceans. 2014. The GEBCO_2014 Grid, version 20150318, www.gebco.net. British Oceanographic Data Centre (BODC).

Hays, G.C. 2003. A review of the adaptive significance and ecosystem consequences of zooplankton diel vertical migrations. Hydrobiology 503, 163–170.

Henin and Cresswell G.R. 2005. Upwelling along the western barrier reef of New Caledonia. Marine and Freshwater Research, 56 (7), 1005-1010. ISSN 1323-1650.

Kara, A. B., Rochford P. A. and Hurlburt H. E. 2000. An optimal definition for ocean mixed layer depth. Journal of Geophysical Research 105, 16,803-16,821.

Klassen, C., M. Amdur, and J. Doull. 1996. Casarett and Doull's Toxicology. McGraw-Hill, N.Y.

Long, E.R., D.D. MacDonald, S.L. Smith and F.D. Calder. 1995. Incidence of adverse biological effects within ranges of chemical concentrations in marine and estuarine sediments. Environmental Management 19, 81-97.

Milliman J.D. 1995. Sediment Discharge to the Ocean from Small Mountainous Rivers: The New Guinea Example. Geo-Marine Letters (1995) 15:127-133.

Montagna, P.A., Baguley, J.G., Hsiang, C-Y. and Reuscher, M.G. 2016. Comparison of sampling methods for deep-sea infauna. Limnology and Oceanography Vol 15 (2): 166-183

NSR. 1988. Environmental Monitoring Program Baseline Report, July. Prepared by NSR Environmental Consultants Pty Ltd for Misima Mines Pty Ltd. CR 206/7.

NSR. 1996. Environmental Baseline Volume 1: Marine Environment. Prepared by NSR Environmental Consultants Pty Ltd for Lihir Management Company Pty Limited. CR 235/30.

NSR. 1998. Ramu Nickel Project Environmental Plan. Appendix 24: Deep-Slope Fisheries Survey, off the Rai Coast, Papua New Guinea. November. Prepared by NSR Environmental Consultants Pty Ltd and Dr Stephen J Newman of Western Australian Fisheries for Highlands Pacific Limited and Nord Pacific.

Pempkowiak, J., Walkusz-Miotk, J., Bełdowski, J. and Walkusz, W. 2006. Heavy metals in zooplankton from the Southern Baltic. Chemosphere 62 (2006) 1697–1708.

Renagi, O., Ridd, P. V., and Stieglitz, T. C. 2010. Quantifying the Suspended Sediment Discharge to the ocean from the Markham River, Papua New Guinea. Continental Shelf Research, 30, pp. 1030–1041.

Ringelberg, J. 2010. Diel Vertical Migration of Zooplankton in Lakes and Oceans. (Dordrecht: Springer Science).

Salomons, W and Förstner, U. 1984. Metals in the Hydrocycle. Springer-Verlag Berlin Heidelberg. 352 pp.

SAMS. 2010a. Draft General Guidelines and Criteria for mining operations in Papua New Guinea (PNG) involving Deep-Sea Tailings Placement (DSTP). Prepared by Scottish Association of Marine Science Research Services Limited.

SAMS. 2010b. Final Report: Independent Evaluation of Deep-Sea Tailings placement (DSTP) in PNG. Prepared by Shimmield, T.M., Blak, K.D., Howe, J.A., Hughes, D.J., Sherwin, T.

Simpson et al. 2013. Revision of the ANZECC/ARMCANZ Sediment Quality Guidelines. Simpson, S.L., Batley, G.E., Chariton, A.A. CSIRO Land and Water Science Report 08/07.

May 2014. Prepared for the Department of Sustainability, Environment, Water, Population and Communities.

U.S. Geological Survey. 2006. National Field Manual for the Collection of Water-Quality Data. A WWW publication accessed on 16 June 2017 at http://water.usgs.gov/owq/FieldManual/Chapter6/conversion.html.

Wan Ying Lim, Ahmad Zaharin Aris, and Mohamad Pauzi Zakaria, "Spatial Variability of Metals in Surface Water and Sediment in the Langat River and Geochemical Factors That Influence Their Water-Sediment Interactions," The Scientific World Journal, vol. 2012, Article ID 652150, 14 pages, 2012. doi:10.1100/2012/652150.